7-17-2007

Geomorphology of Submarine Spring West of Fort Myers, Florida

Shihadah M. Saleem
University of South Florida

Geomorphology of Submarine Spring West of Fort Myers, Florida

by

Shihadah M. Saleem

A thesis submitted in partial fulfillment
of the requirements for the degree of
Master of Science
College of Marine Science
University of South Florida

Major Professor: David F. Naar, Ph.D.
Kent A. Fanning, Ph.D.
Robert H. Byrne, Ph.D.
Barnali Dixon, Ph.D.

Date of Approval:
July 17, 2007

Keywords: submarine hydrothermal vents, multibeam bathymetry, GIS, Florida Platform

Acknowledgements

I thank my committee: Drs. David Naar, Barnali Dixon, Robert Byrne, and Kent Fanning for their guidance, support, and patience over the past years. I would especially like to thank Brian Donahue for his never-ending guidance, invaluable advice, and support during the completion of my research and graduate studies. A special thanks to Teresa Greely, Sande Ivey, Elizabeth Tyner, and Elizabeth Fisher for their friendship. Lastly, I would like to thank my family, my fiancé, Ruben, and my daughter for their love, keeping me focused, and always striving for the best.

Table of Contents

List of Tables

List of Figures

Geomorphology of Submarine Springs West of Fort Myers, Florida

Shihadah M. Saleem

ABSTRACT

In March of 2000, March of 2001, and April of 2002, multibeam bathymetry and backscatter data were collected, which revealed several low-temperature hydrothermal submarine springs in the Mudhole Submarine Springs (MHSS) area that were investigated by SCUBA divers. High-resolution multibeam sonar provides a precise way of defining the geomorphology of the seafloor. The bathymetry data were used to understand (1) vent geomorphology and how it varied from vent to vent; (2) spatial patterns of active vents compared to extinct vents and known land springs identified by Kohout (1977) and Breland (1980); and (3) potential correlations between geochemical and geomorphological characteristics of the vents in the study area. SCUBA observations show that MHSS, Spring #3, New Spring, Northern Rusty, Rusty, and Near Rusty are active springs, while Dormant Spring and Sinister Spring were extinct or inactive at the time of the March 2001 cruise. During the April 2002 cruise the locations of Rusty Spring, New Spring and MHSS were confirmed. Two submarine springs, Creature Hole and Sparky Lee were also confirmed. Spring #3 is the deepest spring and Dormant Spring is the shallowest.

There appears to be a rough spatial correlation between vents located on land and the vents on the seafloor, in which all known vents are either to the west or north of Lake

Okeechobee. Vent distribution in the MHSS study area appears to correlate with the structural pattern of the local seafloor. Backscatter data and SCUBA observations show that fine to medium grain siliciclastic sediment bands overlie limestone hardbottom in a NE-SW orientation. Although vent geomorphologies are generally distinctive, vent activities generally correlate with the steepness of vent depressions. Most active vents had slopes of 6^{o} or greater, with the exception of Rusty Spring and Near Rusty Spring whose slopes ranged from 2.5^{o} and 6^{o}; whereas all the inactive vents had slopes of 5^{o} or less. Most active vents have "V"-shaped profiles versus the "U"-shaped profiles of most of the inactive vents. The inactive springs have shallower maximum depths and shallower ambient seafloor depths than the active vents.

Chapter 1

INTRODUCTION

The driving force for hydrothermal circulation of Florida the submarine springs is due to slow thermal upwelling related to geothermal heat in the Florida carbonate platform. Most land springs are moderately easy to locate and are well-known. Submarine springs, however, are difficult to find and monitor due to overlying murky seawater along the west Florida coastline. Documentation of the geomorphology of the area around vent fields, depth-profiles of the vents, effluent flux, and overall distribution are limited primarily due to lack of data. Geochemical analyses of spring effluent can also provide information about the origin and chemical interactions of seawater along the fluid circulation path.

High-resolution multibeam sonar provides a precise way of defining the geomorphology of the seafloor. During March of 2000, March of 2001, and April of 2002, high-resolution multibeam data and SCUBA diving observations (Naar et al., 2000; Naar and Byrne, 2002) were used to characterize many active and extinct low-temperature hydrothermal submarine springs in the Mudhole Submarine Spring (MHSS) area following the work of Breland (1980) and Fanning et al. (1981). The following questions are addressed by investigating the geomorphology and geographical distribution of the springs in the MHSS area:

1. Do the spatial patterns of local active and inactive vents line up with known vents located far away on land as stated by Kohout (1977) and Breland (1980)?
2. Do seafloor structural trends in the Mudhole Submarine Springs correlate with vent distributions?
3. Does vent geomorphology vary from vent to vent? If so, are the variations related to vent activity?
4. Is there a correlation between the published geochemistry of the vent sites and vent geomorphology?

In order to answer these questions, the geologic background of Florida and its hydrothermal springs will be discussed in detail (Chapter 2). The characteristics of submarine springs will be explained by summarizing the geographical locations of such springs. Chapter 3 will explain how the study was conducted and the methods used to collect, analyze, and display the data. Chapter 4 will describe the observations and results of geomorphologic analyses. Chapter 5 discusses the geomorphology, correlations that exist, and implications of the results. Chapter 6 summarizes the main conclusions and speculations resulting from this study and provides suggestions for future work.

Chapter 2

GEOLOGIC BACKGROUND OF FLORIDA AND ITS SPRINGS

Geomorphology of Florida: Western Continental Shelf

Introduction to Geomorphology and Study Area

Geomorphology is the study of Earth's physical surface. Highstands and lowstands of sea level leave marine terraces, beds of marine shells, submerged coastal dunes, and many other features (Hugget, 2003). Geomorphological techniques and applications can be used to investigate seafloor characteristics, the nature of seabed surfaces (hardbottom vs. soft bottom), sediment transport, and structural trends (Doyle and Sparks, 1980; Finkl et al., 2005). Certain inferences about each vent can be made by utilizing shaded color bathymetry, shaded surface relief and backscatter images. For example, shape and profiles of the vent, the characteristics of the seafloor surrounding the vent depressions, and the orientation of each depression can be investigated and characterized. One can also check the angle of repose for the sedimentary slopes. Soulsby (1997) states the angle of repose "is the angle to the horizontal at which grains start to roll on a flat bed of sediment which is gradually tilted from the horizontal". The angle for non-cohesive sediments depends on the shape, sorting, and packing of the grains. It is affected by the size, mass, angularity, and dampness of the particles and by the force of motion (gravity) accelerated downward. When measuring the angles of sand in

submerged (wet) ripples, dunes, sandwaves, or conical scour holes, the angle of repose is ~28^{o} (Soulsby, 1997).

Shallow Water Carbonates and West Central Florida

Florida is well-known for its karstic topography and carbonate deposits. Ford and Williams (1989) define karst as "terrain with distinctive hydrology and landforms arising from a combination of high rock solubility and well developed secondary porosity". Limestone and dolomite deposits can be easily dissolved by rainwater that seeps into the ground, thus creating cavities and caverns. The development of secondary porosity caused by karst dissolution processes creates a highly heterogeneous aquifer system (Back and Hanshaw, 1970; Lane, 1986; Tihansky and Knochenmus, 2001). Zones of enhanced porosity within these carbonate rocks support high productivity of the principal aquifer in Florida, the Floridan Aquifer (discussed later in this chapter).

The west-central, barrier island coastline of Florida includes two large estuarine systems: Tampa Bay and Charlotte Harbor. The coastline is dominated by siliciclastic sediments and its adjacent inner continental shelf lies at the center of an ancient carbonate platform that started forming during the Jurassic (~150 Ma) (Table 1). Unconsolidated carbonate and siliciclastic sediments represent a thin veneer overlying an irregular base of Miocene limestone bedrock (Arcadia Formation; Hawthorne Formation; Hine et al., 2003). Most of this sediment in the inner shelf represents "reworked Plio-Pleistocene, high-stand quartz sand deposits admixed with sand- to gravel-sized, skeletal carbonate debris, and some reworked Tertiary limestone." (Hine et al., 2003).

Table 1. Geologic and hydrologic characteristics near Forty Mile Bend located approximately 135 km SE of MHSS. Adapted from Kohout (1967).

SYSTEM	SERIES	FORMATION			LITHOLOGY	HYDROLOGIC CHARACTER
		Name	Top (ft.)	Thickness (ft.)		
Quaternary	Pleistocene	Pleistocene and Pliocene deposits	0	20	Shelly Limestone	Water-table aquifer
Tertiary	Miocene	Tamiami Formation	20	180	Marl, clay, sand and limestone	Confining bed, low permeability
		Hawthorn Formation	200	400	Green clay, marl, and sand	Confining bed, low permeability
		Tampa Limestone	600	250	Sandy limestone	Confining bed, fairly low permeability. Wells may flow small amount owing to upward leakage from underlying formations
	Oligocene	Suwanee Limestone	850	350	Limestone	Fairly low permeability; wells usually flow owing to upward leakage from underlying formations
	Eocene	Ocala Limestone	1,200	100	White limestone	*Florida Aquifer* Known as "zone of lost circulation" in the oil industry. Oil-well drillers' comments frequently are as follows: 1,200 ft- "Fresh-water flow" or "lost circulation" 1,900 ft- "Lost circulation" 2,300 ft- "Boulders" 2,700 ft- "Strong salt-water Flow"
		Avon Park Limestone	1,300	500	Chalky limestone	
		Lake City Limestone	1,800	250 *	Tan dolomitic limestone, cavernous	
		Oldsmar Limestone	2,050	1,250 *	Limestone with brown dolomite developed adjacent to large caverns	
	Paleocene	Cedar Keys Limestone	3,300	1,950 *	Dolomite and anhydrite	The "first anhydrite" near top of Cedar Keys Limestone (about 3,300 ft) is the base of the Floridan Aquifer
Cretaceous	Upper Cretaceous	Lawson Limestone	5,250	150 †	Porous Limestone	
		Unnamed Deposits	5,400	2,300 †	White chalk and slate	Lost circulation frequently reported at 8,500 to 9,00 ft. Solution holes 1-inch in diameter at 11,400 ft. in reef-like formation at Forty Mile Bend.
		Atkinson Formation	7,700	100 †	Silty limestone and shale	
	Lower Cretaceous	Undifferentiated Units	7,800	4,000 †	Limestone, anhydrite, dolomite and shale. Sunniland pay zone	
				11,800	Deepest well at Forty Mile Bend.	

*Applin and Applin, 1944, Figure 22.
† Banks, Joseph E., 1960, p. 1739.

Florida Platform (Plateau) and Floridan Aquifer

The Florida Platform extends southward from the North American continent and separates the Atlantic Ocean from the Gulf of Mexico (Stringfield and LeGrand, 1969; Rosenau et al., 1977; Randazzo and Jones, 1997). The emergent part, the state of Florida, occupies only half of the larger portion of the Platform and is offset to the east of its axis (Figure 1). The Florida Platform is a sequence of porous permeable limestone and dolomite strata several thousand meters thick. Sea-level fluctuations played a primary role in the distribution of sediments. The broad, low-lying structure of the Platform is covered by a blanket of sediments ranging in age from Miocene to Holocene. There are valuable natural resources contained within this blanket of sediment, which range from very thin (less than a meter) to thicknesses exceeding 300 meters. They include limestone, phosphorite, heavy minerals, clays, and shell deposits. The western side of the Florida Platform extends approximately 321 km from the coastline into the Gulf of Mexico and is an extension of the limestone karst surface of the Florida peninsula. The western shelf is relatively smooth, but terraced with small mounds and ridges located near the 55-m isobath that were interpreted by Gould and Steward (1955) to be reefs formed during the Pleistocene when sea level was lower.

The Floridan Aquifer is one of the world's largest aquifers and is extensively used for drinking water. A thick sequence of carbonate rocks (limestone and dolomite) of Tertiary age comprises the Floridan aquifer system. This system is defined based on its permeability. The thick rock layers within the aquifer system vary in permeability. Therefore, in most places the system is divided into the Upper and Lower Floridan aquifers, separated by a less permeable confining unit (Figure 2). The confining unit

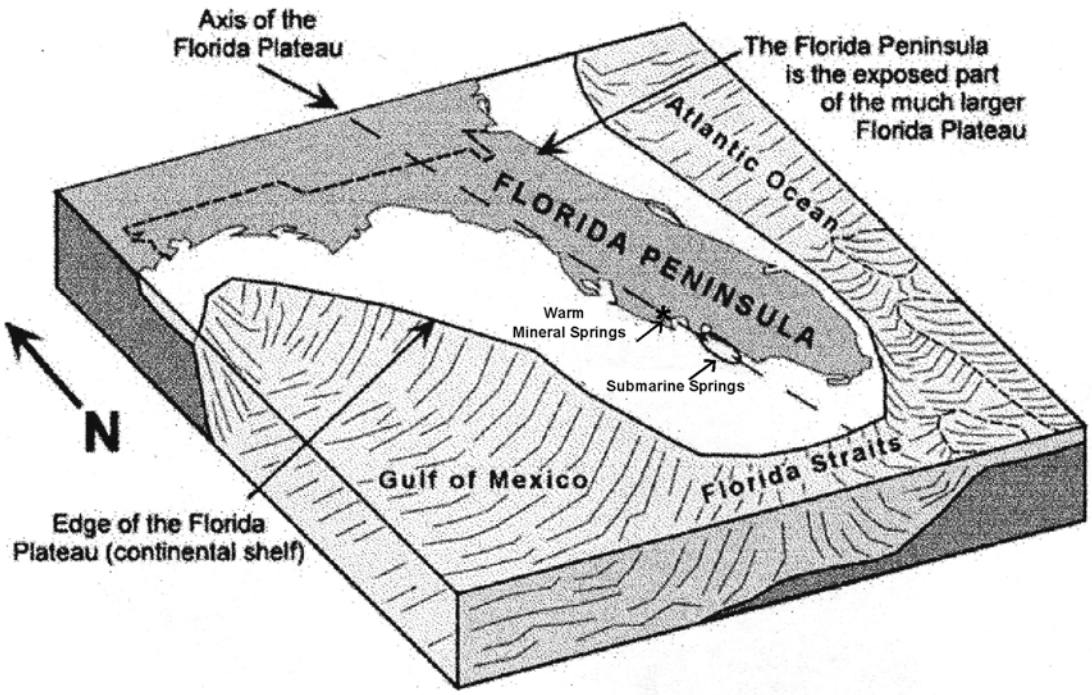

Figure 1. Schematic topographical map of Florida Plateau. Exposed parts (gray) from the Florida Peninsula while submerged parts (white) form the continental shelf. Light gray, hatched area are the abyssal plains of the Gulf of Mexico and Atlantic Ocean connected by the Florida Straits. Saline geothermal springs are found along the axis of the Florida Plateau, approximately indicated by the long-dashed line. Warm Mineral Springs (asterisk) is located on land, north of where the axis intersects the Florida coast. The area of submarine springs is circled with an ellipse. The short dashed line is the Florida state border. Figure modified from Schijf and Byrne (2007).

separating the Upper and Lower Floridan is informally called the middle confining unit (or semi-confining unit where it allows water to leak through more easily). The depth of the middle confining unit varies at different locations and consists of different rock types. The rocks are principally limestone and dolomite. Most of the aquifer water flow takes place where it is unconfined or where the upper confining unit is thin. Within the Lower Floridan aquifer is a deeply buried cavernous zone termed the 'boulder zone'. The boulder zone of southern Florida contains saltwater and lays 500-2,500 m below sea level. It consists of limestone and dolomitic limestone of Eocene age. It is overlain by low permeable Oligocene and Miocene limestone sands, and it overlies an impermeable layer of Paleocene anhydrite (Kohout, 1965, 1967; Henry and Kohout, 1972). Kohout et al. (1965, 1967) proposed that the occurrence of geothermal springs is a result of the highly permeable "boulder zone" of the Floridan Aquifer.

Interfaces of Floridan Aquifer and Submarine vents: Kohout Circulation Theory

The geothermal heating of the Floridan Aquifer was investigated by Kohout (1965, 1967). He hypothesized that a continuous flow of sea water from the Florida Straits enters the deep part of the aquifer, becomes mixed and diluted with freshwater, and flows upward and seaward through the upper part of the aquifer (Figures 3 and 4). Figure 5, a temperature-depth profile, shows a slight temperature increase from 24^{o} C (77^{o} F) to 26^{o} C (79^{o} F) at 304 meters below mean sea level (1,000 feet), as one moves below the confining beds and into the Floridan Aquifer System until a depth of 487 m (~1600 feet). Below the depth of 487 m (~1600 feet) meters the temperature decreases to

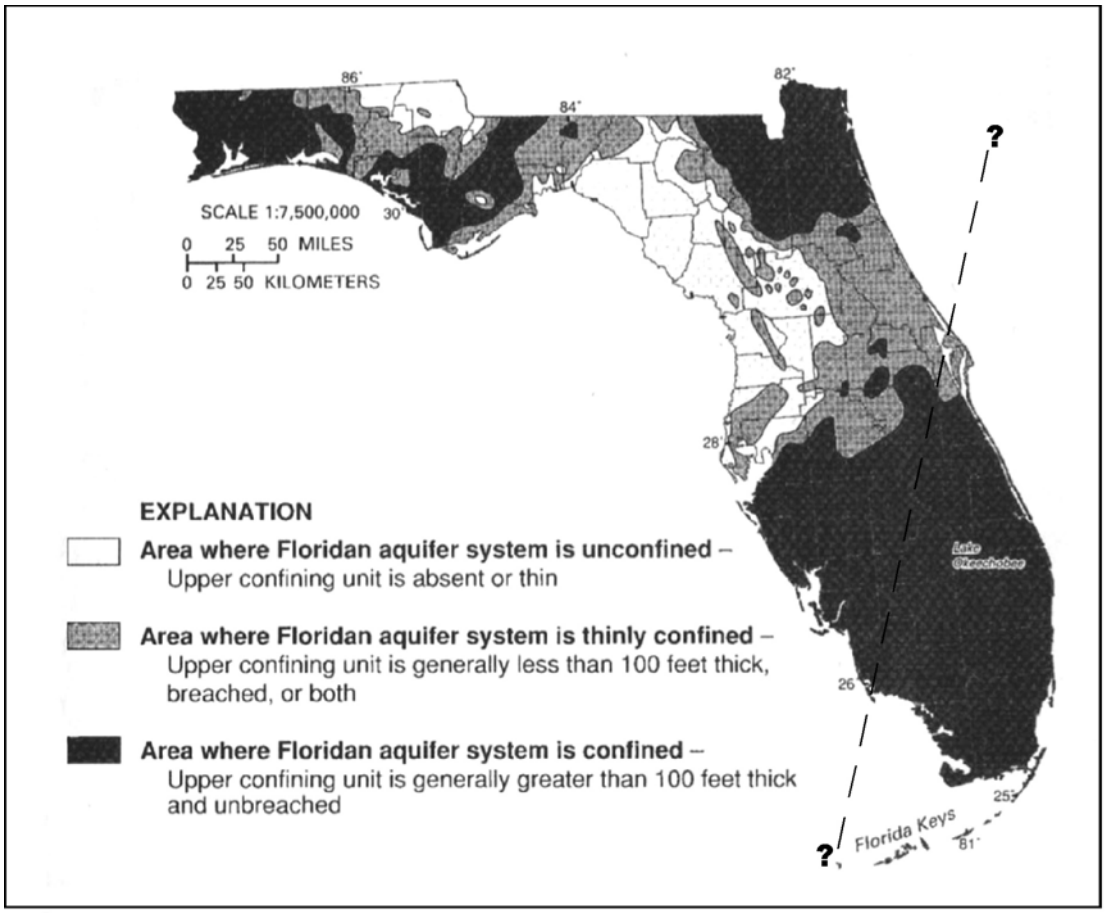

Figure 2. Thickness of the upper confining unit of Floridan aquifer system (Miller, 1986). Modified from Randazzo and Jones (1997). Dashed line marks the southeastern extent of known land and submarine springs (see Figure 6A and 6B).

23° C (74° F) until 944 meters (~3,100 feet). From the top of the anhydrite layer, at 1,000 meters (~3,280 feet), the temperature increases smoothly from 24° C (~76° F) to 113° C (~236° F) at 3,505 meters (~11,500 feet) following the observed geothermal gradient.

Kohout (1965, 1967) postulated that the direction of the penetration of seawater is from the east, the west, and perhaps the south (Figure 6). He also proposed that the semi-permeable anhydrite layer acts as a hot plate, warming the cool seawater as it becomes entrained in the boulder zone (Figure 4). The seawater is then geothermally heated by 5-10° C to almost 40° C as the seawater moves upward through the aquifer. It discharges through the upper part of the aquifer either by upward leakage through confining beds into the shallow aquifer, or through submarine low-temperature springs and seeps on the continental shelf and slope (Kohout, 1965).

The rate of flow at submarine vents can further be regulated by the piezometric pressure (Stringfield, 1936; Kohout, 1965; Kohout, 1977; Rosenau et al., 1977) which can vary from the rising and falling of sea level due to tidal cycles (Fanning et al., 1981). Piezometric pressure (potentiometric surface) is defined as the level to which the water in the upper part of the aquifer (artesian aquifer) would rise if unaffected by friction with the surrounding rocks and sediments. A potentiometric surface is an imaginary surface representing the total pressure head of groundwater and can be depicted on a map by a series of contours of equal water level (Figure 7). Water in the aquifer moves from high to low points on the potentiometric surface and the natural direction is perpendicular to the contours on the potentiometric surface (Stringfield, 1936; Stringfield et al., 1941). The highs are generally considered recharge areas and the lows are discharge areas. Recharge occurs in the peninsular inland areas of Florida whereas discharge generally

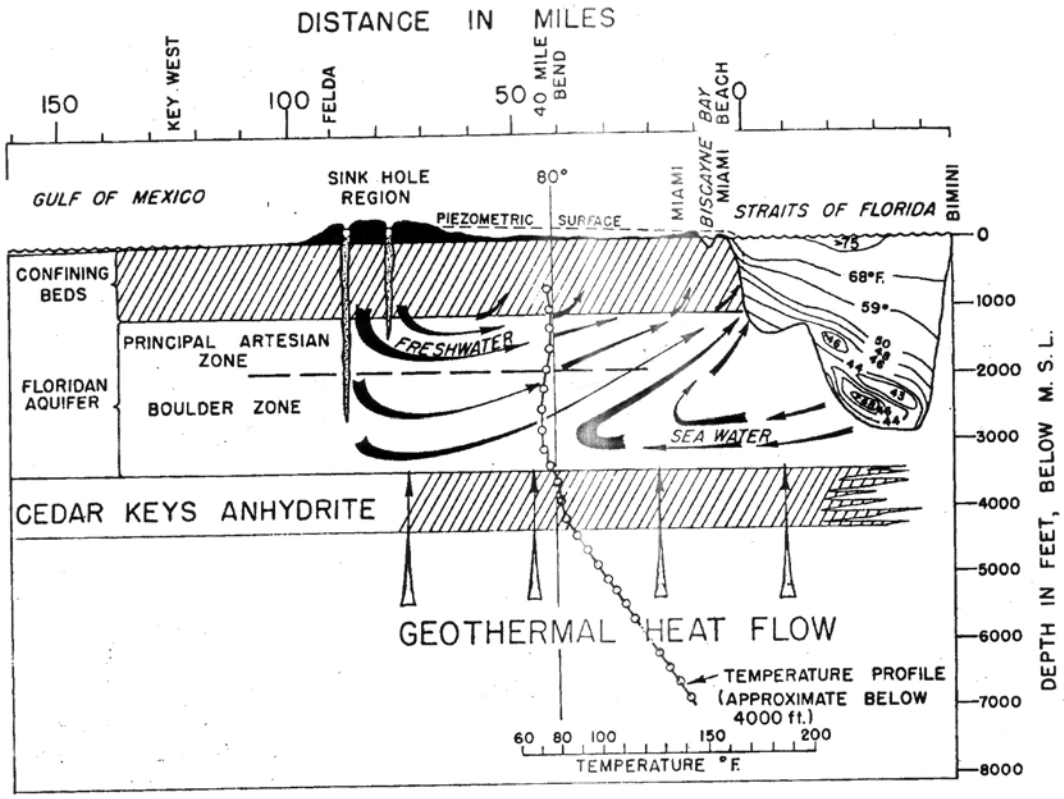

Figure 3. Idealized section through Miami showing concept of cyclic flow of sea water induced by geothermal heating. Figure from Kohout (1965).

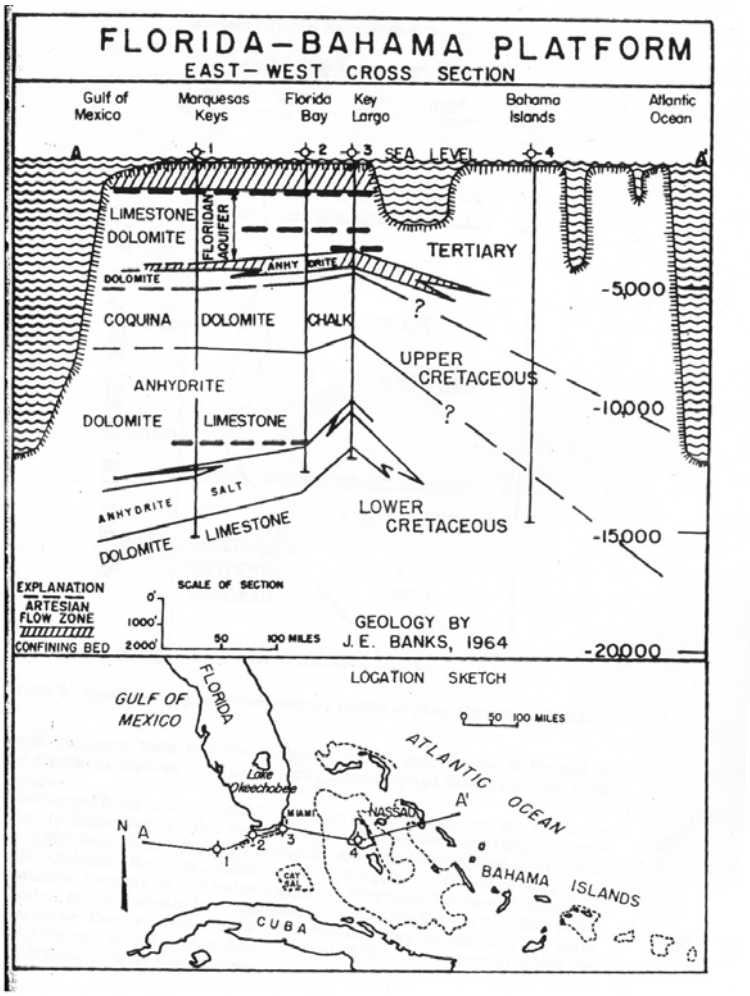

Figure 4. West-east geologic section through southern Florida from the Gulf of Mexico to the Atlantic Ocean. Figure from Kohout (1965).

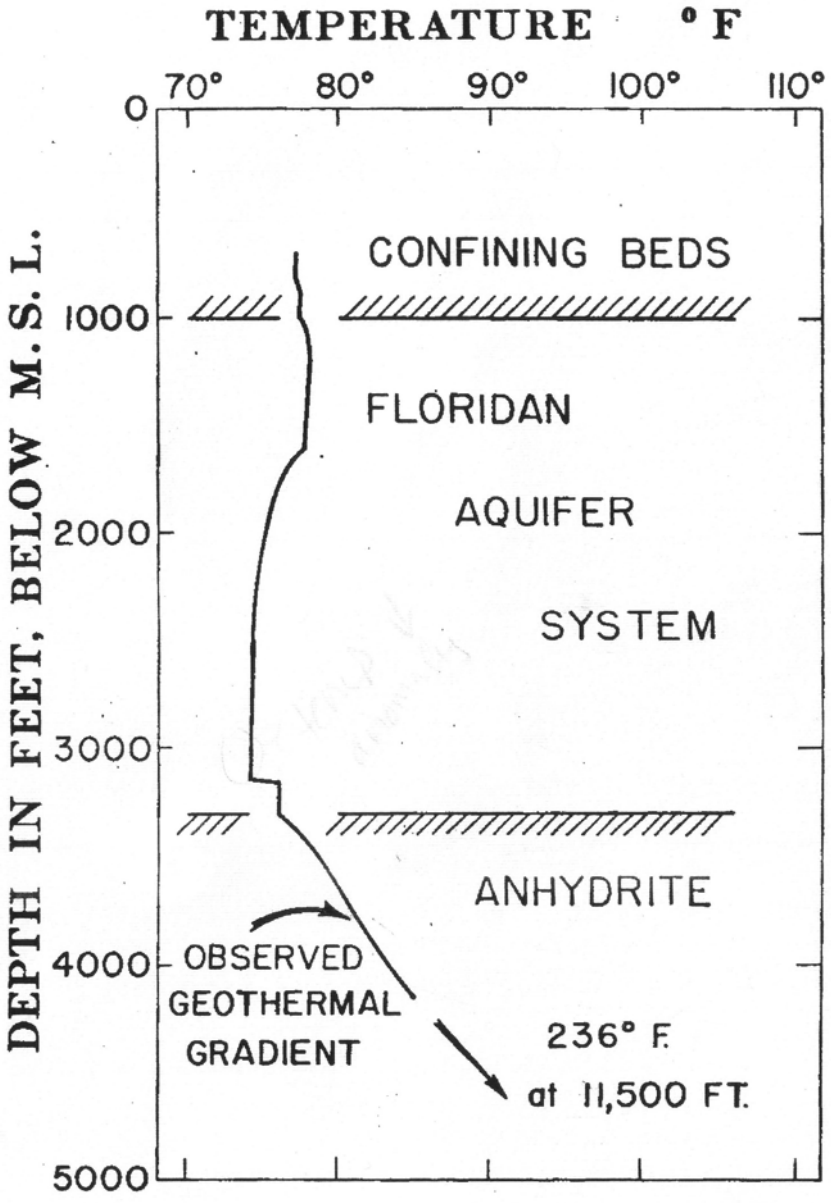

Figure 5. Graph showing temperature-depth profile at Forty Mile Bend, Florida. Figure from Kohout (1965).

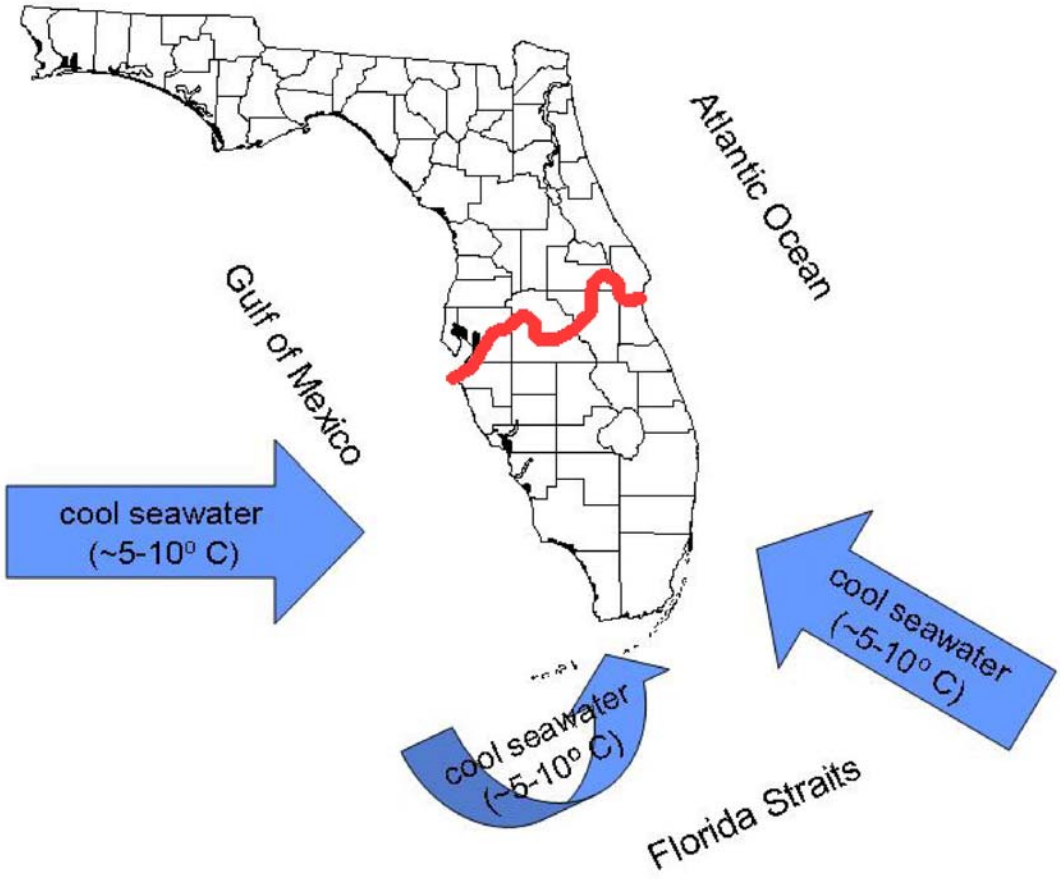

Figure 6. Simple illustration of Kohout (1965) circulation theory. Cool seawater from 500-1,000 m deep around the platform penetrates the permeable zone from the east (Atlantic Ocean), west (Gulf of Mexico) and perhaps the south (Florida Straits). The seawater is initially 5-10^{o} C and becomes geothermally heated to almost 40^{o} C as it percolates toward the interior of the platform. The red line marks the northern boundary of where the southern Floridan aquifer system is confined (see Figure 2). North of the red line most known land and submarine springs occur. Southwest (towards the coast) more submarine springs occur than land springs. The short black lines are the boundaries of the counties within Florida.

occurs in the coastal areas. Kohout (1965) states that in southern Florida the piezometric surface may be as much as 40 feet above land surface where a fresh-or brackish-water flow is usually encountered between 1,000 to 1,300 feet below sea level. As shown in Figure 7, areas of low piezometric pressure are located towards the coast with the occurrence of both major (flow of 100 cfs or more) and large springs (flow less than 100 cfs). The location of the confining units of the Floridan aquifer system and the piezometric lows may be good indicators of where land and submarine springs may exist (Rosenau, 1977).

Land Springs

There are 27 known first-magnitude Florida springs located on land (Figure 8 and Table 2). Tables 2 and 3 show that four first-magnitude springs are found in Wakulla County, three are found in Citrus and Marion Counties, and at least one spring is found in each of the remaining counties located in the panhandle, central, and southwest Florida. Several second or third magnitude springs (Table 2 and Figure 8) are also generally located in the panhandle and central Florida where carbonate rocks are at or near the land surface. The dashed lines in Figures 8 and 9 are old and new spatial correlations that are discussed in Chapter 5. Sixteen offshore submarine springs known to exist along the coasts of Florida (Figure 9) are discussed next.

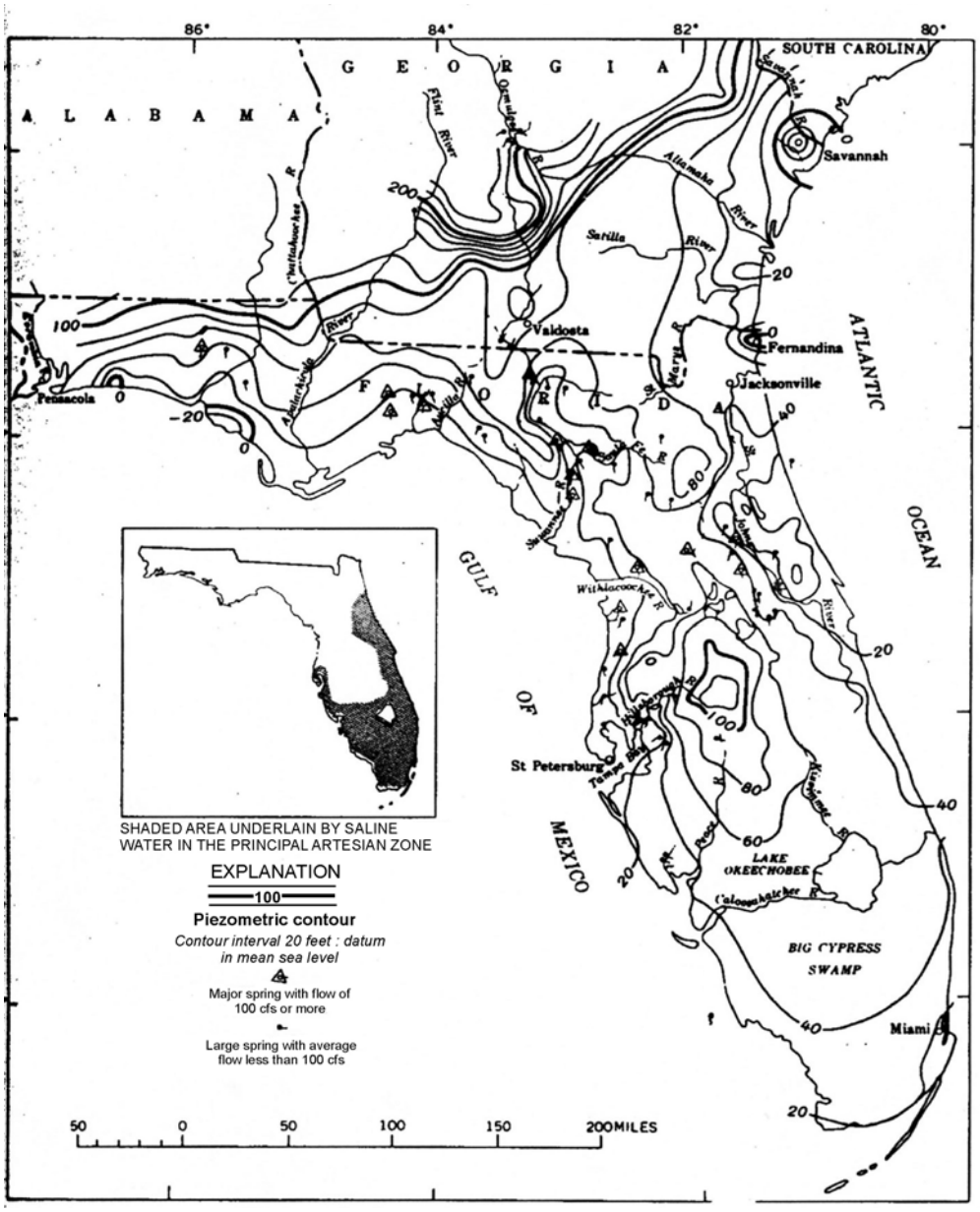

Figure 7. Map showing the piezometric surface of the Principal Artesian Zone (upper aquifer) as of 1960. After Stringfield (1964, p. C166), based on maps of Healy (1962), Stewart and Counts (1958), and Stewart and Croft (1960). Modified from Kohout (1965).

Table 2. Summary of discharge and water quality data collected at Florida's 27 first magnitude springs. [Map number refers to Figure 8 and Table 3]. Values show average flow (ft^3/s, cubic feet per second), (specific conductance µS/cm, microciemens per centimeter at 25 degrees Celsius), and concentrations mg/L, milligrams per liter]. Modified from Spechler and Schiffer (1995).

Map Number	Name	County	Average Discharge (ft^3/s)	Specific conductance (µS/cm)	Chloride (mg/L)	Sulfate (mg/L)
1	Spring Creek Springs	Wakulla	2,000	4,300	1,200	280
2	Crystal River Springs	Citrus	878	4,300	1,400	200
3	Silver Springs	Marion	799	410	9.5	42
4	Rainbow Springs	Marion	711	140	3.5	5.5
5	Alapaha Rise	Hamilton	608	230	6.8	21
6	St. Marks Spring	Leon	517	260	5.7	8.7
7	Wakulla Springs	Wakulla	391	270	5.8	10
8	Wacissa Springs	Jefferson	388	270	5.3	5.4
9	Ichetucknee Springs	Columbia	360	300	5.3	9.4
10	Holton Spring	Hamilton	243	230	11	25
11	Homosassa Springs	Citrus	192	2,700	780	110
12	Blue Spring	Jackson	189	210	2.6	0.3
13	Manatee Spring	Levy	178	410	5.9	24
14	Weeki Wachee Springs	Hernando	174	280	6.3	7.5
15	River Sink Spring	Wakulla	164	190	7.8	12
16	Gainer Springs	Bay	159	120	2.4	0.6
17	Blue Spring	Volusia	158	1,700	420	53
18	Troy Spring	Lafayette	152	330	4.1	8.0
19	Kini Springs	Wakulla	150	200	7.9	13
20	Hornsby Spring	Alachua	148	400	12	53
21	Falmouth Spring	Suwannee	145	340	4.2	9.7
22	Chassahowitza Springs	Citrus	139	520	78	16
23	Fannin Springs	Levy	113	360	4.9	11
24	Natural Bridge Spring	Leon	109	250	5.5	7.3
25	Blue Spring	Madison	106	270	4.4	12
26	Silver Glen Springs	Marion	106	2,000	460	180
27	Alexander Springs	Lake	102	1,100	230	59

Table 3. Classification system for springs according to average discharge (ft^3/s, cubic feet per second; Mgal/d, million gallons per day]. Modified from Spechler and Schiffer (1995).

Magnitude	Average Flow
1	100 ft^3/s or more (65 Mgal/d)
2	10-100 ft^3/s (6.5-65 Mgal/d)
3	1-10 ft^3/s (0.65-6.5 Mgal/d)
4-8	Less than 1 ft^3/s (0.65 Mgal/d)

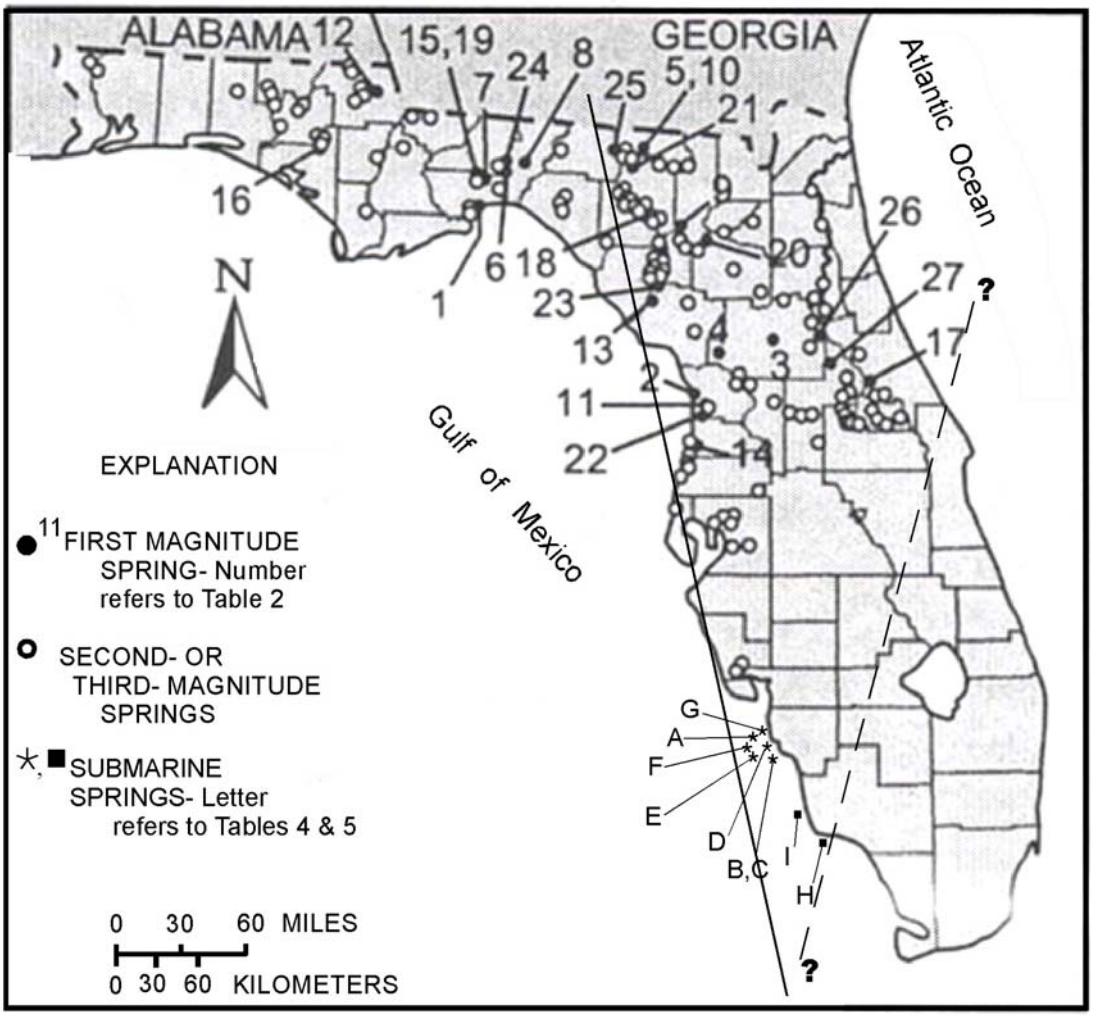

Figure 8. The open and filled circles are the location of selected land springs in Florida. The black asterisks represent the locations of the submarine springs in the MHSS study area during the March 2001 cruise. The black squares represent the verified submarine springs of the April 2002 cruise. Letters A, B, C, D, E, F, G, H, and I are discussed in Tables 6 and 7. The dashed line represents a possible boundary of all known spring locations. Northwest of the boundary line land springs are prevalent throughout Florida, however, southeast of the boundary no springs are observed. Long black solid line represents the approximate location of the axis of the Florida Platform. Long dashed line roughly coincides with the confined southern Floridan Aquifer (see Figure 2). Modified from Spechler and Schiffer (1995).

Submarine Springs

Previous studies of other submarine springs

The term “submarine spring” identifies a spring that discharges below sea level in a coastal salt-water environment (Rosenau, 1977; Wilcove, 1975). Sixteen Florida springs listed as offshore or submarine springs have been documented (Figure 9). All of the springs occur near the shoreline, but this may be a result of their accessibility. Eight submarine springs are located off the coast of the panhandle, five are located off the central (Tampa Bay) coast, two off the north-eastern coast, and only one off the southwestern coast (Fort Myers) (Figure 9). The discharges are usually fresh to brackish water (Hunn and Cherry, 1969; Rosenau, 1977; Donoghue et al., 1995). During certain tidal stages submarine springs occasionally produce a “boil” or “slick” on the surface of the water. The MHSS study area seems to be the only documented area off the west coast of Florida where certain “hot spots” or active venting appear to remain fairly constant through the years (Kohout, 1965, 1967; Breland, 1980; Fanning et al., 1981; Naar and Byrne 2001; Byrne and Naar, 2002).

Mudhole Submarine Spring (MHSS) and the Study Area

Mudhole Submarine Spring: Previous Data

The earliest known reference in the literature to Mudhole Submarine Spring is by Brooks (1961), who mentions the ‘Mud Boil’ only in passing, stating that the ‘rising water contains considerable amounts of suspended sediment and the odor of hydrogen sulfide is prevalent in the vicinity’. The Mudhole Submarine Spring (MHSS) is located approximately 11 miles offshore from Fort Myers Florida (Figures 10 and 11). Reports

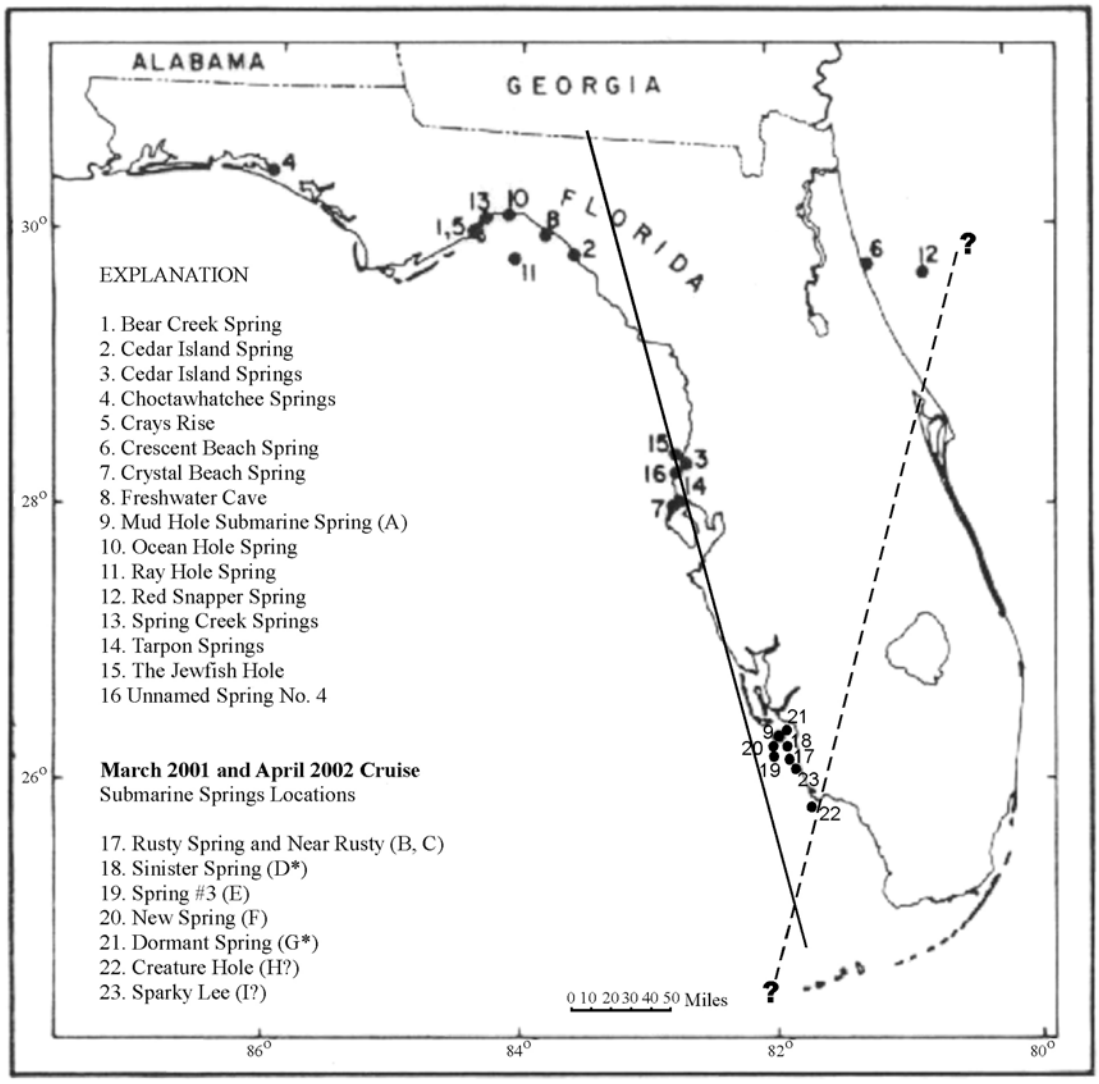

Figure 9. Submarine Springs of Florida. Source: Springs of Florida, Florida Geological Survey Geological Bulletin No 31. Long solid line represents the approximate location of the axis of the Florida Platform. Long dashed line roughly coincides with the confined southern Floridan Aquifer (see Figures 2,8 and Tables 6, 7).

from fisherman and others led to the naming of this spring due to highly turbid plumes sometimes observed in overlying waters. Numerous studies of MHSS have been conducted to locate the origin of the vent effluent, to measure the temperature of the vent fluids, and to analyze the fluid chemistry (Brooks, 1961; Kohout, 1965; Kohout, 1967; Breland, 1980; Fanning et al., 1981). The discharge temperature at several prominent orifices within the MHSS depression (Figure 12) exhibited a temperature of 35^{o} C (95^{o} F). Temperatures were measured using a human fever Fahrenheit thermometer (Kohout, 1967). Kohout (1965) proposed that the origin of the MHSS effluent is from inland movement of the cold seawater from the Florida Straits through the cavernous sections of the Florida Aquifer. Chemical analyses (Fanning et al., 1981; Breland, 1980) corroborate that the vent effluent is closely related to seawater, and is modified as it percolates through the Florida Platform.

Breland (1980) conducted several studies of MHSS during six research cruises between 1977-1979. He described the physical and chemical characteristics of the spring, and measured temperatures and relative effluent fluxes from the spring. Using side-scan sonar and SCUBA diver observations Breland (1980) concludes:

"The bottom surrounding is generally flat and sandy, and very few hard substrates in the surrounding area. The spring itself is a conical depression of ~100 meters across at the top sloping down on the floor area roughly 25 meters across… Crevices are present in the sandy bottom next to the lip of the rocky depression. A final drop of 1-2 meters occurs abruptly across a rock ledge ringing the deepest part of the depression… Shell debris and coarse material cover most of the floor, with exposed rock in several places" (Figure 11).

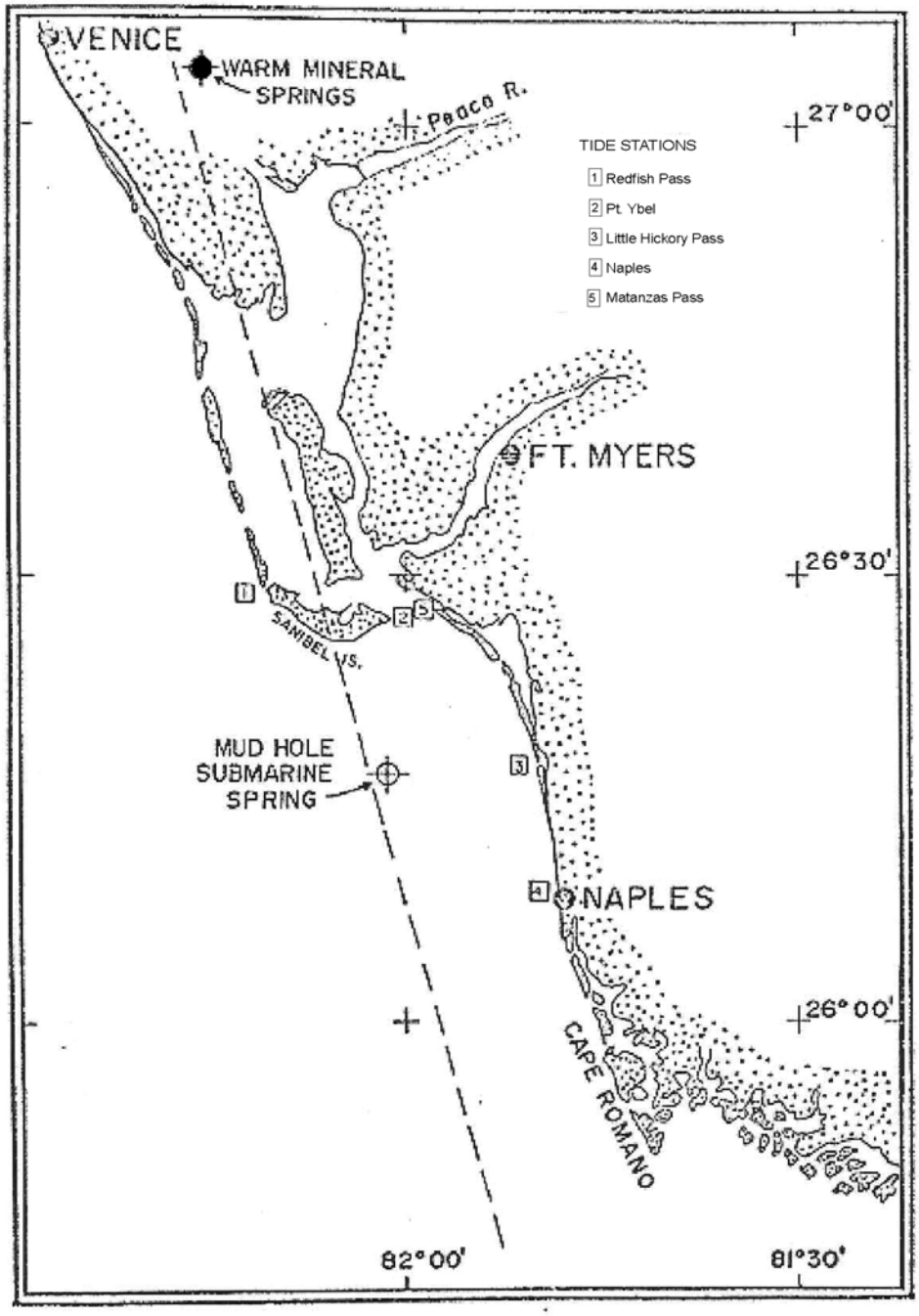

Figure 10. The lower southwest coast of Florida showing location of tide gauging stations. Dashed line approximates the axis of the Florida Platform and the trend line of hydrothermal vents proposed by Breland (1980). Modified from Breland (1980).

Figure 11A. and B. Right (A): Merged illustration of Naar 2001-2002 cruise track lines shown in red and Breland 1980 figure of the lower southwest coast of Florida showing location of tide stations (refer to Figure 10). Small blue dots denote the Mud Hole Submarine Springs study area. H and I represent two vent sites verified during this study. Bottom (B): 2001 MHSS study area 3D shaded relief mean depth, interpolated image. Minimum depth of 0.5 meters and a maximum depth of 20.8 meters. Image shown with aggressive surface editing, although some north-south track parallel "striping" still occurs due to tide and sound velocity uncertainties. Letters A, B, C, D, E, F, and G denotes the locations of all the vents found to date, except H and I which are found outside this survey. Refer to Table 4. Note: Figure 11A is modified from Figure 10 and Figure 11B is enlarged later in Figures 15.

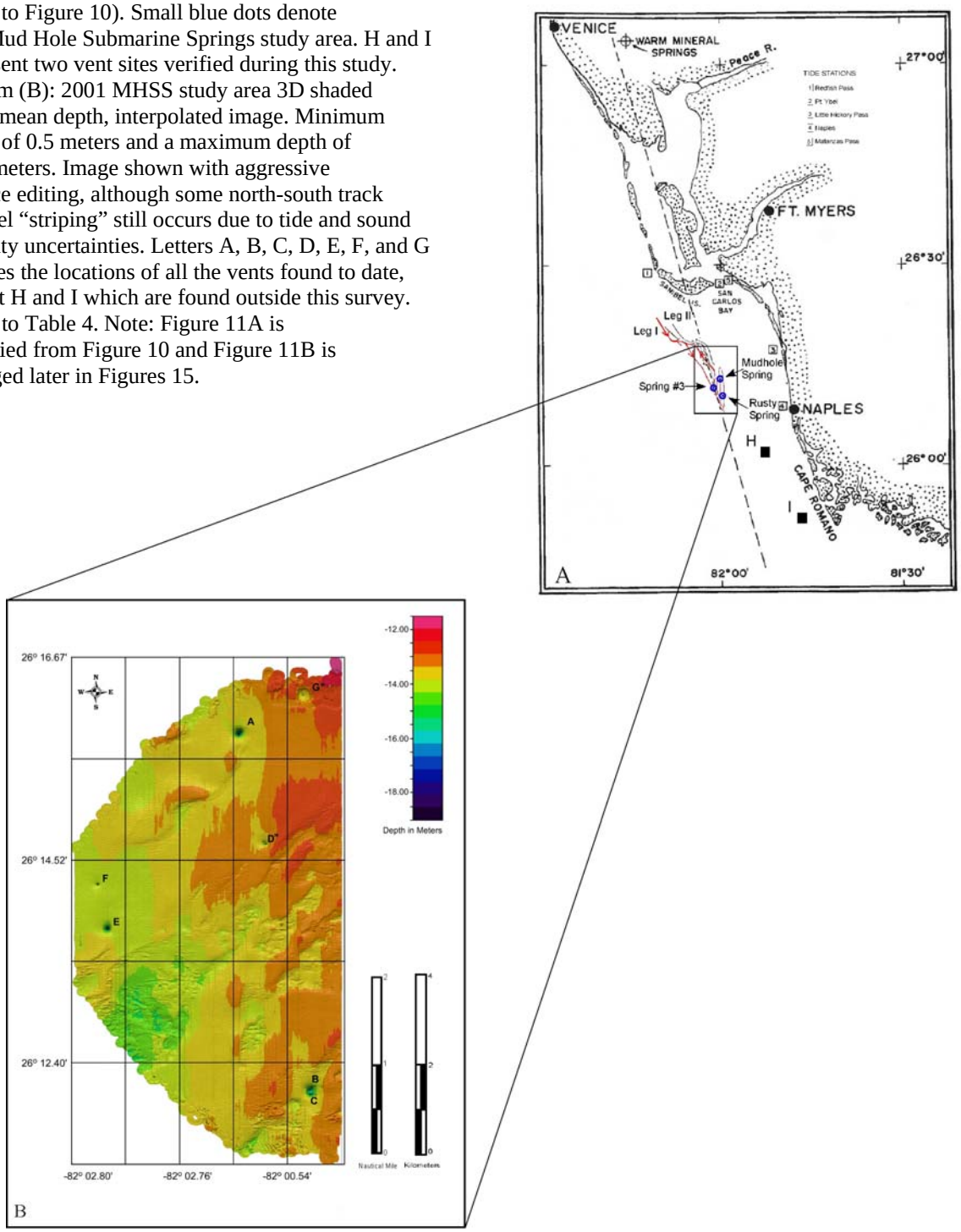

There also appeared to be several vents within the depression, and discharges in various places on the depression floor (Figures 12 and 13). Through SCUBA diver observations it was concluded that the rate of underlying flow or seepage controls the sediment type of a particular area. Strong flows from the major vents are associated with exposed limestone while, in “seepage areas”, warm water gradually rises from coarse shell and rubble debris-bottom. There were also other warm water seepages that exhibited very slow upward water movement detected beneath the sediment-water interface. These areas were often underlain by silt or fine sand. In June 12-17, 1979, SCUBA divers observed ~0.3 m of the bottom had been scoured away around the large central rock in MHSS (Breland, 1980). Such evidence suggests that the geomorphology of the bottom depression may change over periods of several months, particularly between March and June.

Fanning et al. (1981) described four techniques used to find the springs. These include: use of sonar depth profiling, observation of turbid plumes in overlying waters, use of side-scan sonar, and observation of large sea turtles. Positive identification of heated effluent was obtained by SCUBA divers with hand-held thermometers, or when conditions were risky and visibility low, probe temperatures were lowered from the surface to the bottom. After seven survey cruises between December 1977 and March 1980, six depressions were found which contained either warmed sea water, vents discharging heated effluent, or both (Table 4). Fanning et al. (1981) focused on the following key issues when investigating the MHSS study area: (1) whether or not MHSS is an isolated spring; (2) the chemical composition of effluent currently discharging from

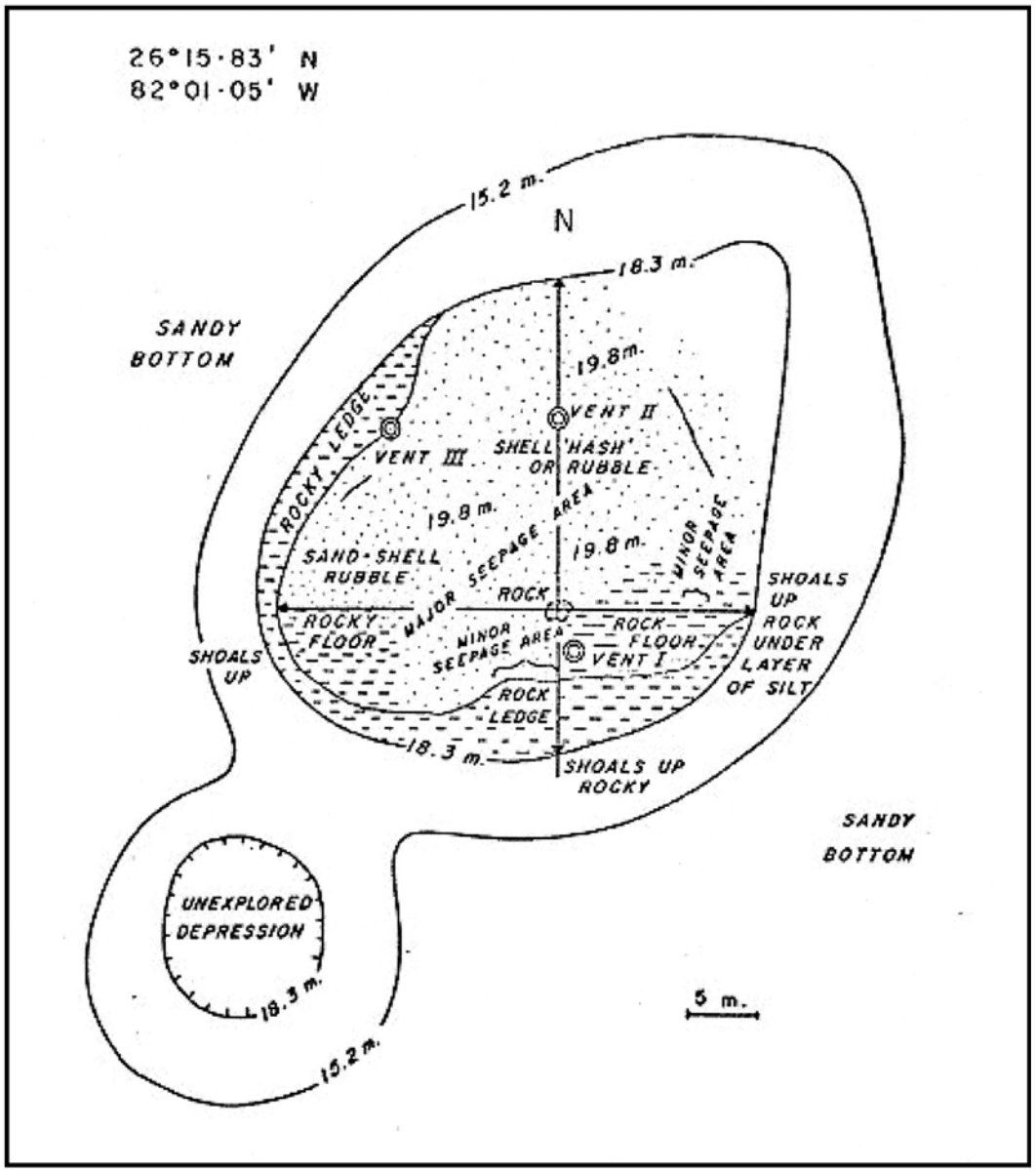

Figure 12. Mud Hole Submarine Spring Depression. Modified from Breland (1980).

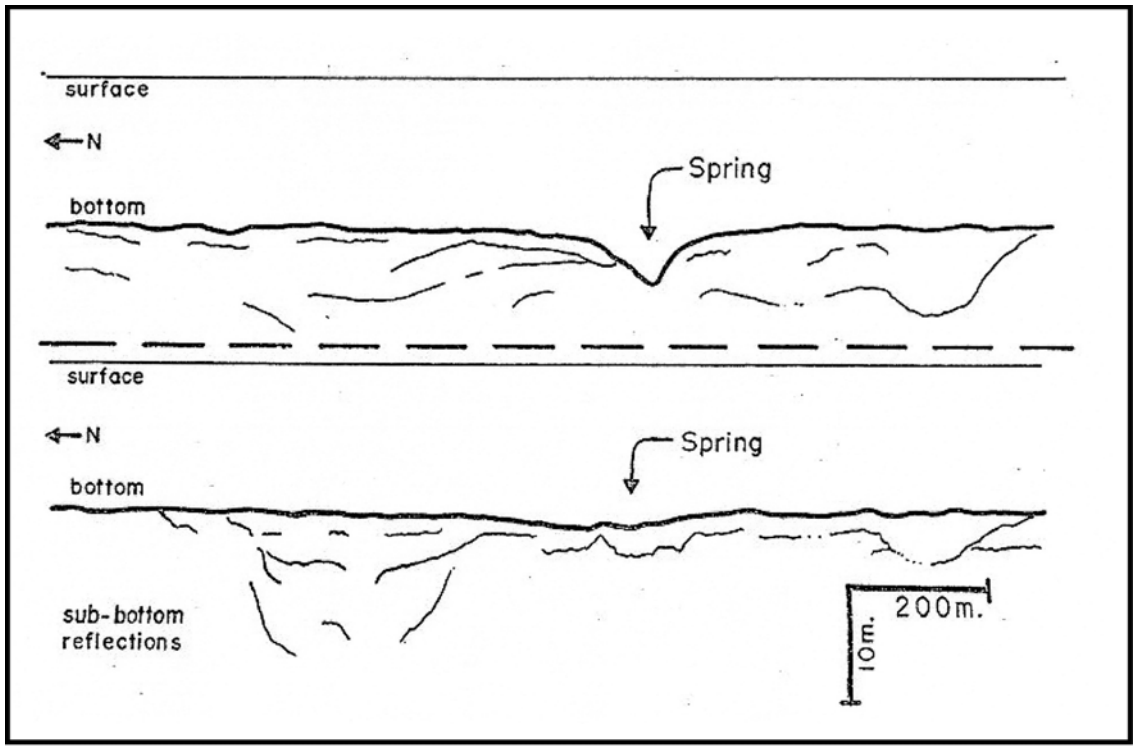

Figure 13. Two representative sub-bottom seismic traces from the MHSS. Modified from Breland (1980).

the spring; and (3) if the vent discharge experienced any changes during its passage through Florida Platform as proposed by the Kohout (1965) model. The stream velocity monitored from the MHSS vent showed a regular variation from a high of 30 cm/s at 3 hour elapsed time to a low of 26 cm/s at 8.5 hours (Fanning et al., 1981). The average discharge rate for MHSS over a nine-hour period was calculated to be 25 l/s. The flow velocity (linear flow rate) appeared to correlate with the tide records from a nearby tide station (Fanning et al., 1981). High flow rates of MHSS correlated with the local low tide and low flow rates correlated with the local high tide (Fanning et al., 1981).

The chemical properties of the effluent were very similar to the surrounding seawater (Table 5). According to Table 5 the salinity of MHSS, spring III, and spring V ranged from ~34.93 to 35.07‰, which is closely related to the shelf water salinity (~35.5‰) and deep Gulf water (500-1000 m) salinity (~35.2‰). This indicates that the fluid discharging from the spring vents is seawater (Fanning et al., 1981). However, the calcium and magnesium concentrations of the spring effluent (major ions in solution) showed substantial differences. Fanning et al. (1981) stated that, at a chlorinity of 19.3‰, sea water from MHSS had 35% more calcium and 5% less magnesium per kilogram than normal seawater with the same chlorinity. The most preferable explanation for the calcium and magnesium variations was the process of dolomitization (Fanning et al., 1981). Specifically, as the seawater percolated through the highly porous zone at 500-1000 m depth in the aquifer, magnesium was exchanged for calcium within the aquifer limestone while dolomitization took place (Fanning et al., 1981).

Table 4. Physical features of thermal springs in the area of springs off the west Florida coast. The areas refer to the depressions and the depths refer to the maximum distance from the shelf floor to depression floor. Modified from Fanning et al. (1981).

Spring Designation	Number of Visits	Position	Effluent temperature (°C)	Comments
MHSS (I)	6	26° 15.83' N, 82° 01.05'W	35.7	Turbid surface plume Area: 1000 m^2 Depth: 7 m
Steward (II) Spring (SS)	1	26° 12.50'N, 82° 57.92'W	--	Turbid surface plume Bottom water 5° C warmer than in depression Depth: 3 m
III	3	26° 13.57'N, 82° 02.43'W	34.5	Area: 35 m^2 Depth: 9 m
IV	1	26° 14.50' N, 82° 00.81'W	33.9	Depth: 2 m
V	3	26° 11.88'N, 82° 00.29'W	34.4	Area: 10,000 m^2 Depth: 3 m
VI	1	26° 16.03'N, 82° 00.39'W	--	Divers found warm turbid water in depression Depth: 2 m

Table 5. Composition of heated submarine springs on the West Florida shelf and adjacent ocean waters. The reliability of the values is shown by standard deviation of the analytical method or of replicates from samples of the same water, whichever is larger. Each spring had one sample with oxygen concentrations greater than 100 micromole/kg; those samples were excluded due to contamination with oxygen. Modified from Fanning et al. (1981).

Parameter	Type of water sampled				
	MHSS	spring III	spring V	shelf water	deep Gulf water (500–1000 m)
Salinity (‰)	34.932 ± 0.020	34.965 ± 0.020	35.074 ± 0.020	35.5–35.8 [c]	34.9–35.2 [d]
Chlorinity (‰)	19.33 ± 0.08	19.38 ± 0.08	19.45 ± 0.08	19.5 [a]–19.8 [c]	19.3–19.5 [a]
Salinity/chlorinity	1.807 ± 0.007	1.804 ± 0.007	1.803 ± 0.007	1.804 ± 0.007 [c]	1.80655 [a]
SiO_2 (μmole/kg)	92 ± 5	93 ± 1	79 ± 1	2–4 [c]	18–23 [b]
O_2 (μmole/kg)	14 ± 7	7 ± 2	8 ± 2	220–230 [c]	130–140 [b]
Alkalinity (meq/kg)	2.19 ± 0.04	–	–	2.41–2.45 [c]	–
pH (at 25°C)	7.36 ± 0.15	–	7.40 ± 0.02	8.26 ± 0.02 [c]	–
PO_4^{3-} (μmole/kg)	0.34 ± 0.15	0.28 ± 0.05	0.88 ± 0.05	0.0–0.3 [c]	1.6–1.9 [b]
NO_3^- (μmole/kg)	0.10 ± 0.09	0.05 ± 0.05	0.07 ± 0.05	0.2 [c]	25–40 [b]
NO_2^- (μmole/kg)	0.05 ± 0.06	0	0.09 ± 0.05	0–0.1 [c]	–
NH_3 (μmole/kg)	0.90 ± 0.22	1.2 ± 0.5	0.90 ± 0.5	0.1–0.3 [c]	–
H_2S (μmole/kg)	4.0 ± 0.9	–	–	0	0
Chlorinity ratio					
SO_4^{2-} [(mg/kg) (‰)$^{-1}$]	142 ± 1	–	–	140 [a]	140 [a]
boron	0.221 ± 0.003	–	0.224 ± 0.003	0.227–0.231 [c]	0.232 [a]
Na^+	554.0 ± 0.3	–	–	556 [a]	556 [a]
K^+	20.4 ± 0.05	–	–	20.6 [a]	20.6 [a]
Mg^{2+}	63.4 ± 0.3	–	–	66.8 [a]	66.8 [a]
Ca^{2+}	28.8 ± 0.2	–	–	21.3 [a]	21.3 [a]
F^-	0.066 ± 0.0002	–	–	0.0673 [a]	0.0673 [a]
Number of samples	9	1	2	4	–

[a] Calculated after Wilson [19].
[b] Used courtesy of D. Atwood and G. Berberian, Atlantic Oceanographic and Meteorological Laboratory, National Oceanic and Atmospheric Administration, Miami, Fla.
[c] Measured by the authors.
[d] Based on data of Nowlin and McLellan [20].

Chapter 3

METHODS

Data Acquisition

Study Area: MHSS Cruises

As part of the State University System Educational and Training Grant administered by the Florida Institute of Technology, Byrne and Naar (2001) and Byrne and Naar (2002) revisited the MHSS study area during March 2001 and April 2002 cruises (Figure 11) aboard the R/V Suncoaster. The vents were located within ~2 m accuracy during the multibeam surveys (Tables 6 and 7). Four "new" submarine vents were identified (Table 6) during March 2001. Mudhole Spring, Rusty Spring (#5), and Spring #3 had been previously identified by Fanning et al. (1981). These three active springs were also 'active' during the second cruise in April 2002, as confirmed by SCUBA divers. Three additional springs were confirmed to exist after locations were provided by local fishermen during the April 2002 cruise (Table 7). These three new springs are: Creature Hole, Sparky Lee, and New Spring. However, observations from SCUBA divers concluded Creature Hole appeared to be extinct at that time (Table 7), (Naar, 2001; Byrne and Naar, 2002). 'Extinct' springs are springs that are thought to have had warm effluent seepage at one time, but were inactive at the time of the cruise. Thus, the multibeam

Table 6. Compiled information of submarine spring area from Naar and Byrne research cruise Leg II of March 2001. A, B, C, D, E, F, and G denotes the location of the springs in the 3D shaded relief , mean depth, sun illumination, and backscatter figures.

Mudhole Cruise Summary 2001 – Leg II			
Spring Designation	**Position**	**Fanning et al. (1981) Designations**	**Comments**
Previously Known Sites:			
Mudhole Spring (A) "Active"	26° 15.837'N 82° 01.047'W	I	Approx. 15 m across one margin defined by ledge, center is a flat area of 62 ft depth. From center, seafloor gradually slopes up to the 48 ft depth of surrounding area. Many distinct areas with concentrated flow and innumerable small seep areas.
Rusty (B) "Active"	26 ° 12.060'N 82° 00.302'W	V	Max depth is 54 ft depth, found at small area adjacent to a ledge (approx. 4 m long and 1 m high). Approx. 3 areas under of just in front of ledge with strong flow of spring effluent, and many smaller "vents". Surrounding this ledge is large area over which very slow seeps can be found, depth of "seep field" is approx. 48 ft, and seems very flat to divers.
Recently Discovered Sites:			
Near Rusty (C) "Active"	26° 12.060'N 82° 00.250'W	--	While looking for Rusty Spring, divers located this area, marked by small cluster of rocks (1.5m^2) from which effluent was flowing.
Sinister Spring (D) "Inactive"	26° 14.688'N 82° 00.765'W	IV	On first attempt to locate this spring divers encountered a small "seep field" (approx. 3m^2). While no defined vents, significant amount of effluent seeping from shell hash lined area. Area was surrounded by flat line sand and divers did not find features (slopes) as seen on bathymetry map. Depth was 53 ft at the "seep field". On second attempt divers encountered a slope leading to a depression filled with sand, through sand were multiple small 6-8 inch active vents. Sand thickness was ~2'. Max depth was 53 ft. Divers also was able to locate the "seep field" originally found, and it was ~30 m due west. Active in 1981, but now inactive.
Spring #3 (E) "Active"	26 ° 13.793'N 82 ° 02.418'W	III	Very steep slope leading to a small center area (~2 m^2) where there is a definite source of spring effluent. Due to steep walls, sponge material collects and seems to act as a "diffuser" making a defined "vent" difficult to detect though seems to be significant flow. Depth of center is 72 ft.
New Spring (F) "Active"	26 ° 14.265'N 82 ° 00.385'W	--	Very similar to Spring #3 though it is shallower. It has a steep slope (from 48-58 ft) to a base covering of 3-4 m^2. Base is filled with sponge material and very fine sand. In some areas sand covered sponges so thickly it created a "false bottom". There is a 1 m long cement culvert pipe along with several cement filled crates that were clearly used as markers and may be reason for 2 m difference in depth found by divers and depth suggested in map.
Dormant Spring (G) "Inactive"	26° 16.245'N 82° 00.388'W	VI	Active in 1981, but now inactive.

Table 7. Confirmed location of known springs and newly discovered springs from Naar and Byrne cruise report 2002.

Mudhole Cruise Summary April 2002			
Spring Designation	Date	Location	Comments
Previously Known Sites:			
Rusty Spring (B) "Active"	11 April	26° 12.053'N 82° 00.275'W	Confirmed spring location from previous, 2 dives completed, samples collected. Highest iron concentrations.
New Spring (F) "Activity uncertain"	12 April	26° 14.378'N 82° 02.503'W	New location
Mudhole Spring (A) "Active"	12 April	26° 15.839'N 82° 01.047'W	Confirmed location from previous years, 2 dives completed, samples collected for data comparison.
Recently Discovered Sites:			
Creature Hole (not shown in 2001 MHSS images) "Inactive"	10 April	25° 44.531'N 81° 40.672'W	New location, lead from fisherman, 2 dives completed, appeared to be an extinct vent, no samples collected.
Sparky Lee (not shown in 2001 MHSS images) "Activity uncertain"	11 April	26° 12.913'N 81° 53.953'W	New location, lead from fisherman.
Sparky Lee (not shown in 2001 MHSS images) "Activity uncertain"	12 April	26° 12.895'N 81° 53.956'W	No Information

system discovered and/or confirmed seven previously unmapped and unsampled vent sites. Five of seven vents were active.

Geophysical and geochemical data were collected during these cruises. Geophysical data consisted of high resolution multibeam bathymetry and backscatter data. Both multibeam and backscatter data were processed from the March 2001 cruise, which covered the most area. Short surveys of each vent site were conducted during some older multibeam cruises, but are not displayed here because of poorer quality resulting from navigation problems. Chemical data consisted of CTD (Conductivity, Temperature, and Depth) casts used for multibeam sound velocity profiles, and on-board chemical analyses on water samples taken by divers using 60 mL syringes placed in vent orifices. Small sea water samples, left unacidified (50 mL) were further analyzed by ion chromatography, while the larger acidified samples (>100 mL) were used for subsequent ICP-MS (Inductively Coupled Plasma Mass Spectrometry) analysis. Further description of geochemical analyses and methods can be found in Schijf and Byrne (2007), Naar and Byrne (2001), Byrne and Naar (2002), Rosenau et al. (1977), Breland (1980), Fanning et al. (1981), and Kohout (1965).

The 2001 MHSS data are used to investigate (a) how vent geomorphology may vary from vent to vent, (b) the seafloor structural trends of the MHSS area, (c) the spatial patterns of active vents and extinct vents with respect to known vents on land (as reported by Kohout et al. (1977) and Breland (1980)), and (d) whether published geochemical data correlate with the geomorphological characteristics of the vents.

Multibeam Bathymetry

The Kongsberg Simrad EM-3000 system was used to collect high-resolution multibeam bathymetry and backscatter data for both the 2001 and 2002 cruises. The system maps the shallow ocean floor using a 300 kHz acoustic frequency. The Simrad EM-3000 system measures depth with a ~15 cm RMS accuracy after post-processing. The system produces a 130-degree transverse swath with 127 overlapping 1.5^{o} x 1.5^{o} beams (Parrott et al., 1999; Berman, 2002; Berman et al., 2005; McIntyre, 2003; Wolfson, 2005; McIntyre et al., 2006; and Wolfson et al., 2007). The transducer emits sound waves, at a maximum ping rate of 20 pings per second, from the base of a pole mounted to the port side of the vessel (Naar et al., 1999; Zaleski and Flood, 2001; http:// www.kongsberg.com). The Applanix Positioning and Orientation System for Marine Vessels (POS/MV 320 system) is a GPS/Inertial navigation system. The system measures vessel location and attitude (roll, pitch, heading, and heave) of the vessel using two global positioning satellite antennas (GPS) and an inertial motion unit (IMU) sensor. This information is integrated with the multibeam echo soundings to eliminate the effects of vessel movement, and provide accurate position and orientation of the seafloor as mapped by the multibeam sonar.

Multibeam Backscatter

In addition to bathymetric data, the EM3000 also provides backscatter data that yields additional quantitative data that can be used for qualitative descriptions of seabed characteristics (Davis et al., 1996; Huvenne et al., 2002). Backscatter refers to the amount of acoustic energy reflected back to a transducer. These data are sensitive to the geometry

and roughness of the seafloor as well as the seafloor composition (e.g., grain size, sediment type, and/or biological coverage). A gray-scale image from black to white is generated based on the strength of the signal within a range of 0-255 (e.g., Blondel and Murton, 1997). A seafloor with sediment characteristics of rocks, gravels, coarse shells, or steep slopes, will exhibit a high backscatter. Areas with low backscatter may represent fine sediments, especially sands or acoustic shadows (i.e., where a rock or ledge prevents sound from reaching a portion of the seafloor). In the figures, areas with high backscatter are represented as dark shades, while low backscatter is shown as light shades.

Data Processing

Caris: HIPS and SIPS

The Caris HIPS and SIPS software package was utilized to post-process the multibeam bathymetry and backscatter data from the MHSS study area (Figs. 14, 15, 16, and 17). The HIPS package was used to clean bathymetry data by the automatic and manual outlier flagging removal method. Flagging eliminates the processing of pooor quality data without deleting the data from the raw data file. A flowchart of the order of applications used is shown in Figure 18.

Caris: Tides

The tide levels at the approximate location of the study area were obtained from the NOAA (National Oceanic and Atmospheric Association) archives. The tide data were recorded every six minutes at the NOAA station 8725520 in Fort Myers, Florida during March 1-14th, 2001 using a mean lower low water (MLLW) chart datum. MLLW chart

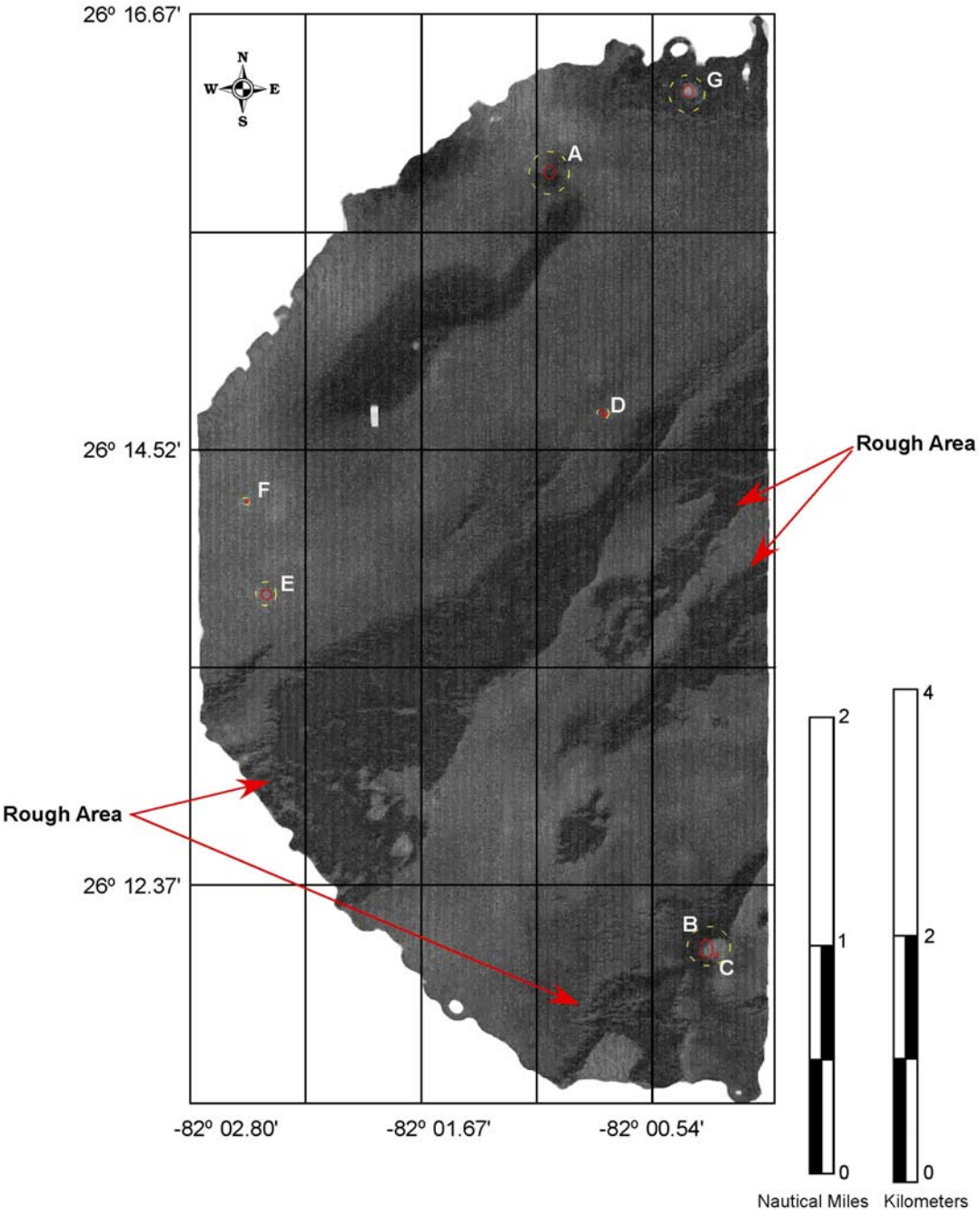

Figure 14. 2001Mudhole Submarine Spring (MHSS) study area. Backscatter, interpolated image. Gray scale images generated on a signal strength range of 0-255 db. Dark gray to black areas may represent rocks, gravels, coarse shell or steep slopes (high backscatter). Light gray to white areas may represent fine sediments, especially sands or acoustic shadows (low backscatter). White letters (A-G) denotes the location of the springs. Mudhole Submarine Spring (A), Rusty Spring (B), Near Rusty Spring (C), Sinister Spring (D*), Spring #3 (E), New Spring (F), and Dormant Spring (G*). The letters with the asterisks are inactive springs. Refer to Table 6 for further information about springs. The red circles represent the location of the orifice of each spring, while the dashed yellow circles show the extent of the overall depression of each spring. Red arrows show some areas of "roughness".

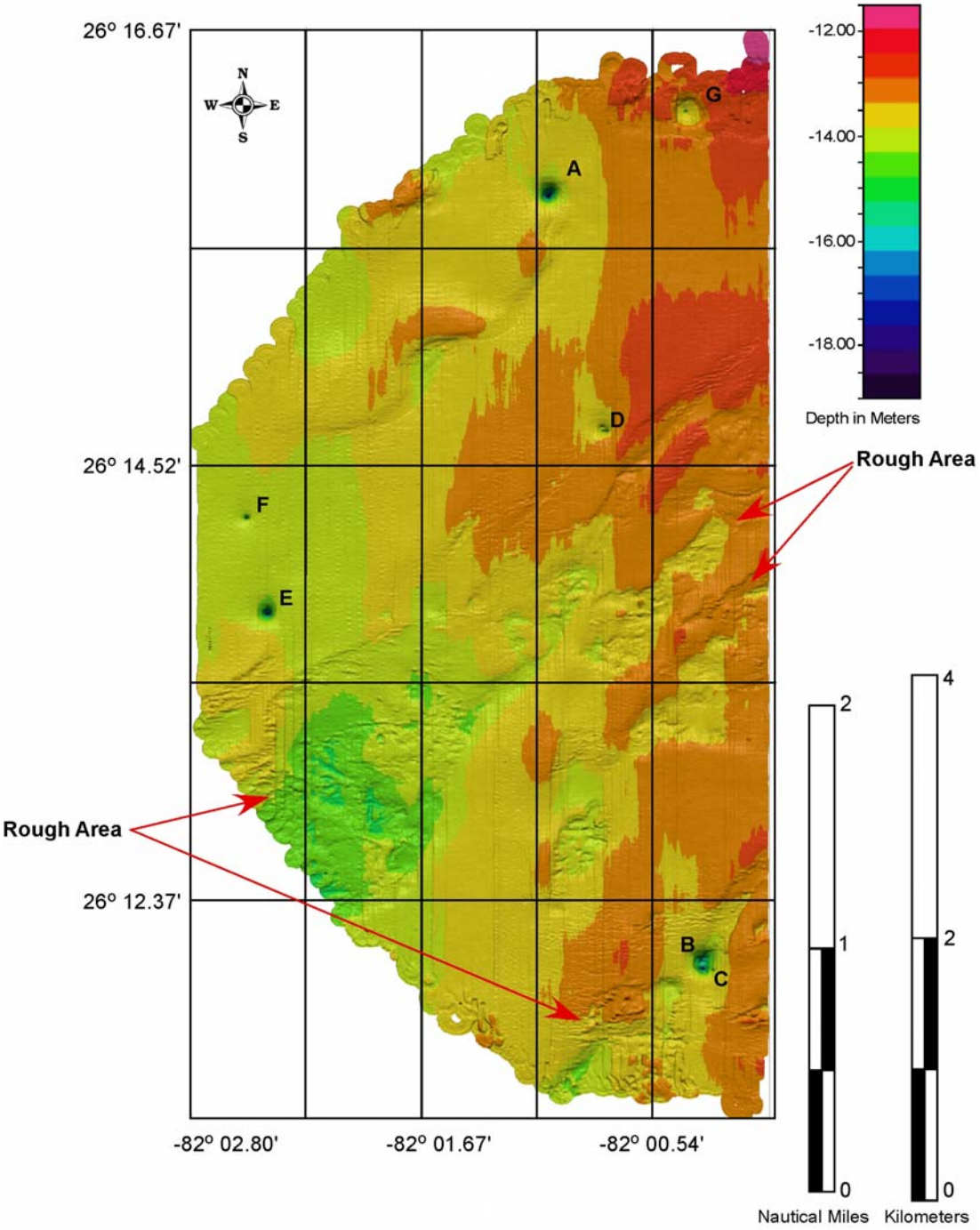

Figure 15. 2001 Mudhole Submarine Spring (MHSS) study area. Mean depth, N-S interpolated shaded color bathymetry. Image shown with aggressive surface editing, although some "striping" still occurs due to tide and sound velocity uncertainties. Black letters (A-G) denotes the location of the springs. Mudhole Submarine Spring (A), Rusty Spring (B), Near Rusty Spring (C), Sinister Spring (D*), Spring #3 (E), New Spring (F), and Dormant Spring (G*). The letters with the asterisks are inactive springs. Refer to Table 6 for further information about springs. Red arrows show some areas of roughness.

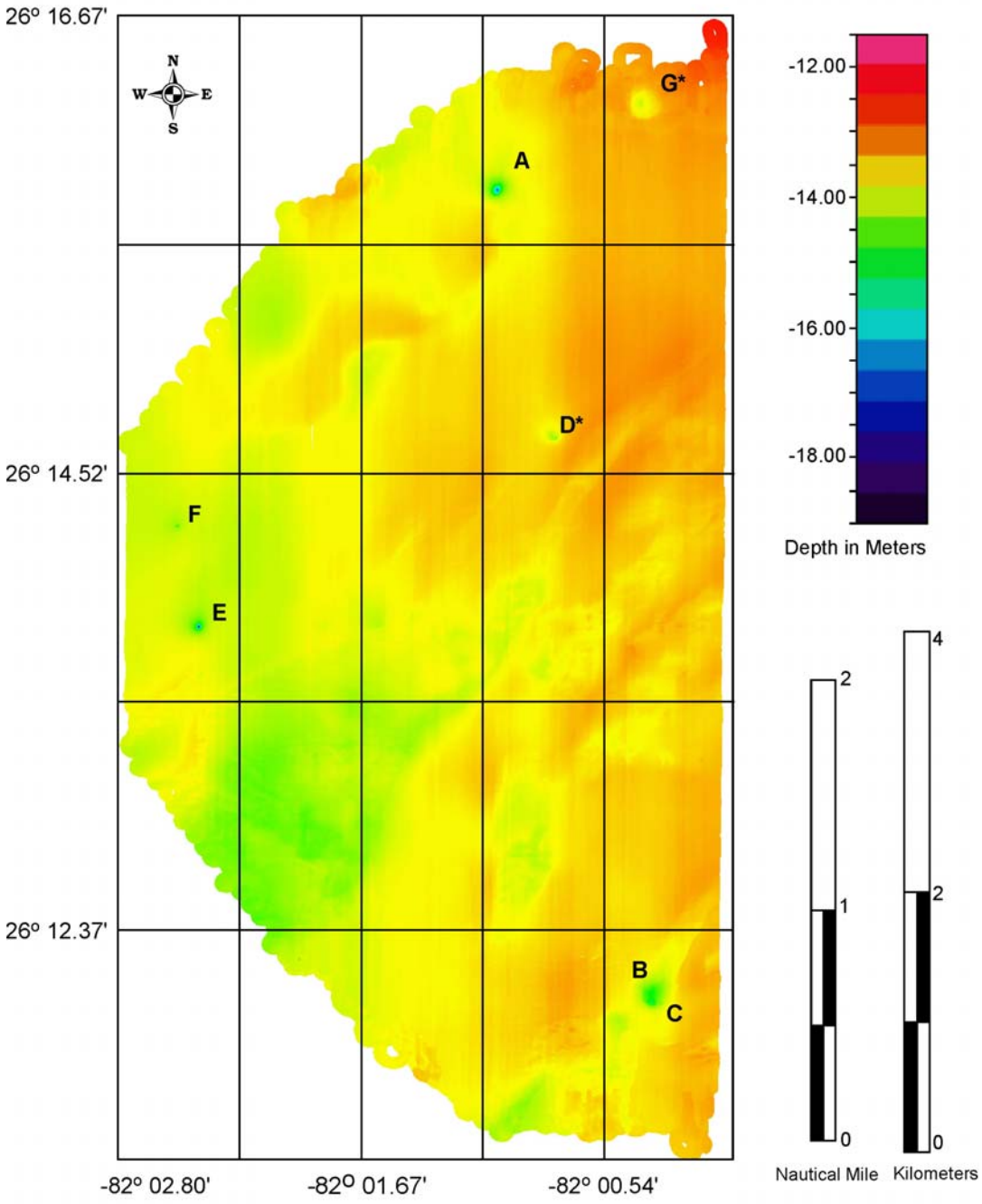

Figure 16. 2001 Mudhole Submarine Spring (MHSS) study area. Mean depth, interpolated image. Image shown with aggressive surface editing, although some "striping" still occurs due to tide and sound velocity uncertainties. Black letters (A-G) denotes the location of the springs. Mudhole Submarine Spring (A), Rusty Spring (B), Near Rusty Spring (C), Sinister Spring (D*), Spring #3 (E), New Spring (F), and Dormant Spring (G*). The letters with the asterisks are inactive springs. Refer to Table 6 for further information about springs.

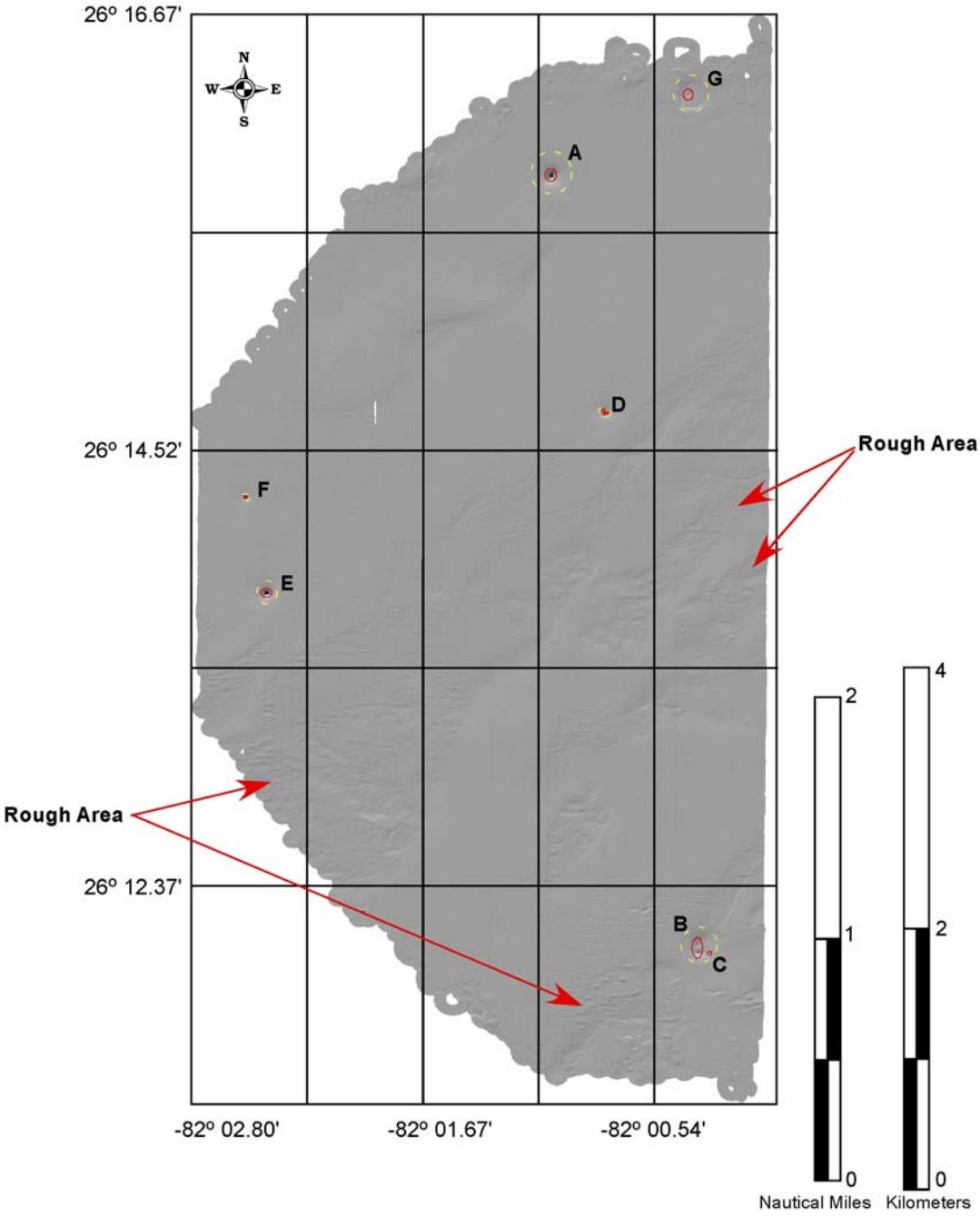

Figure 17. 2001Mudhole Submarine Spring (MHSS) study area. Shaded surface relief, interpolated image. Vertical exaggeration of 7 with an elevation of 46 degrees and an azimuth of 350 degrees. Black letters (A-G) denotes the location of the springs. Mudhole Submarine Spring (A), Rusty Spring (B), Near Rusty Spring (C), Sinister Spring (D*), Spring #3 (E), New Spring (F), and Dormant Spring (G*). The letters with the asterisks are inactive springs. Refer to Table 6 for further information about springs. The red circles represent the location of the orifice of each spring, while the dashed yellow circles show the extent of the overall depression of each spring. Red arrows show areas of "roughness".

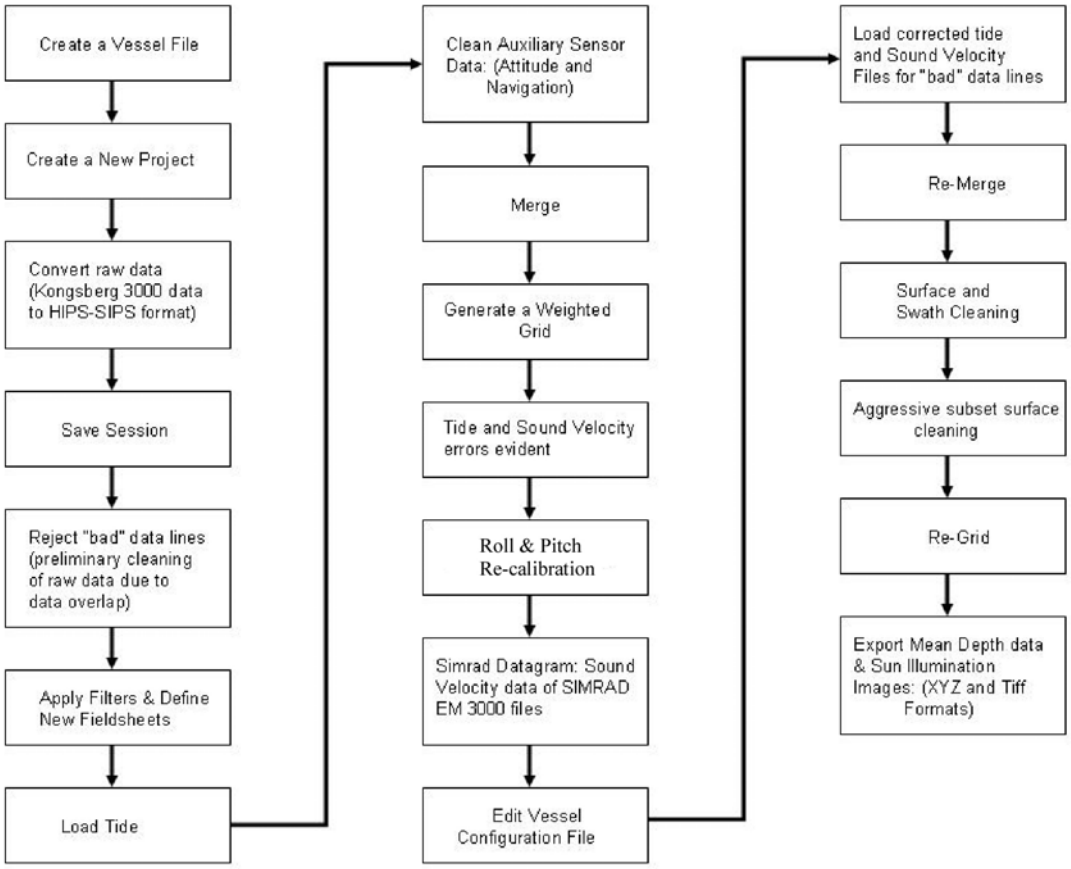

Figure 18. Processing flow chart for bathymetric and backscatter data.

datum is the average of the lower low water height of each tidal day observed over the National Tidal Datum Epoch. Several survey lines in March 3, 12, and 13 were offset approximately ~1.5 meters higher or lower than the surrounding data lines. Such offsets are a result of: a tide problem, i.e. sea level at study site did not match the distant NOAA tide station, an improper setting of the heave filter, or some other unknown problem. Although some survey lines were normalized after "regridding", a number of data lines continued to display a north-south along-track artifact. Therefore, the tide data of selected survey days were downloaded into a Microsoft Excel format and adjusted based on the offset amount and time. Once tide data were adjusted, the tidal data were reloaded and regridded. Some remaining north-south along-track artifacts are still slightly evident, but are reduced by an order of magnitude from previous versions of the processed data.

Caris: Pitch and Roll Calibration

The data lines were recalibrated using Caris' HIPS and SIPS Calibration module in the HDCS program. Pitch refers to the rotational motion of the vessel around the port/starboard axis (X). Roll refers to the rotational motion of the vessel around the fore/aft axis (Y). Pitch and roll from the Simrad Datagrams of raw data and cruise reports were inputted into the Vessel Configuration file as Sound Velocity Profile 1 (SVP1), which contained the X,Y, Z offsets of the transducer from the center of rotation. The data used for the top pole X,Y, Z mount and the bottom pole X,Y, Z as well as the pitch and roll from the preliminary input survey are shown in Tables 8 and 9. Note: dates are shown in Julian time. Re-calibration of the selected lines was performed, allowing for adjustments of the survey data for pitch and roll. The adjustments made to the selected

survey lines were saved in the vessel configuration file and re-merged with the entire dataset.

Caris: *Sound Velocity Corrections*

Despite the corrections described above, some inherent along-track north-south "striping" artifacts still exist in the data mosaics (Figures 15 and 16). These artifacts appeared to be related to the use of incorrect sound velocity profiles. To modify the sound velocity profile with an EM 3000 system using Caris, one must obtain the data shown in Tables 8 and 9. These values were obtained directly from the raw data or data processing as described above. When many across-track depth profiles of the seafloor are stacked and averaged, the resulting profile should be flat. If it is not, e.g., it is systemically curved up (smile) or down (frown), it is likely that the sound velocity profile being used is incorrect. The survey lines that exhibited these types of sound velocity errors were from March 2nd, and March 3rd of 2001. The average across-track depth profiles used in the Sound Velocity Editor were obtained from the Simrad Installation Datagram, and a new sound velocity profile was created and applied by a trial-and-error method. In the newly created sound velocity profile a value of 1534 m/s was applied to the entire dataset. Although some sound velocity uncertainties still appeared in the image, the data were significantly improved. Where data overlapped, additional aggressive surface editing (i.e., flagging outliers) was performed to reduce the north-south along-track artifact.

Table 8. Sound velocity, pitch and roll parameters from Caris Vessel Configuration File. The top and bottom pole mount values were obtained from the Simrad datagrams (e.g., see Table 9). X, Y, Z are in meters, roll and pitch are in degrees following the Caris manual reference frame convention.

Julian Date	Top X	Top Y	Top Z	Bot X	Bot Y	Bot Z	Roll	Pitch
2001-061 (March 2, 2001)	-3.140	-5.120	2.770	-3.140	-5.120	2.770	0.250	-6.00
2001-062 (March 3, 2001)	-3.140	-5.120	2.770	-3.140	-5.120	2.770	0.100	-6.00
2001-071 (March 12, 2001)	-3.140	-5.120	2.770	-3.140	-5.120	2.770	-0.200	0.180
2001-072 (March 13, 2001)	-3.140	-5.120	2.770	-3.140	-5.120	2.770	-0.200	0.180

Table 9. The pole mount offset values that were retrieved from the Simrad Datagram. The table indicates which Simrad value belongs in which field in the VCF (Wong and Gourley, 2003).

Simrad field	HIPS SVP1 VCF Field	Values
S1Z	Pole Top Z & Pole Bottom Z	2.770, 2.770
S1X	Pole Top Y & Pole Bottom Y	-5.120, -5.120
S1Y	Pole Top X & Pole Bottom X	-3.140, -3.140

Fledermaus: Data Visualization

A suite of associated programs, also made by IVS (Interactive Visualization Systems), were used to generate and manipulate data (Figure 19). Fledermaus, a high-powered 3D data visualization program, was used to generate digital elevation models and profiles of the vent areas. Additional information follows in the Data Analysis section.

Data Analysis

Slope Analyses

Before the slope analyses were performed, the data were exported from the Caris program as an X,Y, Z ASCII file to be used by the suite of Fledermaus programs. The X,Y, Z ASCII file of the study area was first imported into the Average Gridder ("avggrid"). The Average Gridder is designed to produce a regular gridded surface from irregularly spaced points. Using a gridding algorithm controlled by input parameters, the MHSS data file was exported as a ".dtm" (digital terrain model), and a ".geo" (geo-referenced information) file for use in another program called "DMagic" (Data Magician). DMagic is an application designed to prepare objects for visualization in Fledermaus. Once the data were imported into DMagic, the Surface Shader tool was used to shade the surface based on mean depth by manipulating the shadow direction of the sun and lighting parameters. The Surface Shader can be used to visualize features and has the ability to create 3D surfaces with true cast shadows. Cast shadows highlight fine

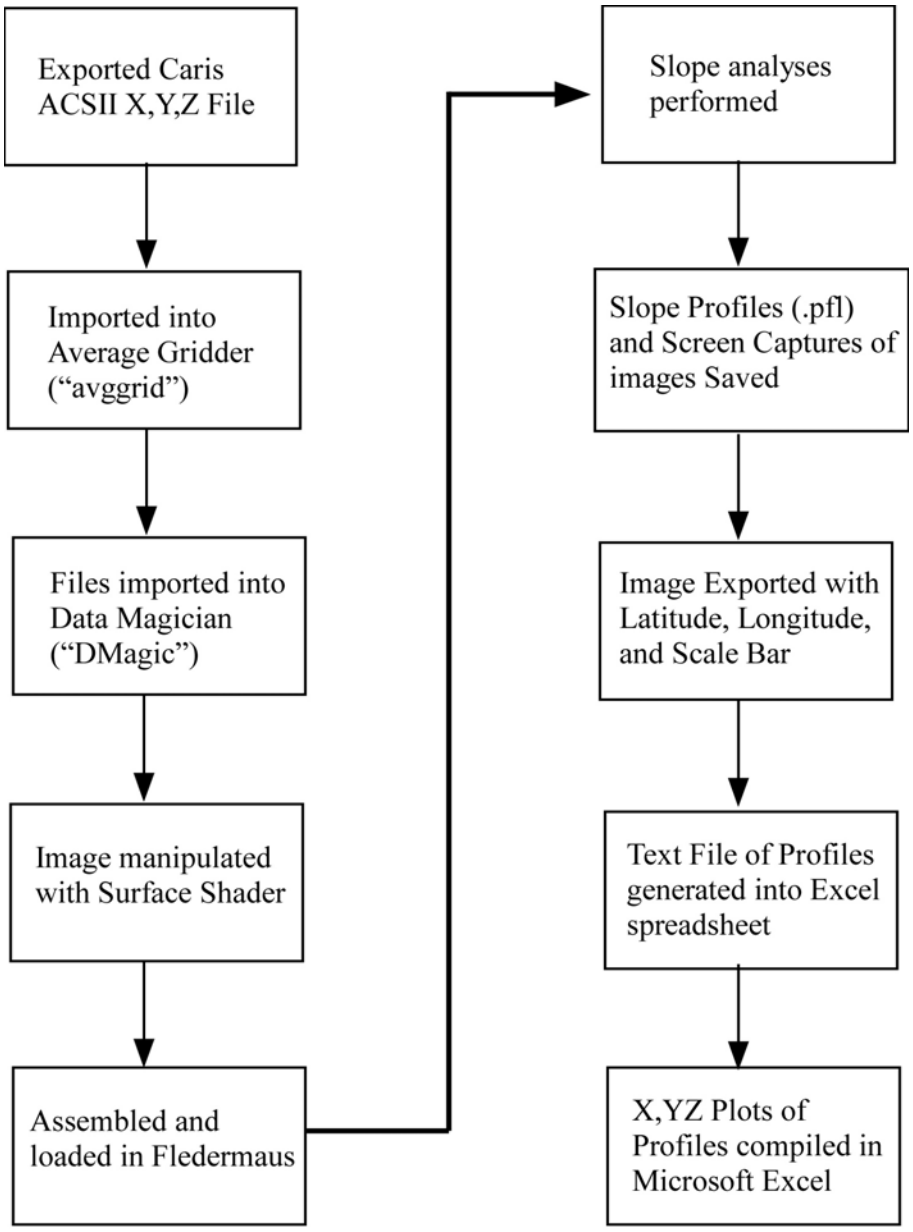

Figure 19. Processing flow chart of exported X, Y, Z data into suite of Fledermaus programs for slope analyses and images of study area.

details on the surface and produce a much more realistic and intuitive 3D model of the surface. Six parameters of the illumination model were adjusted to the desired 3D image. These parameters are: light position, light direction, intensity of ambient light, specular component, shadow softness, and vertical exaggeration of heights. The sun direction can be rotated to any azimuth from 0 to 360 degrees, while the shadow length can be adjusted from 0 to 4 meters in length (thus the height of the sun). The sunlight direction is from the northwest at an angle of 315^{o}. The length of the shadows from the northwest was set to 0.50 m (an approximate sun angle of 79^{o} from horizontal). The ambient light control was set to 47.4, which affects the amount of light that appears in cast shadows. High ambient light makes that entire image brighter and shadows less distinct. The specular component was set to 20.6 (medium glossy-matte finish), which controls the extent of glossy highlight. High specular content makes the surface appear to be very glossy, while low specular content provides a matte finish. Shadow softness controls the sharpness or softness of the shadow edges. The vertical scale is the height of the surface that can be artificially increased or decreased to change the shadow length. The vertical scale was set to 24:6. Once the image was saved as a scientific data object (SD), the object was assembled in Fledermaus.

The assembled MHSS file was loaded into the Fledermaus and slope profile analyses were performed on each submarine spring in the study area. A slope profile was saved as a text file and individual images of each spring were exported using the Screen Capture function. Twelve hundred meter cross sections of the all submarine spring profiles with a vertical exaggeration of 40:1 were made and utilized for slope analyses. In the text file each point in the profile is written out to the file as a distance along the

profile and an x,y and height/depth (z) position. The text files were then imported into Microsoft Excel, where X, Z plots based on distance and ambient seafloor depth were generated.

The same slope profiles imported into Mircosoft Excel spreadsheets were used to generate graphs of the extents of the depressions surrounding the vents. The extent of the depression was based on the overall width (north to south and west to east) of the depression as it extended towards a “flatter” ambient seafloor bottom from the origin (defined as the deepest part of the vent).

Chapter 4

OBSERVATIONS AND RESULTS

Slope and Geomorphological Analyses

Geomorphological analyses are performed using bathymetry data for quantitative slope measurements. Backscatter data (Figure 14), color-shaded bathymetry data (Figure 15), and "sun-illuminated" bathymetry (Figure 17) are used for qualitative analysis. Although the bathymetry images contain minor north-south “striping” artifacts, much information can still be inferred about the study area. According to the processed backscatter data (Figure 14), dark gray to black areas are likely to represent limestone, rocks, gravels, coarse shell, or steep sonar-facing slopes (high backscatter), whereas light gray to white areas are likely to represent fine sediments, especially sands or acoustic shadows (low backscatter). For each vent 1200 meter-long profiles were generated in a N-S and E-W direction centered on the deepest part of each vent. The northern, southern, eastern, and western slopes of each vent were measured using the steepest part of the profile. A summary of the depression dimensions are measured from the deepest part of the vent to where the seafloor slope matches the ambient seafloor slope.

Mudhole Submarine Spring

Mudhole Submarine Spring (A) is an active spring located at 26^{o} 15.837' N and 82^{o} 01.047'W. The maximum depth is ~18.7 meters below sea level. The northern extent is -338 meters and the southern extent is 127 meters (Figure 20). The eastern extent of the depression is 164 meters, and the western extent is -170 meters (Figure 21). The very circular bathymetric shape of MHSS depression suggests (Figure 22) some scouring may have occurred from effluent discharging from the orifice. The slope of both the northwestern (a, b) and southeastern (a', b') "slopes" of the depression profile (Figure 22) are ~10^{o}. The vent has a "V"-shape cone and is symmetrical. The W-E (dashed lined, a-a') and N-S (solid line, b-b') profiles of MHSS are very similar. The width of the upper part is ~300 meters across, and becomes progressively narrower with depth.

According to the backscatter image (Figure 14 and Figure 23) MHSS has a high backscatter return. Thus, it can be inferred that the immediate depression may be mostly composed of gravels and coarse shells in agreement with Breland's (1980) interpretation (Figure 12). The moderately steep slope of ~10^{o} does not appear to affect the backscatter much because both flat and steep areas occur with similar backscatter strength. The area surrounding the depression appears to have the same sediments, with some sands or fine sediments creating a more flat seafloor bottom (also matching Figure 12). Approximately southeast of the depression there appears to be a broad mound of rocks and/or coarse shell (northeast of a mound surrounded by yellow-orange color in Figure 15)

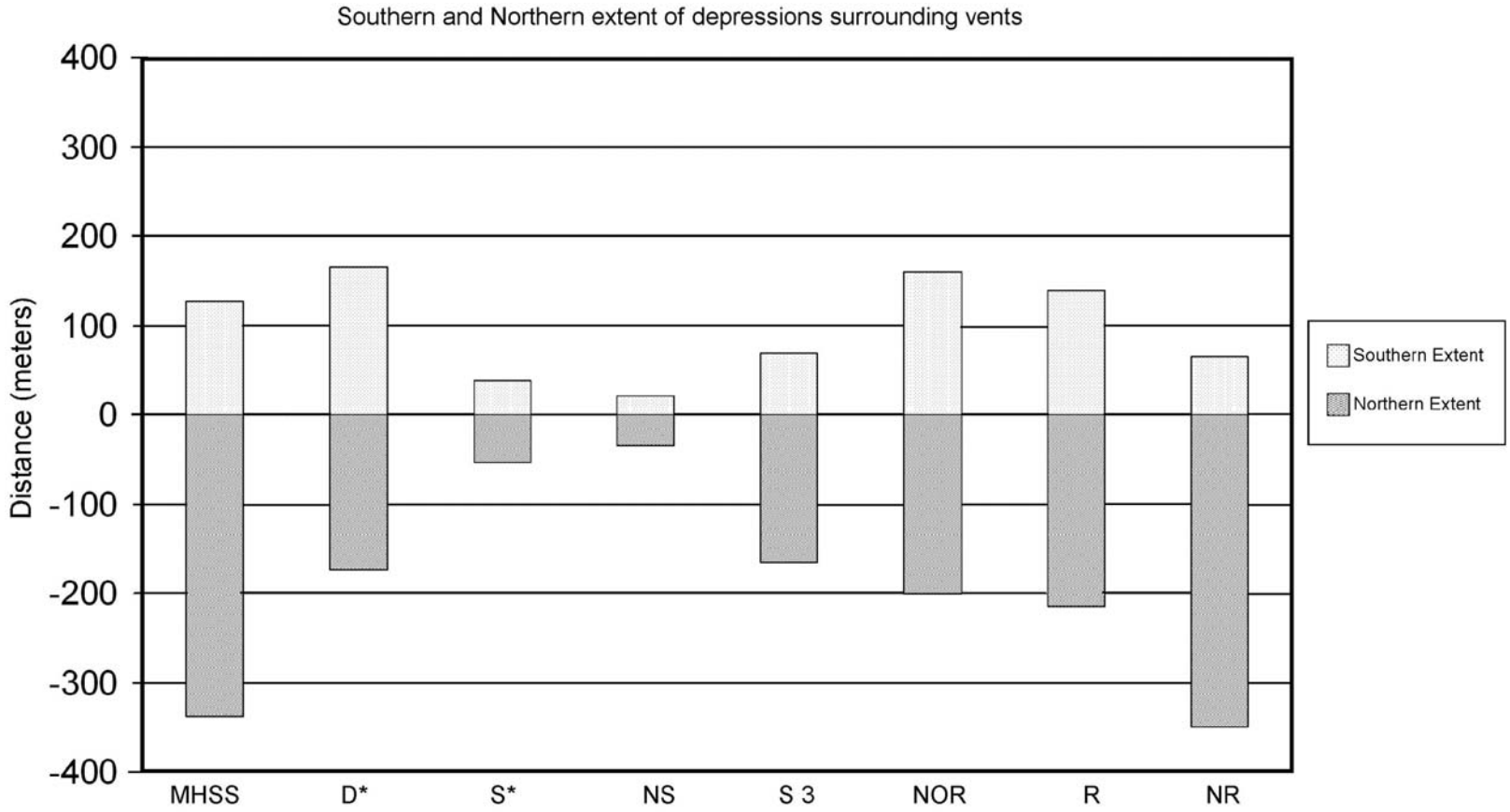

Figure 20. Southern and Northern extent of depressions surrounding vents. "MHSS" is Mudhole Submarine Spring, "D*" is Dormant Spring, "S*" is the entire Sinister Spring depression (includes NW, SW and SE vents), "NS" is New Spring, "S 3" is Spring #3, "NOR" is Northern Rusty Spring, "R" is Rusty Spring and "NR" is Near Rusty Spring. The letters with the asterisks represent the springs that appear inactive at the time of the cruise.

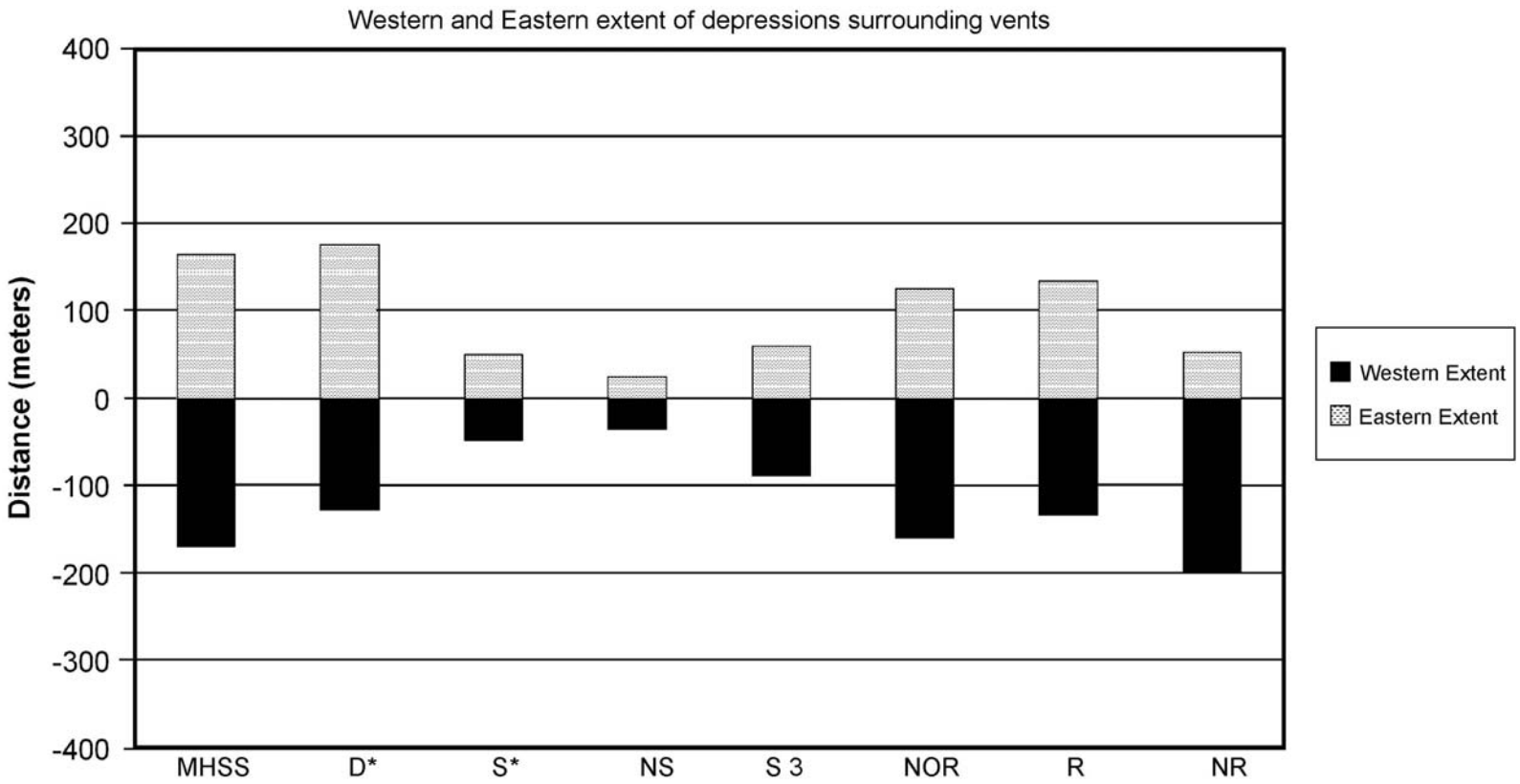

Figure 21. Western and Eastern extent of depressions surrounding vents. "MHSS" is Mudhole Submarine Spring, "D*" is Dormant Spring, "S*" is the entire Sinister Spring depression (includes NW, SW and SE vents), "NS" is New Spring, "S 3" is Spring #3, "NOR" is Northern Rusty Spring, "R" is Rusty Spring and "NR" is Near Rusty Spring. The letters with the asterisks represent the springs that appear inactive at the time of the cruise.

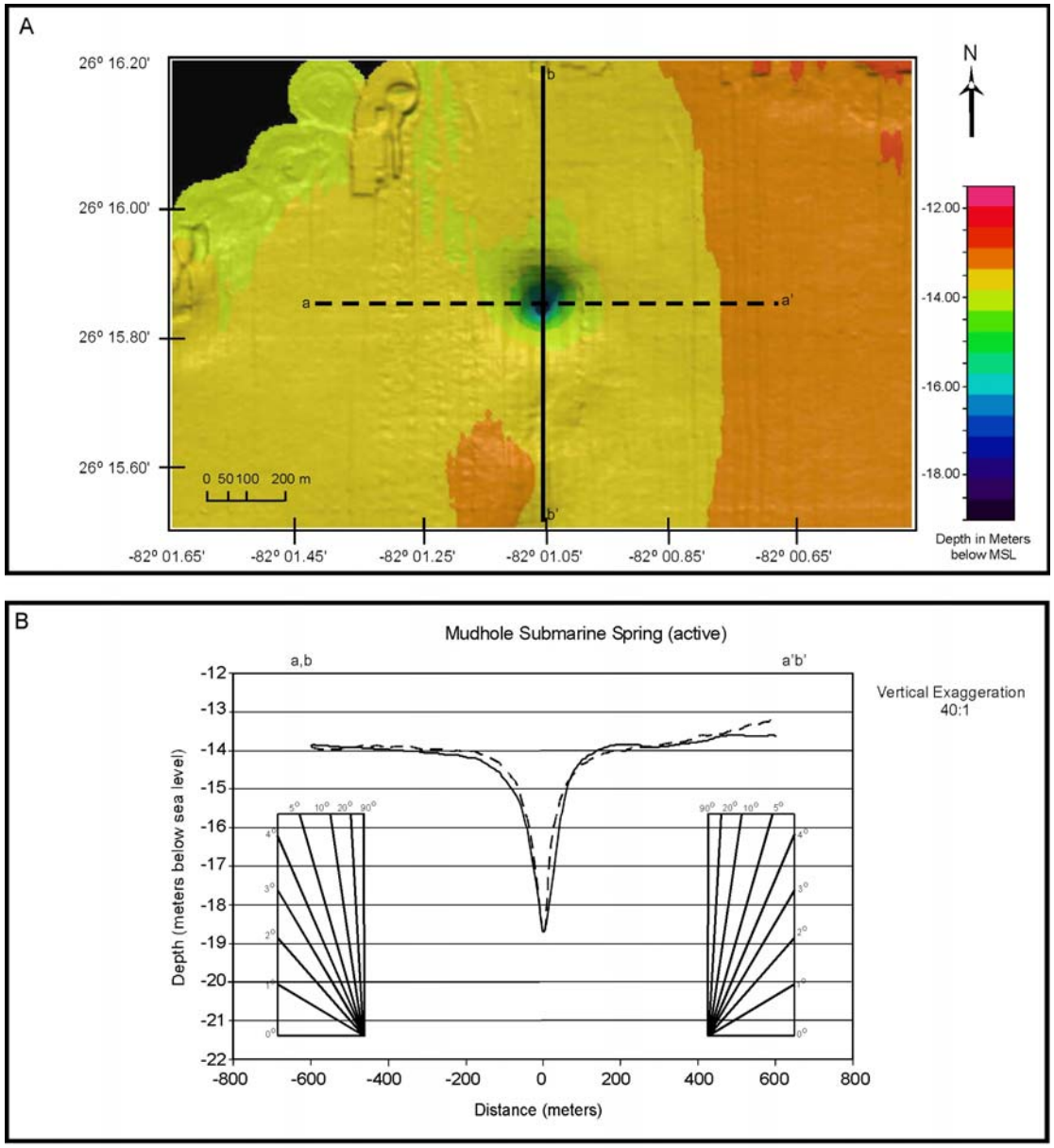

Figure 22. The upper image (A) is a shaded color bathymetry of MHSS. The lower image (B) is a cross section profile image of MHSS. The distance of each profile measures 1200 meters across. The dashed line (a-a') is the west to east profile, and the solid line (b-b') is the north to south profile. The active MHSS has a vertical exaggeration of 40:1.

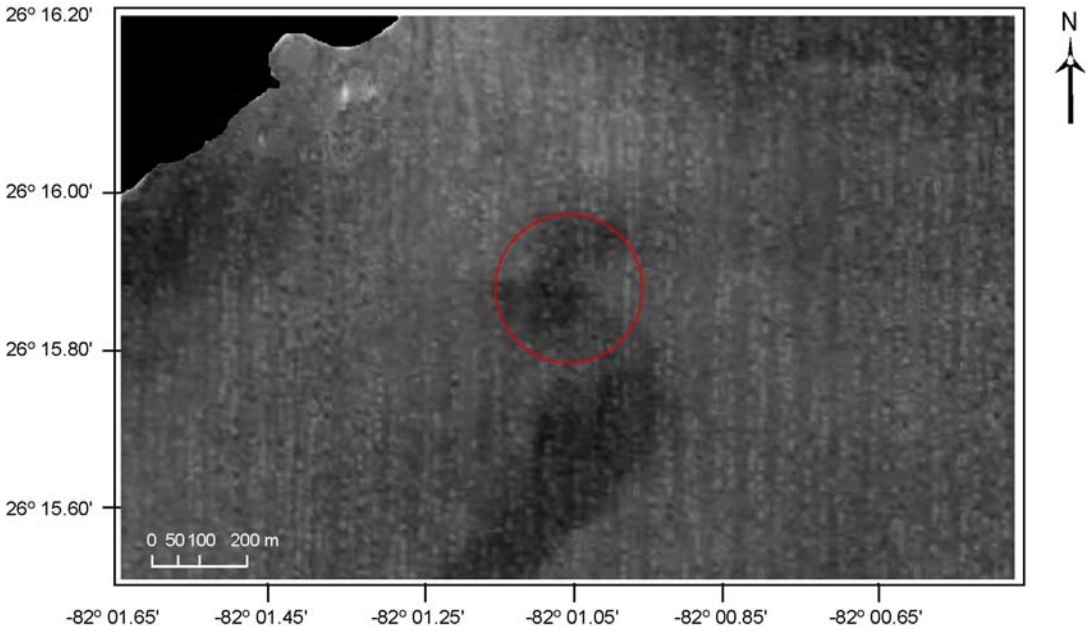

Figure 23. Backscatter image of MHSS (A). Red circle represents the location of the entire depression of active MHSS. Dark gray to black areas may represent limestone rocks, gravel, coarse shell or steep slopes (high backscatter). Light gray to white areas may represent fine sediments especially sands or acoustic shadows (low backscatter).

Rusty Springs Depression

Three active vents are located within the Rusty Spring depression (B, C): Northern Rusty Spring, Rusty Spring, and Near Rusty. Northern Rusty Spring is located at north of Rusty Spring at 26^{o} 12.105'N and 82^{o} 00.298'W. The maximum depth is ~16.1 meters below sea level. The northern extent is -200 meters and the southern extent is ~160 meters (Figure 20). The eastern extent is 160 meters, and the western extent is -125 meters (Figure 21). According to the shaded bathymetry (Figure 24), Northern Rusty is located in a diverse setting. The western and eastern slopes of the vent (Figure 21) have a slope of ~3^{o}. The northern slope (represented by the solid line, b) has a slope of ~2^{o}, and the southern slope (represented by the solid line, b') has a slope of ~6^{o} (this southern slope also includes the profile of Rusty which is located exactly north of Rusty). The W-E (a-a') width is ~250 meters across. Compared to MHSS, the shape of Northern Rusty's has more of a broad "U"-shape and is asymmetrical.

Rusty Spring is located south of Northern Rusty at 26^{o} 12.060'N and 82^{o} 00.302'N (Figure 25). The maximum depth is ~16.9 meters. The northern extent is -215 meters and the southern extent is 139 meters. The eastern extent is 134 meters and the western extent is -136 meters. The western slope of the vent is 4^{o}, the eastern slope is 3^{o}, the northern slope is 2^{o} and the southern slope is 6^{o}. The shape of Rusty Spring is "U"-shaped and asymmetrical.

Northern Rusty Spring and Rusty Spring are located in an area of both high and low backscatter (Figure 14 and Figure 26). The immediate depression of the spring

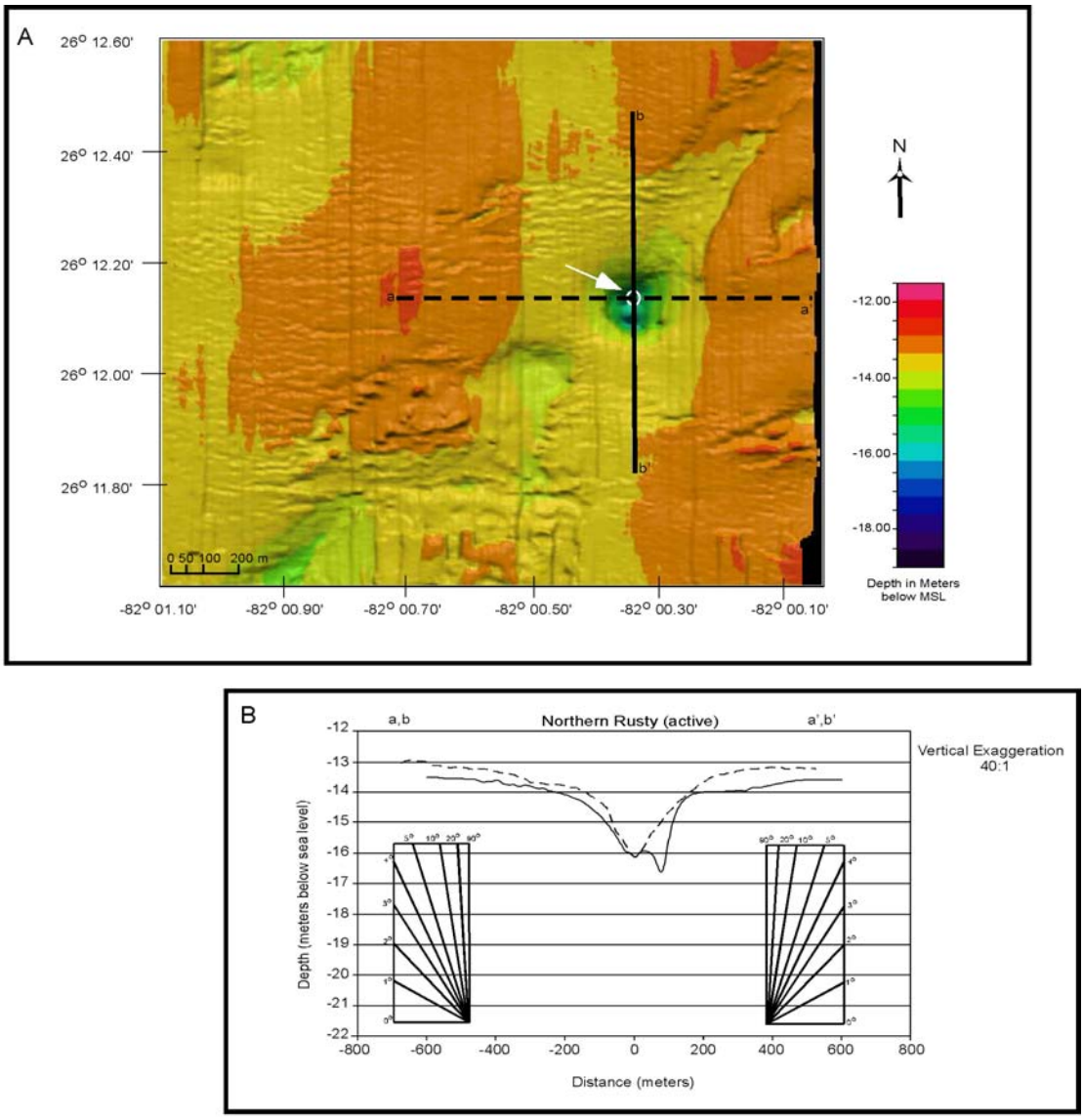

Figure 24. The upper image (A) is shaded color bathymetry of Northern Rusty. Within the depression are three distinct vents sites: Northern Rusty, Rusty Spring and Near Rusty. Northern Rusty's location is shown by the white circle and white arrow. The lower image (B) is a cross section profile image of Northern Rusty. The distance of each profile measures 1200 meters across. The dashed line (a-a') is the west to east profile, and the solid line (b-b') is the north to south profile with a vertical exaggeration of 40:1. Note Figure A and B are offset so that the profile lines in the upper image (A) directly correspond to the profiles in the lower Figure (B).

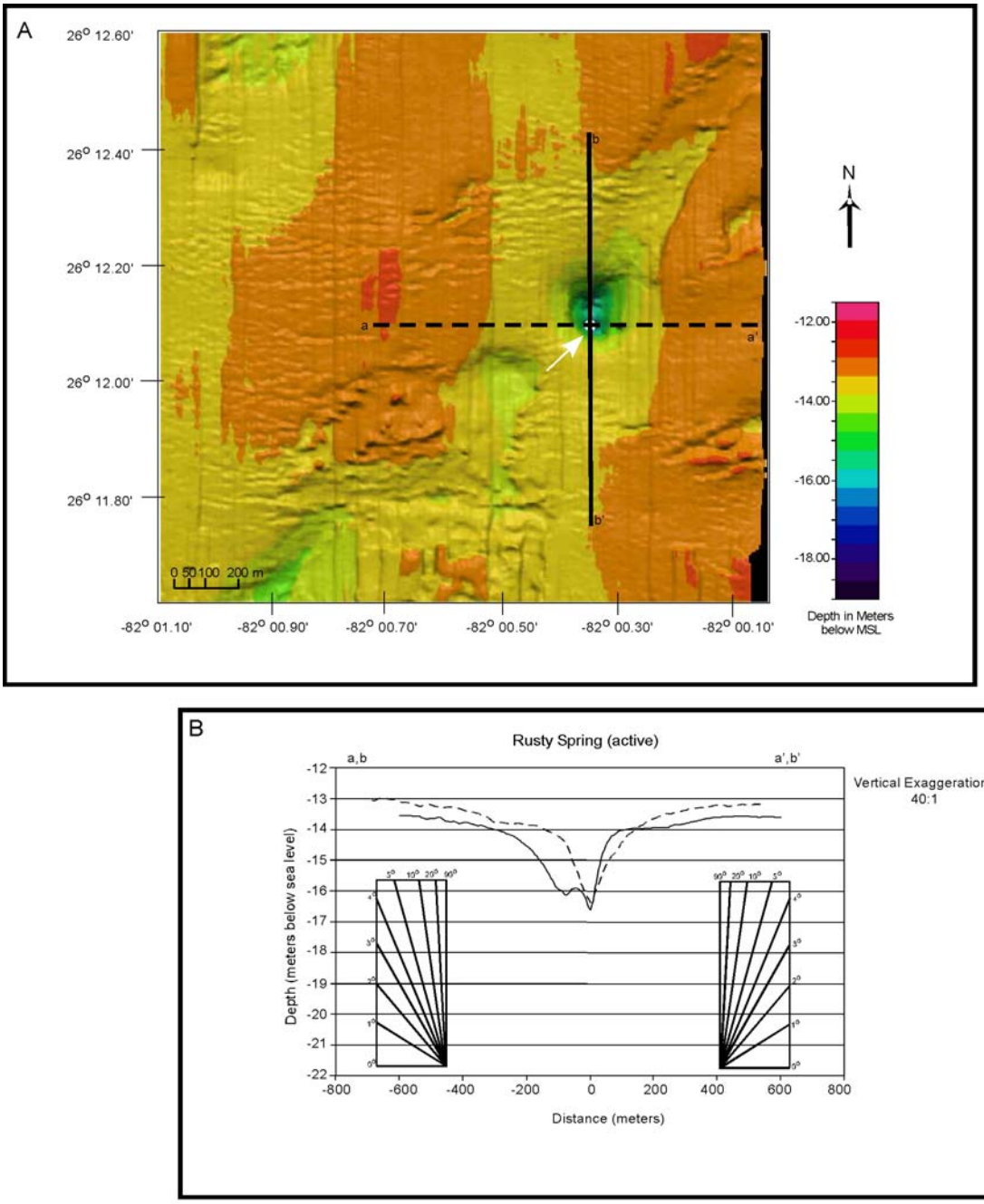

Figure 25. The upper image (A) is shaded color bathymetry of Rusty Springs. Within the depression are three distinct vents sites: Northern Rusty, Rusty Spring and Near Rusty. Rusty Spring's location is shown by the white circle and white arrow. The lower image (B) is a cross section profile image of Northern Rusty. The distance of each profile measures 1200 meters across. The dashed line (a-a') is the west to east profile, and the solid line (b-b') is the north to south profile with a vertical exaggeration of 40:1. Note Figure A and B are offset so that the profile lines in the upper image (A) directly correspond to the profiles in the lower Figure (B).

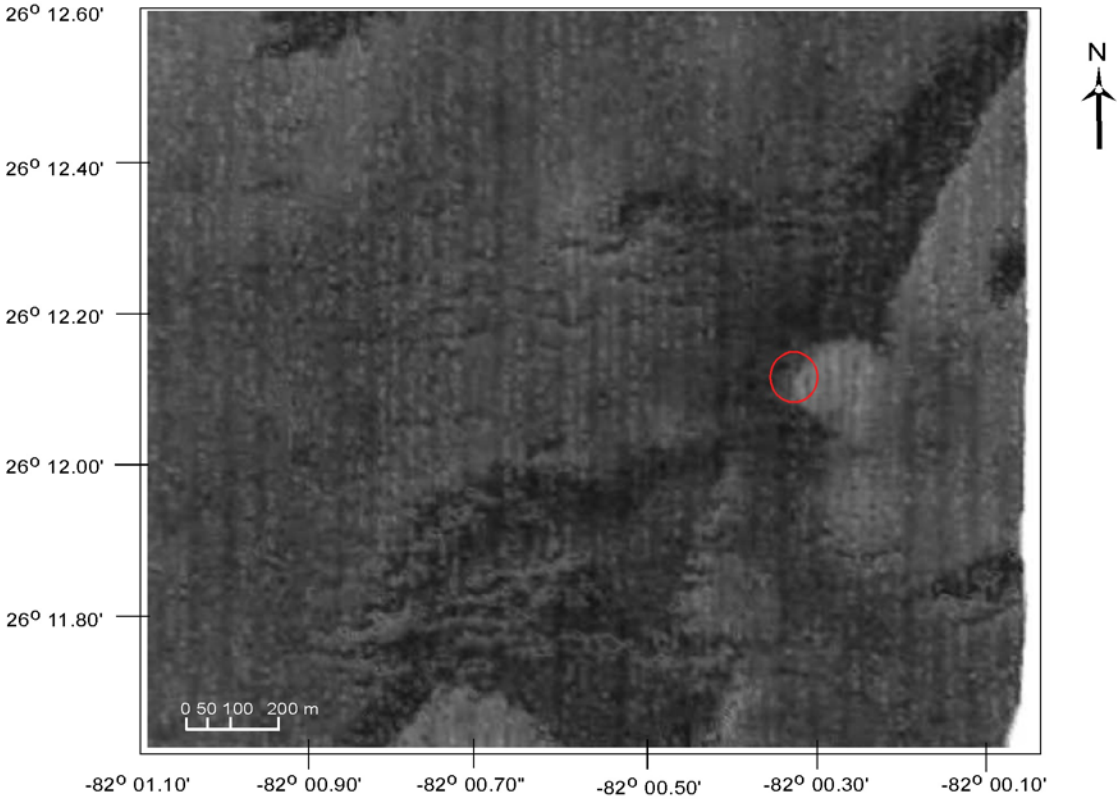

Figure 26. Backscatter image of Northern Rusty and Rusty Spring (B). Red circle represents the location of the entire depression of active Rusty. Dark gray to black areas may represent limestone rocks, gravel, coarse shell or steep slopes (high backscatter). Light gray to white areas may represent fine sediments especially sands or acoustic shadows (low backscatter).

appears to consist mostly of coarse shell, rocks, and gravel, while the overall depression of the spring appears to have fine sediments towards the southeastern slope. Northern Rusty has an irregular shape, possibly due to the presence of unconsolidated sediments, the flux of effluent, and bottom currents. There appears to be a scouring of the entire depression towards the northeast, with possible sand ripples to the north. Dark areas (high backscatter) trending northeast and southwest may be areas of hardbottom, with coarse shells rocks and gravel surrounding Northern Rusty and Near Rusty Springs

Near Rusty (C) is an active spring located east of Rusty Spring at 26^{o} 12.060'N and 82^{o} 00.250'W. The maximum depth is ~14.9 meters. The W-E and N-S extents of Near Rusty include the entire Rusty Springs depression. The northern extent is -350 meters and the southern extent is ~65 meters. The eastern extent is 53 and the western extent is -200 meters. The profile (lower figure B) of Near Rusty Spring in Figure 27 is enlarged to observe and measure the overall shape and slope of the vent. Notice the difference in the axes of the enlarged profile, depth below sea level is between -14.2 meters to -15.2. The distance is between -40 to 40 meters. Near Rusty's western slope has a slope of $<\sim 1^{o}$ and eastern slope has a slope of $\sim 3^{o}$ (dashed line, a-a'; Figure 27). The slope of the northern is $\sim 1^{o}$ and the southern slope (solid line, b-b') is 3^{o}. The W-E (a-a') width of the upper part of the orifice is ~12 meters across.

The immediate depression of Near Rusty is mostly located in fine sediments, and the W-E (a-a') profile of the vent has a "U" shape and is asymmetrical. There appears to be a slight "hump" or mound that separates Northern Rusty, Rusty, and Near Rusty Springs. What these humps are composed of is uncertain, but it is suspected to be a sedimentary deposit.

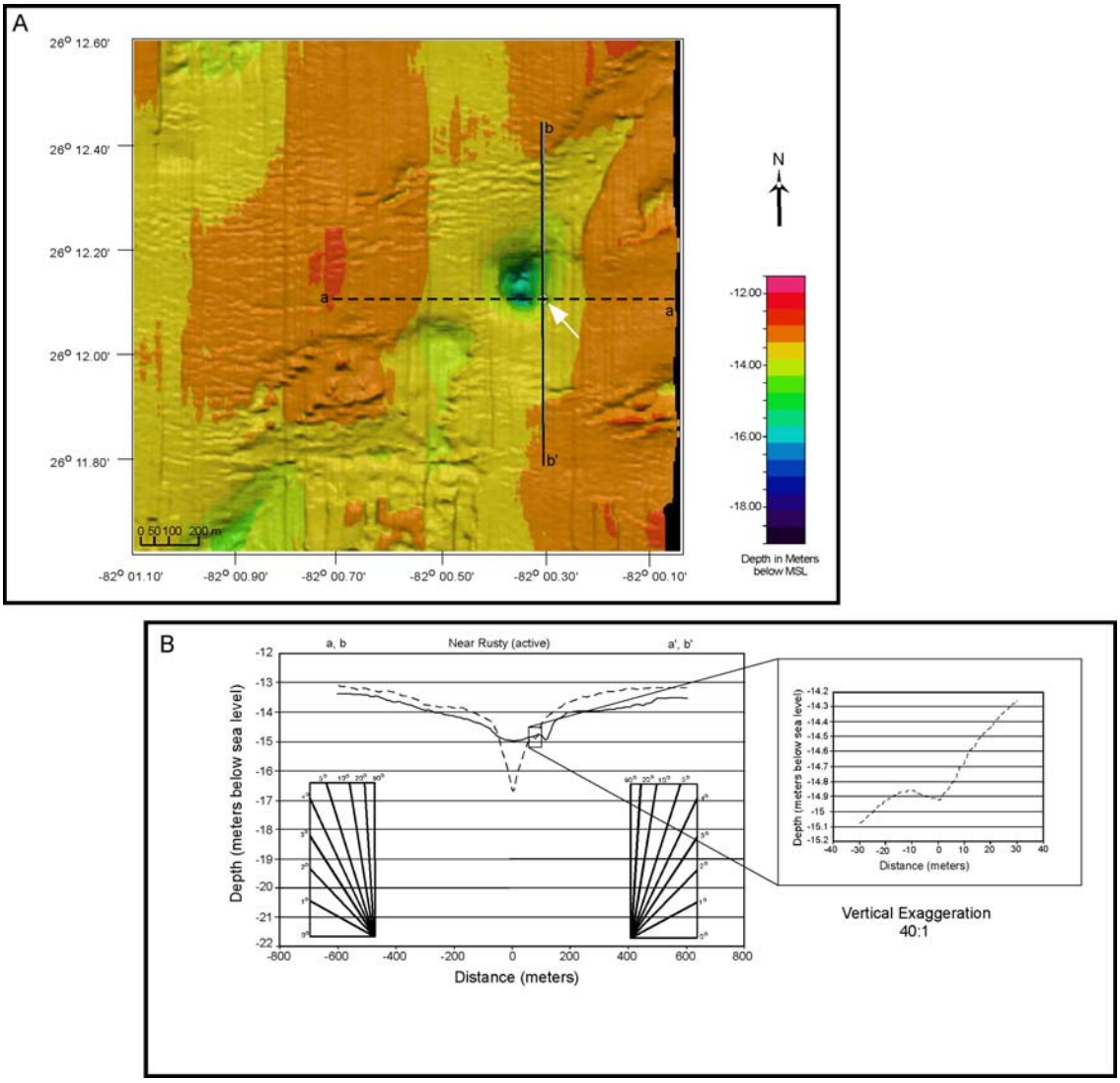

Figure 27. The upper image (A) is shaded color bathymetry of Near Rusty. Within the depression are three distinct vents sites: Northern Rusty, Rusty Spring and Near Rusty. Near Rusty's location is shown by the white arrow. The lower image (B) is a cross section profile image of Northern Rusty. The distance of each profile measures 1200 meters across. The dashed line (a-a') is the west to east profile, and the solid line (b-b') is the north to south profile with a vertical exaggeration of 40:1. Note Figure A and B are offset so that the profile lines in the upper image (A) directly correspond to the profiles in the lower Figure (B). An enlargement of Near Rusty's W-E profile is provided to the right of the overall profile of the depression. Note the change in axes.

Near Rusty is also located in an area of both high and low backscatter (Figure 14 and Figure 28). Compared to Rusty and Northern Rusty, Near Rusty's immediate depression appears to consist of mostly fine sediments.

Sinister Spring Depression

Sinister Spring (S*) is an inactive depression located 26^{o} 14.688'N and 82^{o} 00.765'W. Within the depression of Sinister Spring are three distinct vents (Figures 29, 31 and 32). The maximum depth of the northwest vent of Sinister Spring is ~14.5 meters below sea level, the southwest vent is ~14.7 meters below sea level and the southeast vent is ~14.8 meters below sea level. The eastern extent of the depression is 49 meters and the western extent is -48 meters. The northern extent is -53 meters and the southern extent is 38 meters (Figures 17 and 18).

The western slope of the northwest (NW) vent of the Sinister Spring depression has a ~2^{o} slope, while the eastern slope has a slope of ~2^{o} (dashed line, a-a'; Figure 29). The northern slope of the vent ~1^{o} and the southern slope is ~2^{o} (solid line, b-b'). Sinister's NW vent has a broad "U" shape and width (W-E, a-a') of ~200 meters across. The second vent is located southwest of the depression (Figure 30). The slope of the western slope of the southwest vent of the depression is ~2^{o}, and the eastern slope is ~3^{o} (Figure 30). The northern slope has a slope of ~1^{o} and ~3^{o} for the southern slope. Sinister's southwest vent has more of a "U" shape and width (W-E, a-a') of ~150 meters across.

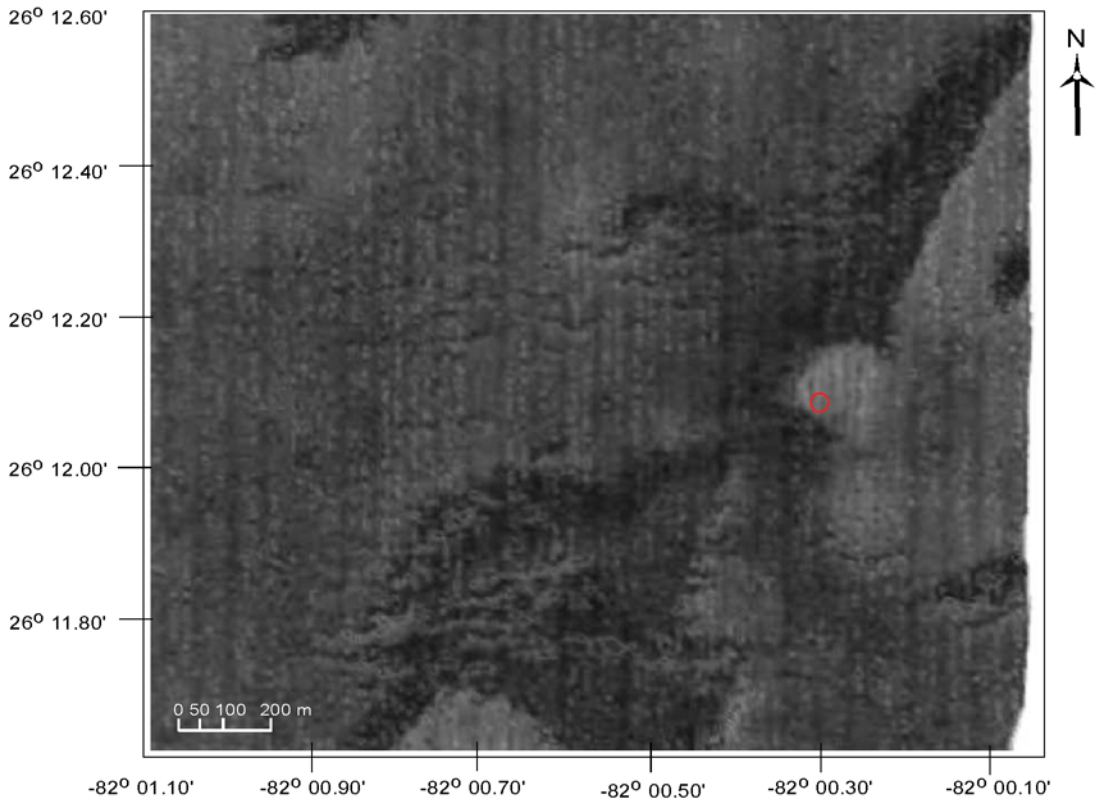

Figure 28. Backscatter image of Near Rusty Spring (C). Red circle represents the location of the entire depression of active Rusty. Dark gray to black areas may represent limestone rocks, gravel, coarse shell or steep slopes (high backscatter). Light gray to white areas may represent fine sediments especially sands or acoustic shadows (low backscatter).

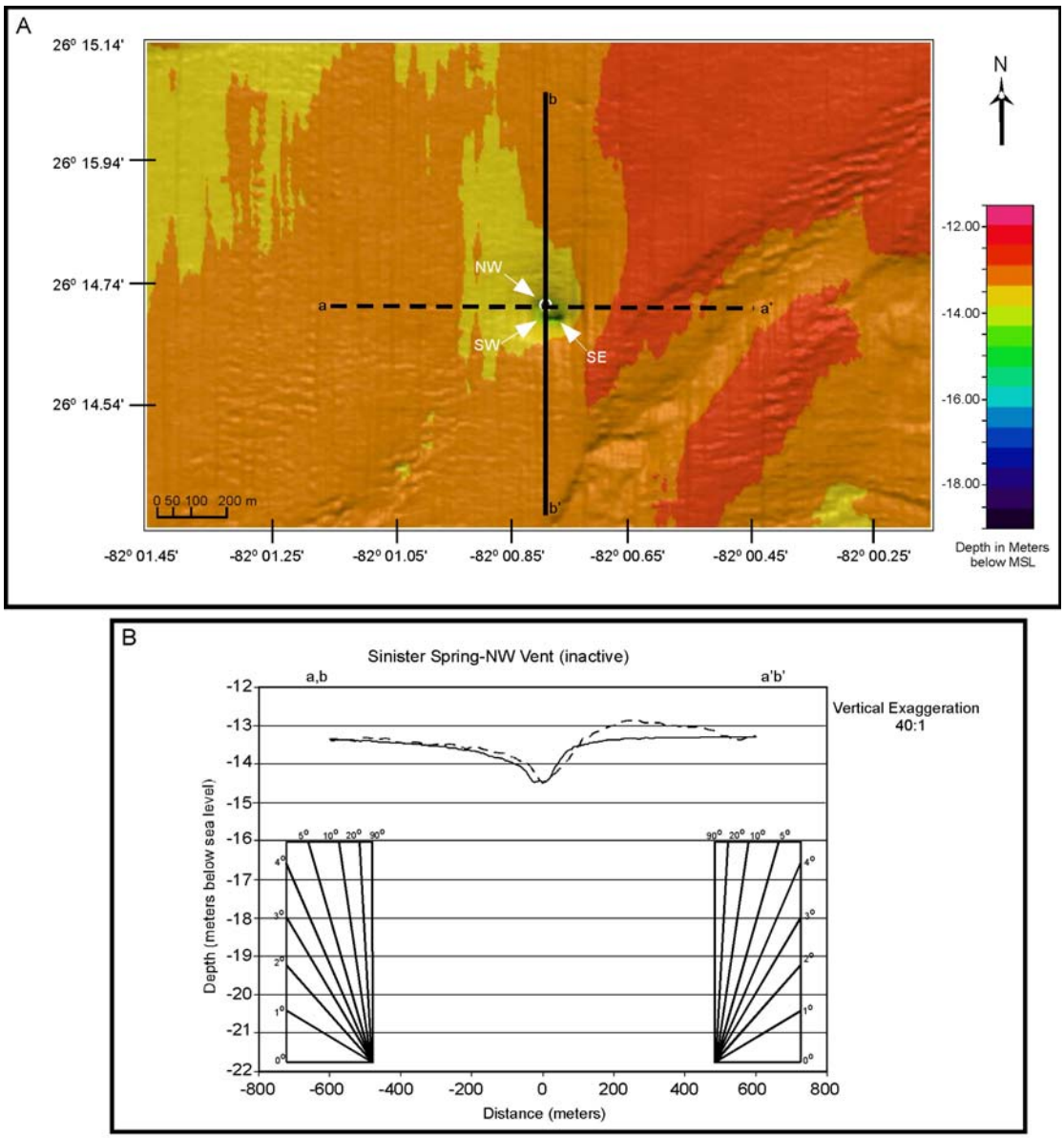

Figure 29. The upper image (A) is shaded color bathymetry of NW Sinister Spring. Within the depression are three distinct inactive vents: Northwestern vent, Southwestern vent, and Southeastern vent. The Northwestern vent (NW) location is shown by the white arrow. The lower image (B) is a cross section profile image of the northwestern vent of Sinister Spring. The distance of each profile measures 1200 meters across. The dashed line (a-a') is the west to east profile, and the solid line (b-b') is the north to south profile with a vertical exaggeration of 40:1. Note Figure A and B are offset so that the profile lines in the upper image (A) directly correspond to the profiles in the lower Figure (B).

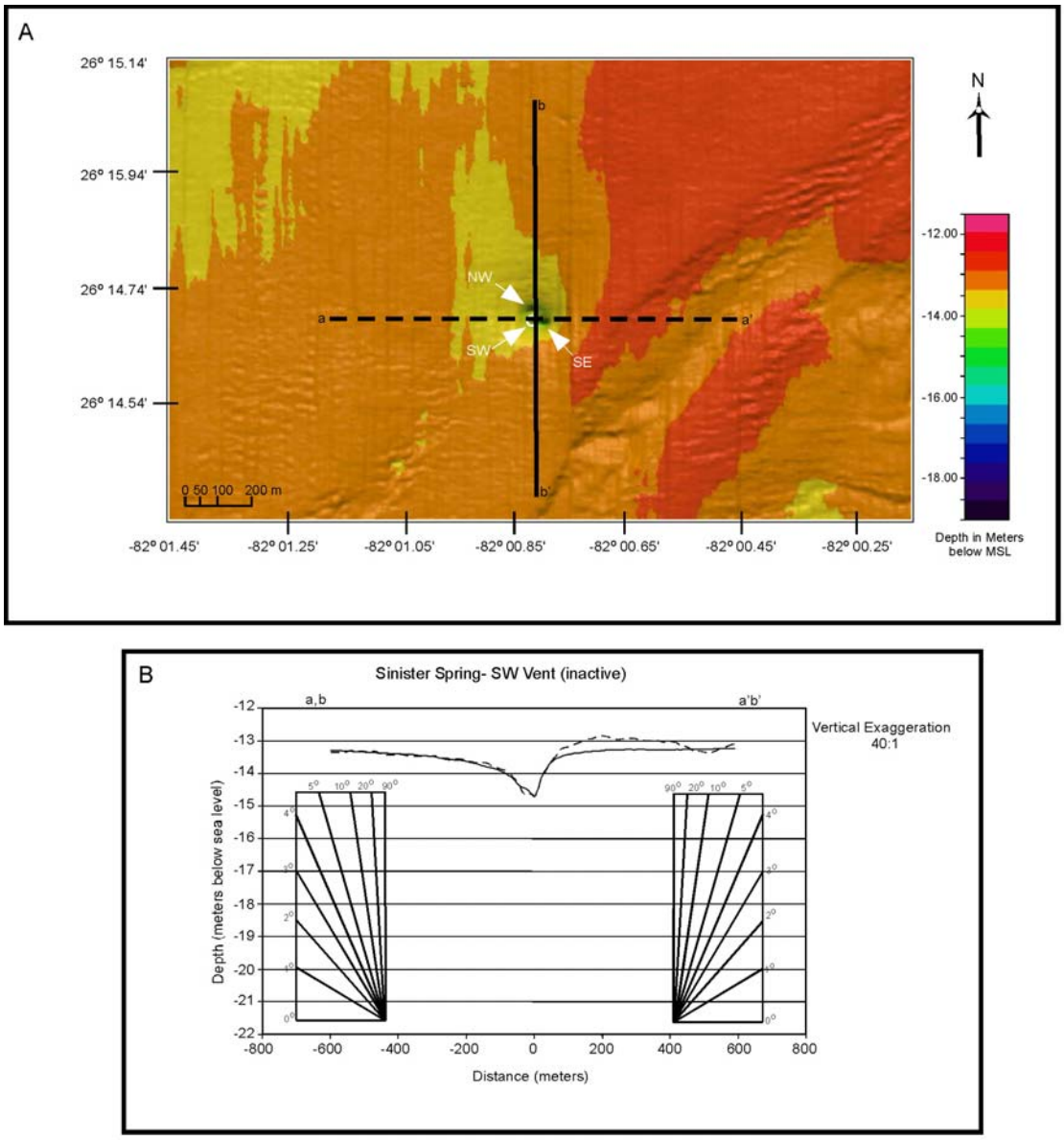

Figure 30. The upper image (A) is shaded color bathymetry of SW Sinister Spring. Within the depression are three distinct inactive vents: Northwestern vent, Southwestern vent, and Southeastern vent. The Southwestern vent (SW) location is shown by the white arrow. The lower image (B) is a cross section profile image of the northwestern vent of Sinister Spring. The distance of each profile measures 1200 meters across. The dashed line (a-a') is the west to east profile, and the solid line (b-b') is the north to south profile with a vertical exaggeration of 40:1. Note Figure A and B are offset so that the profile lines in the upper image (A) directly correspond to the profiles in the lower Figure (B).

The third inactive vent is located southeast of the depression, with its western slope having a slope of ~ 2^{o}, and ~5^{o} for its eastern slope (Figure 31). The northern slope has a slope of ~3^{o}, and the southern slope has a slope of 5^{o}. The SE vent has two distinct shapes, the W-E profile exhibits more of a "U" shape, while the N-S profile has a "V"-shape (Figure 31). The width (W-E, a-a') is ~150 meters across.

The entire depression (depression) of Sinister Spring is located in an area with probable coarse shells, rock, and gravel, which exhibits high backscatter intensity (Figure 14 and Figure 32). Directly southeast and southwest of this depression is an area of "roughness", which is likely to be a limestone hardbottom slope trending northeast (Figure 30).

Spring #3

Spring #3 (E) is an active spring located at 26^{o} 13.793'N and 82^{o} 02.418'W. The maximum depth is ~19.3 meters below sea level. The northern extent is -166 meters and the southern extent is 69 meters (Figure 20). The eastern extent is 60 meters and the western extent is -88 meters (Figure 21). The slope of the western slope of Spring #3 is ~10^{o} and the eastern slope has a very steep slope 30^{o} or more (dashed line, a-a'; Figure 33). The northern slope has a slope of ~13^{o} and the southern slope is also nearly 30^{o} (solid line, b-b'). Spring #3 has a "V" shape depression with its upper part measuring (a-a') ~196 meters across.

Spring #3 is not apparent in the backscatter image (Figures 14 and 34). It is located in an area of low backscatter intensity, probably consisting of fine sediments possibly sands and organic debris.

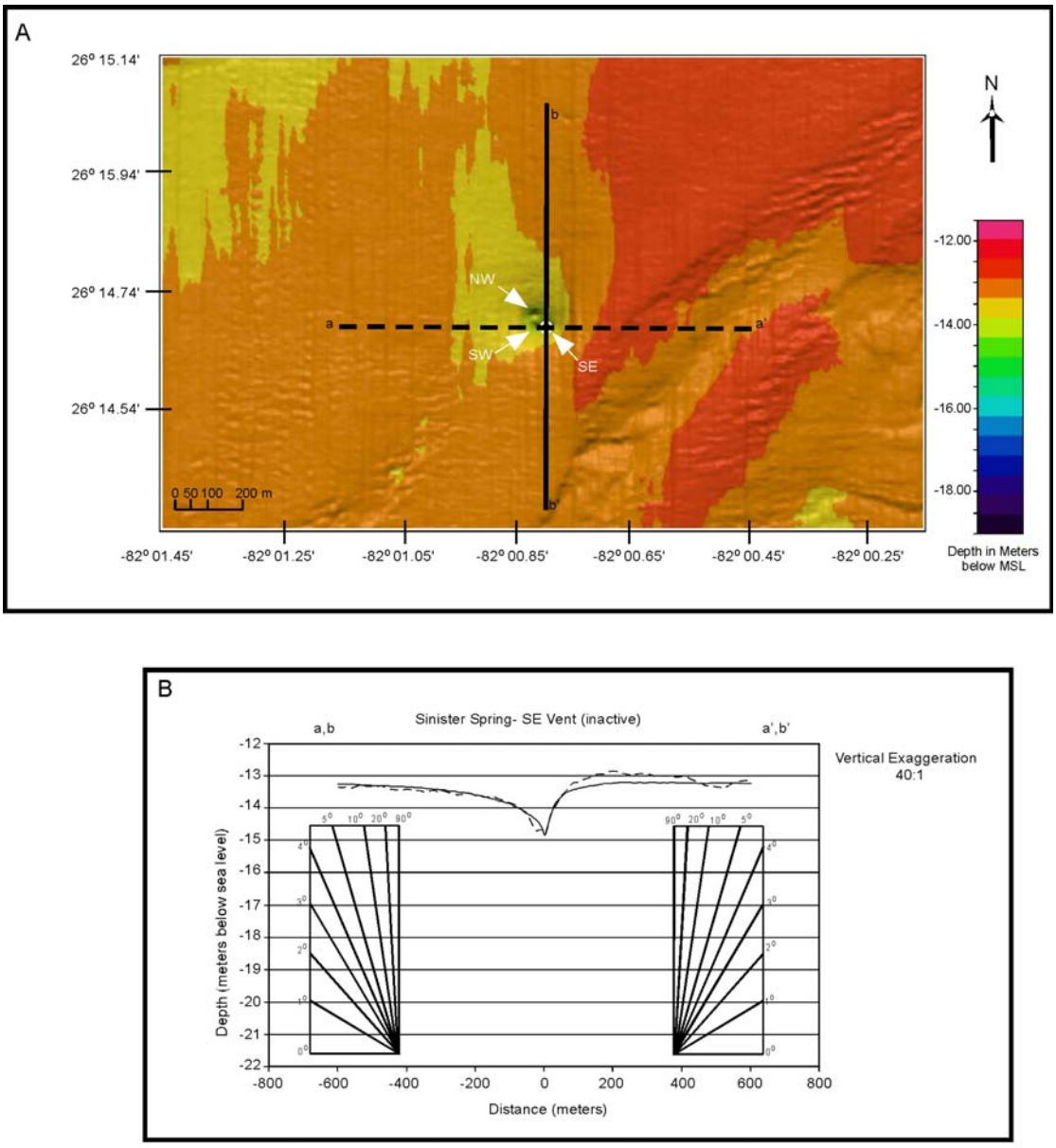

Figure 31. The upper image (A) is shaded color bathymetry of SE Sinister Spring. Within the depression are three distinct inactive vents: Northwestern vent, Southwestern vent, and Southeastern vent. The Southwestern vent (SW) location is shown by the white circle and the white arrow. The lower image (B) is a cross section profile image of the northwestern vent of Sinister Spring. The distance of each profile measures 1200 meters across. The dashed line (a-a') is the west to east profile, and the solid line (b-b') is the north to south profile with a vertical exaggeration of 40:1. Note Figure A and B are offset so that the profile lines in the upper image (A) directly correspond to the profiles in the lower Figure (B).

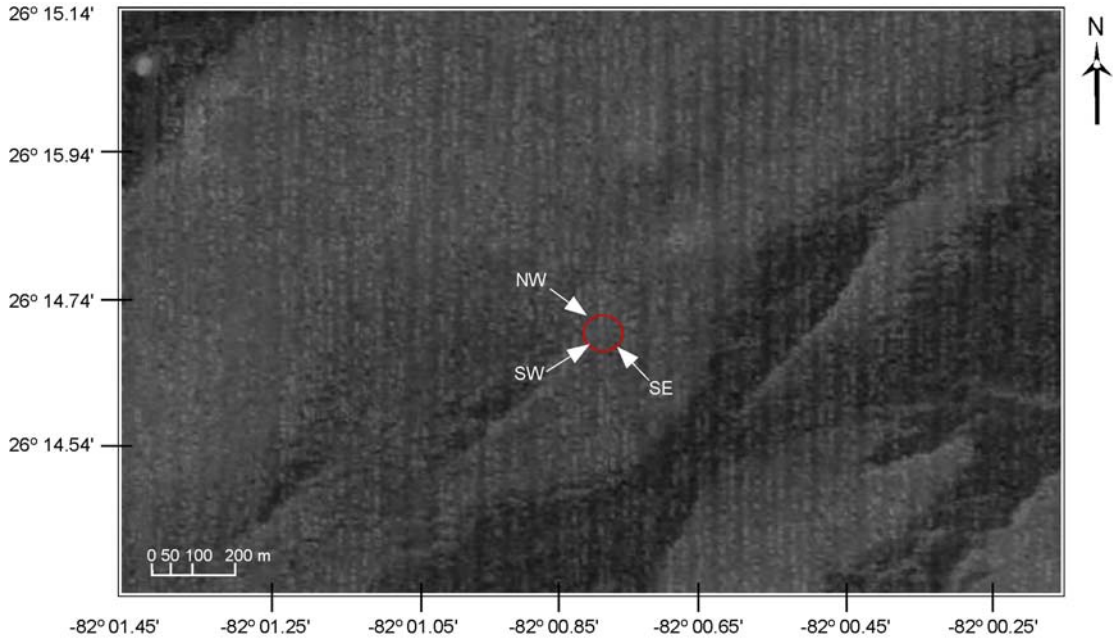

Figure 32. Backscatter image of the entire Sinister Spring (D) depressin. Red circle represents the location of the entire depression of active Rusty. Dark gray to black areas may represent limestone rocks, gravel, coarse shell or steep slopes (high backscatter). Light gray to white areas may represent fine sediments (low backscatter).

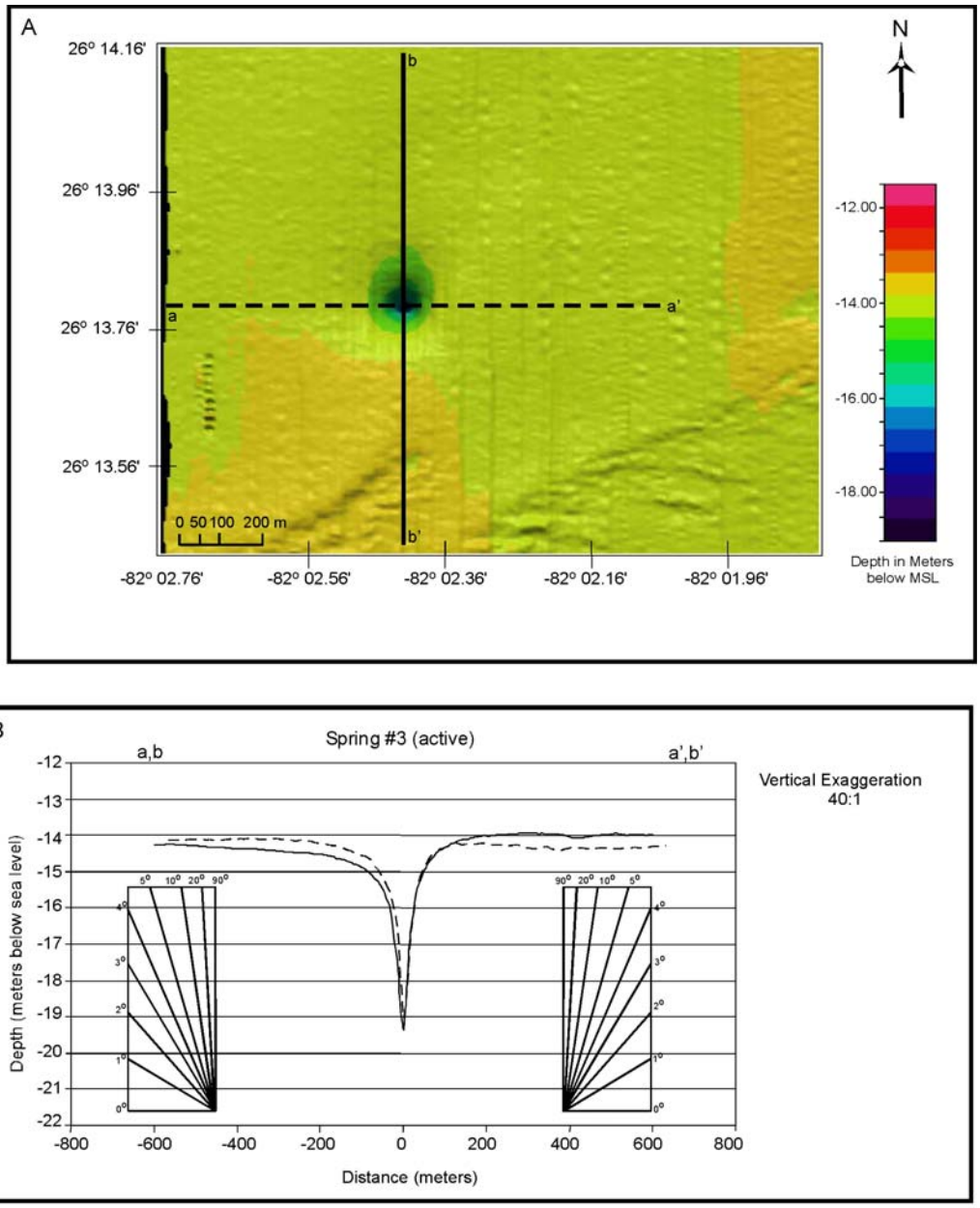

Figure 33. The upper image (A) is a shaded color bathymetry of Spring #3. The lower image (B) is a cross section profile image of Spring #3. The distance of each profile measures 1200 meters across. The dashed line (a-a') is the west to east profile, and the solid line (b-b') is the north to south profile with a vertical exaggeration of 40:1. Note Figure A and B are offset so that the profile lines in the upper image (A) directly correspond to the profiles in the lower Figure (B).

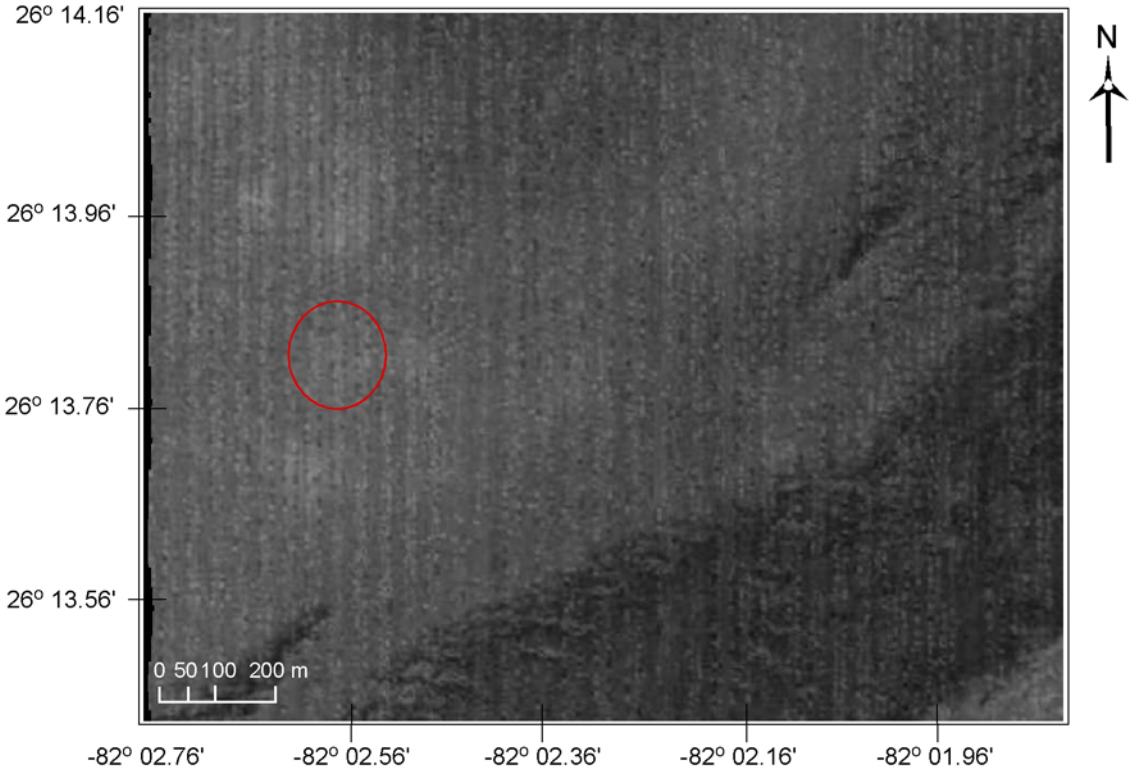

Figure 34. Backscatter image of Spring #3 (E). Red circle represents the location of the entire depression of active Spring #3. Dark gray to black areas may represent limestone rocks, gravels, coarse shell or steep slopes (high backscatter). Light gray to white areas may represent fine sediments especially sands or acoustic shadows (low backscatter).

New Spring

New Spring (F) is an active spring located at 26^{o} 14.265'N and 82^{o} 00.385'W. The maximum depth is ~15.8 meters. The northern extent is -34 meters and the southern extent is 21 meters (Figure 20). The eastern extent is 25 meters and the western extent is -36 meters (Figure 21). The slope for all four slope directions of New Spring is ~10^{o} (Figure 35). The N-S (b-b') and W-E (a-a') profiles are very similar and almost symmetrical. The shape of the depression is "V"-shaped, and the upper part (a-a') is ~75 meters across (Figure 35).

New Spring is also located in a medium backscatter area, probably consisting of sands in a shallow, nearly flat area (Figures 14 and 36).

Dormant Spring

Dormant Spring (G) is an inactive spring located at 26^{o} 16.245' N and 82^{o} 00.388' W in the upper northeastern corner of the study area. The maximum depth of the vent is ~14.5 meters below sea level. The northern extent is -174 meters and the southern extent is ~166 meters (Figure 20). The eastern extent of the depression is ~175 meters, and the western extent -128 meters (Figure 21). The western slope of Dormant Spring has a slope of ~2^{o}, while its eastern slope is ~1^{o} (dashed line, Figure 37). The northern and southern slopes are ~1^{o}. Dormant Spring has a very irregular shape, it appears to have a combination of both "V" and "U" shaped depression. The upper portion (a-a') is ~250 meters across.

Dormant Spring is located near an area of medium to low backscatter intensities, suggesting the occurrence of sands, and/or sediments s (Figures 14 and 38).

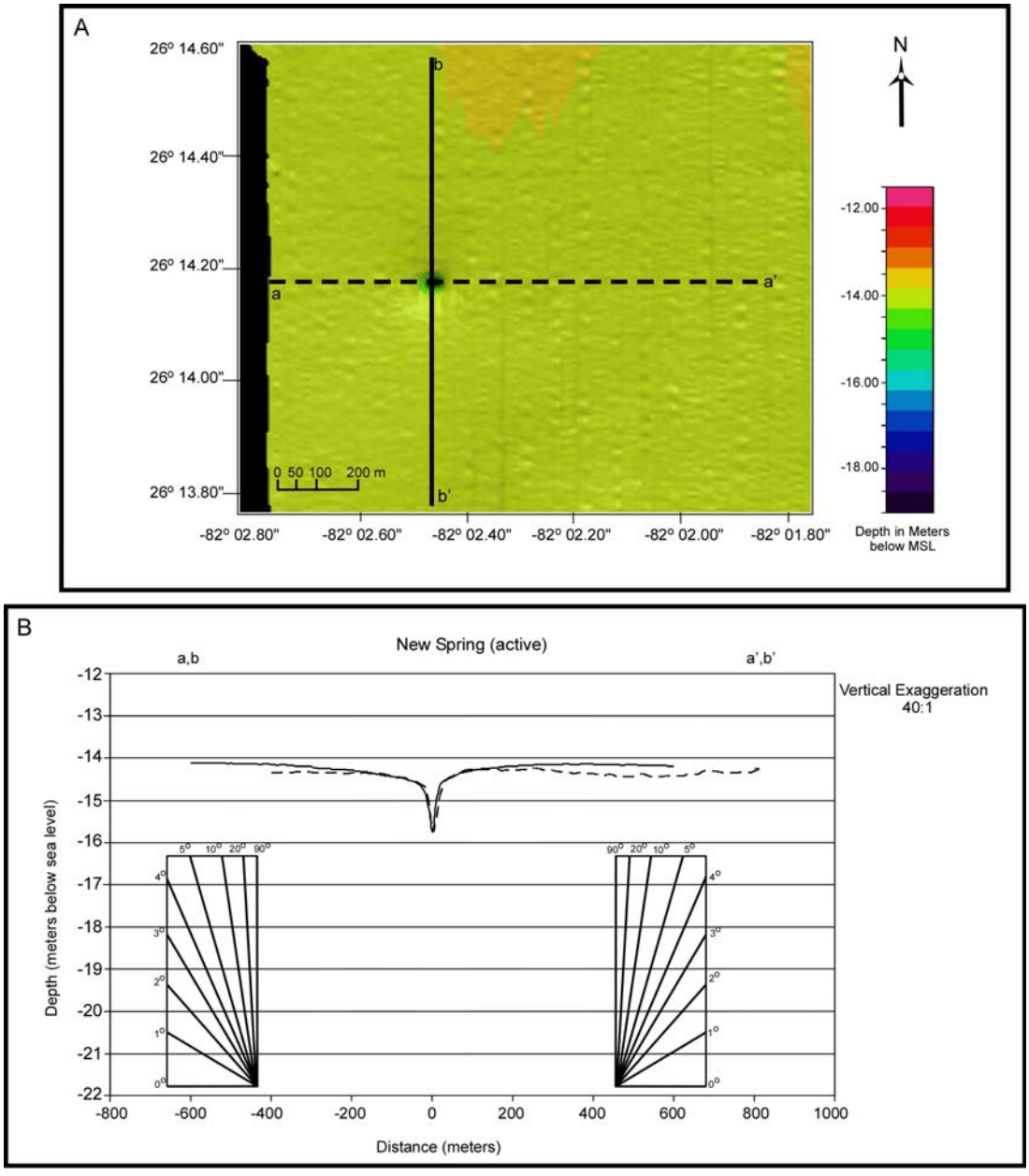

Figure 35. The upper image (A) is a shaded color bathymetry of New Spring. The lower image (B) is a cross section profile image of New Spring. The distance of each profile measures 1200 meters across. The dashed line (a-a') is the west to east profile, and the solid line (b-b') is the north to south profile with a vertical exaggeration of 40:1. Note Figure A and B are offset so that the profile lines in the upper image (A) directly correspond to the profiles in the lower Figure (B).

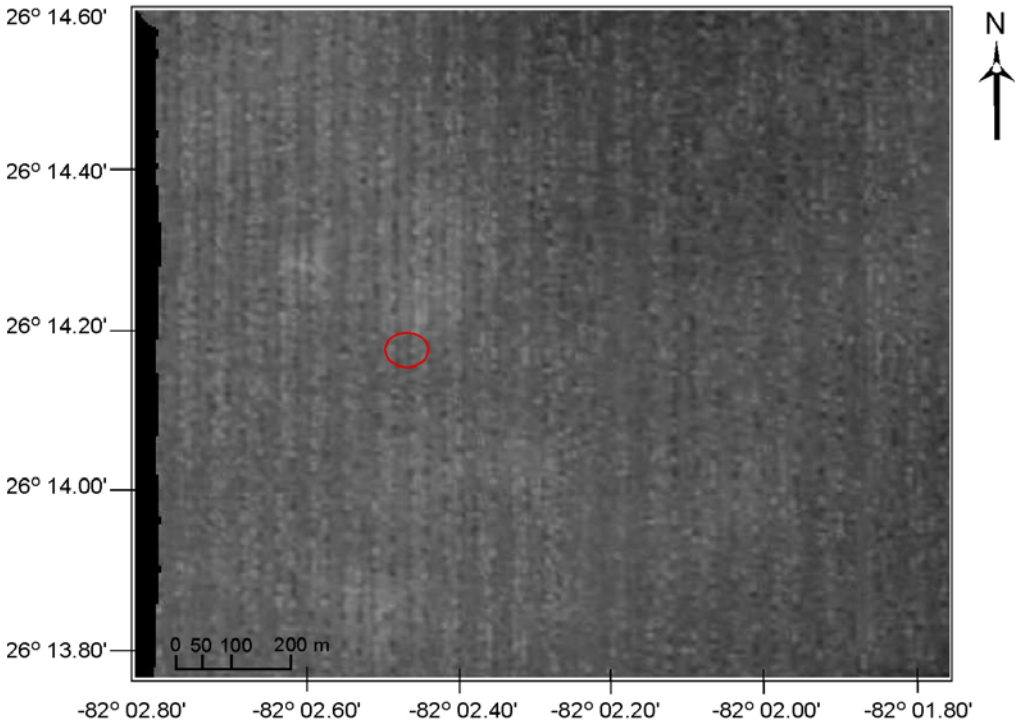

Figure 36. Backscatter image of New Spring (F). Red circle represents the location of the entire depression of active New Spring. Dark gray to black areas may represent limestone rocks, gravels, coarse shell or steep slopes (high backscatter). Light gray to white areas may represent fine sediments especially sands or acoustic shadows (low backscatter).

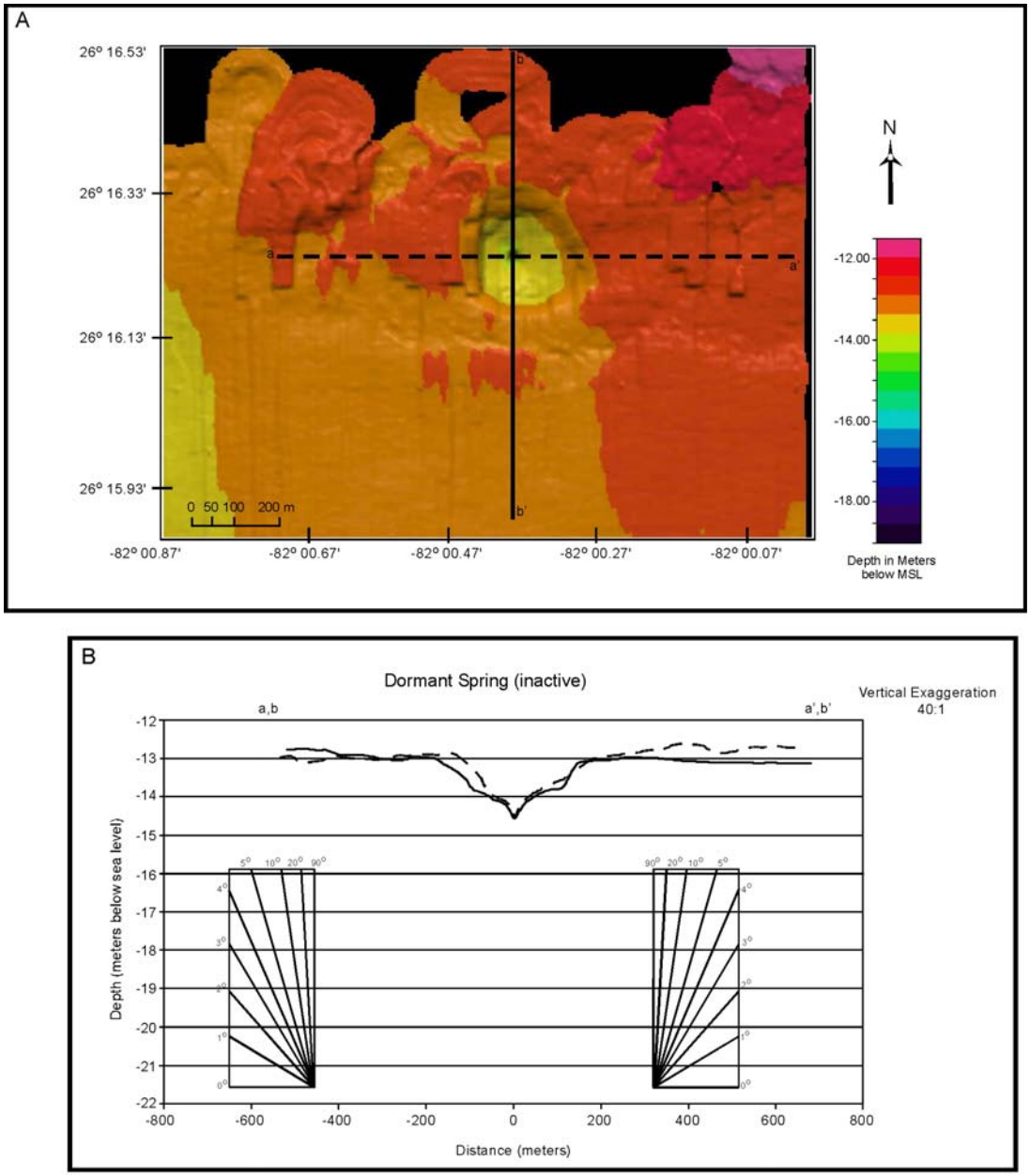

Figure 37. The upper image (A) is a shaded color bathymetry of Dormant Spring. The lower image (B) is a cross section profile image of Dormant Spring. The distance of each profile measures 1200 meters across. The dashed line (a-a') is the west to east profile, and the solid line (b-b') is the north to south profile with a vertical exaggeration of 40:1. Note Figure A and B are offset so that the profile lines in the upper image (A) directly correspond to the profiles in the lower Figure (B).

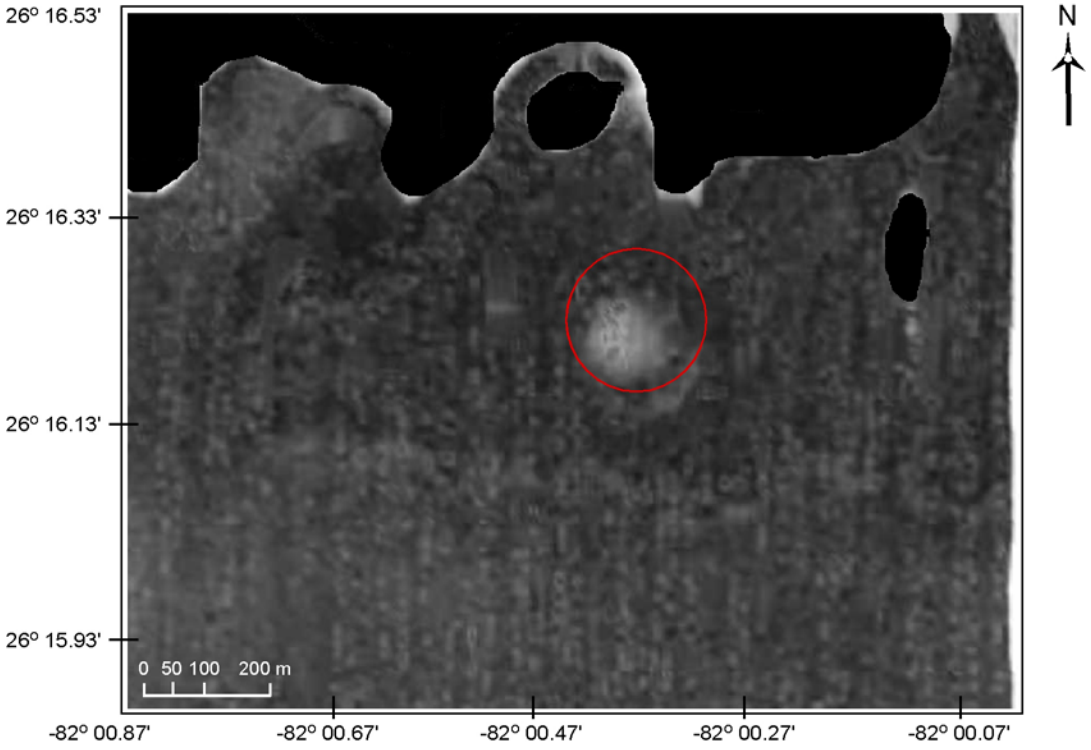

Figure 38. Backscatter image of Dormant Spring (G). Red circle represents the location of the entire depression of inactive Dormant Spring. Dark gray to black areas may represent limestone rocks, gravels, coarse shell, or steep slopes (high backscatter). Light gray to white areas may represent fine sediments especially sands or acoustic shadows (low backscatter).

It is important to note that the area surrounding Dormant Spring (Figure 37) has inherent may have some possible errors associated with the “turns” between the start and ending of track lines during data collection creating the appearance of an ‘uneven’ seafloor bottom.

Summary of Analyses

Structural Trend of Study Area

The structural trend of the MHSS study area was interpreted from the backscatter data (Figure 14), SCUBA observations, and the roughness of the bathymetry data (Figure 15). The backscatter image was used to generate a geologic interpretation map (Figure 39) that shows the locations of probable sediments (most likely fine to medium grain siliciclastic sediments with some carbonate material) and hardbottom (most likely limestone and/or carbonate shell hash). There is a general NE-SW structural trend with rough areas primarily located in the middle and south of the survey (Figures 14 and 39). These outcroppings are probably limestone bedrock represented as the dark or black areas in the backscatter image (Figure 14). The NE-SW trending sediment ridges are also observed west of Clearwater and Sarasota, Florida (Wolfson et al., 2007; McIntyre et al., 2006).

Slopes and Shape of Depression

Table 8 summarizes the slopes of the western, eastern, northern and southern slopes of the vents as well as the W-E (dashed line, a-a’) of the depression. New Spring and MHSS have the steepest slopes and are nearly symmetrical at 10^{o}. Spring #3

depression has the steepest eastern and southern slopes at 30^{o}. Spring #3 also has the steepest (13^{o}) northern slope. Dormant Spring and Sinister, the two inactive springs, have the gentlest slopes on the western of 2^{o}.

It is interesting to note that the inactive springs, Dormant Spring and Sinister, have a west to east "U" shape of the depression (with the exception of the Northern and Rusty Springs). Although the shape of Dormant Spring's depression is a combination of both shapes, the slopes of the depression of these inactive springs are much wider compared to the active springs. MHSS, Spring #3, and New Spring have a very distinct "V" shape and steep slopes, suggesting a strong effluent flow from its orifice. If the flow from the vent remains fairly constant and strong through time, the accumulation of sediments is less likely to occur in the depression. If the rate of the effluent is slow and not constant than more sediment may accumulate in the depression (infilling). The symmetry of the vent was determined using the W-E (dashed black line) profile. Most of the active vents (MHSS, Spring #3, and New Spring) exhibited symmetry to its W-E depression, while the two inactive vents (Dormant Spring and Sinister Spring depression) revealed an asymmetrical W-E depression. Although, the three vents within the Rusty Springs depression are active, the W-E depressions are asymmetrical. The reason for this variability is uncertain.

Extent of depression surrounding vents: Similarities and Differences

The northern extents of the depressions are greater than the southern extents (Figure 23). Such a pattern can be explained by a long term average of seawater in a northerly direction. This explanation will be further discussed in the next chapter.

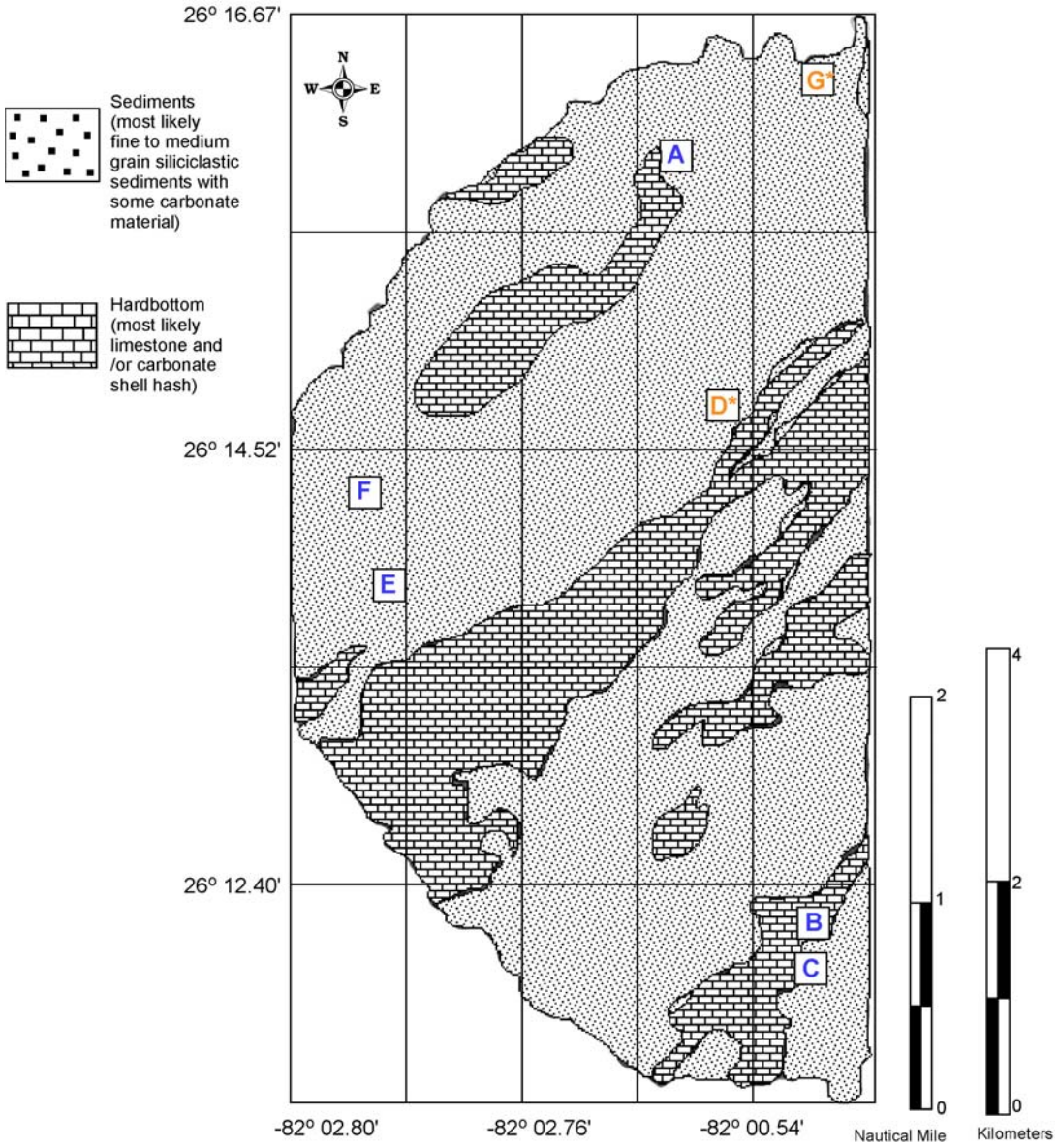

Figure 39. Geologic interpretation map of 2001 MHSS study area. Refer to backscatter image in Figure 14 and bathymetric image in Figure 15. The letters in orange and with an asterisk are inactive springs, Dormant Spring (G*) and Sinister Spring (D*). The blue letters are active springs: MHSS (A), Rusty (B), Near Rusty (C), Spring #3 (E), and New Spring (F). Sediment samples had not been obtained from study site, therefore interpretations are assumed from backscatter data and SCUBA observations.

Table 10. The slopes of western, eastern, northern, and southern slopes of the vents. The table also summarizes the shapes and symmetry of the west to east (dashed line a-a') depression of each spring.

Activity of Spring	Spring Name		Western Slope	Eastern Slope	Northern Slope	Southern Slope	Shape of the W-E depression (dashed line a-a')
ACTIVE	MHSS (A)		10°	10°	10°	10°	"V" shape symmetrical
	Rusty (B)		4°	3°	2°	6°	"V" shape asymmetrical
		Northern Rusty	3°	3°	2°	6°	"U" shape asymmetrical
	Near Rusty (C)		<1°	3°	1°	3°	"U" shape asymmetrical
	Spring #3 (E)		10°	30°	13°	30°	"V" shape symmetrical
	New Spring (F)		10°	10°	10°	10°	"V" shape symmetrical
INACTIVE	Dormant Spring (G)		2°	1°	1°	1°	"V" and "U" shape asymmetrical
	Sinister Spring (D)	NW	2°	2°	2°	2°	"U" shape asymmetrical
		SW	2°	3°	1°	3°	"U" shape asymmetrical
		SE	2°	5°	3°	5°	"U" shape asymmetrical

The N-S artifact is too small (cm's) to account for this observation (10's cm). The depression surrounding MHSS has the greatest northern extent at 338 meters. New Spring (NS) has the least (shortest) northern extent at 34 meters. The southern extent of the depression surrounding Dormant (D*, “inactive”) is the greatest at 166 meters, while the southern depression surrounding New Spring (NS, “active”) is ~21 meters. The extent of the depressions surrounding Sinister (S*, “inactive”), New Spring (NS, “active”) and Spring #3 (S 3 “active”) have the least extent in both the southern and northern directions. In the backscatter image (Figure 14), the springs are located in medium dark to light gray areas, interpreted to be most likely fine to medium grain siliciclastic sediments with some carbonate material. Although Sinister Spring was inactive at the time of the cruise, the three depressions suggest three individual point sources of previous effluent flow. Diffuse flow within the seepage field may have occurred leading to its present northern and southern shape. The activity of New Spring and Spring #3, with only one possible point source of effluent flow and steep slopes (Table 8), suggests that its flow may be stronger and less diffuse. However, the northern, southern, eastern, and western extents of New Spring are much shorter than the other springs (Figures 20 and 21). This may suggest the activity may be recent or exceptionally strong.

The western and eastern extents of the depressions are variable (Figure 21). The depression surrounding Dormant Spring (D*, “inactive”) has the greatest eastern extent at 175 meters, and New Spring (NS, “active”) has the smallest extent at 25 meters. At 170 meters, the depression surrounding MHSS is greatest at the western extent and New Spring has the least extent at -36 meters. Sinister (S*, “inactive”), New Spring (NS,

“active”) and Spring #3 (S 3, “active”) have the smallest vent extents, both eastern and western.

Ambient Seafloor Depths

According to Figure 40, which compares the depth of the vent below seafloor and the ambient seafloor depth, filled polygons represent springs that are inactive, and open polygons are springs that are active. The depth of a vent below seafloor (Z) is the difference between the maximum depth of the vent (Y) and the ambient depth around the vent (X). Dormant Spring and Sinister Spring are the shallowest vents below the seafloor according to the ambient seafloor depth. The depth of Dormant Spring below the seafloor is 2 meters, and the ambient seafloor depth of -12.8 meters. The depth of the northwestern (NW) and southwestern (SW) vents of Sinister Spring’s depression is 1 meter with an ambient seafloor depth of 13.3 meters. The depth of the southeastern (SE) depression is 1.5 meters and the ambient seafloor depth is 13.3 meters. MHSS and Spring #3 have the deepest depths below the ambient seafloor depths. The depth of both vents below seafloor is 5 meters, and the ambient seafloor depths of MHSS and Spring #3 are -13.8 meters, -14.3 meters. Northern Rusty and Rusty have the same depth below seafloor at 3 meters and both have an ambient seafloor depth of 13.5 meters. Near Rusty has the same ambient seafloor as Northern Rusty and Rusty Spring, although the maximum depth of Near Rusty is shallower at 14.9 meters. New Spring’s ambient seafloor depth is the deepest area of the study area at 14.4, and its depth is 1 meter depth below the seafloor.

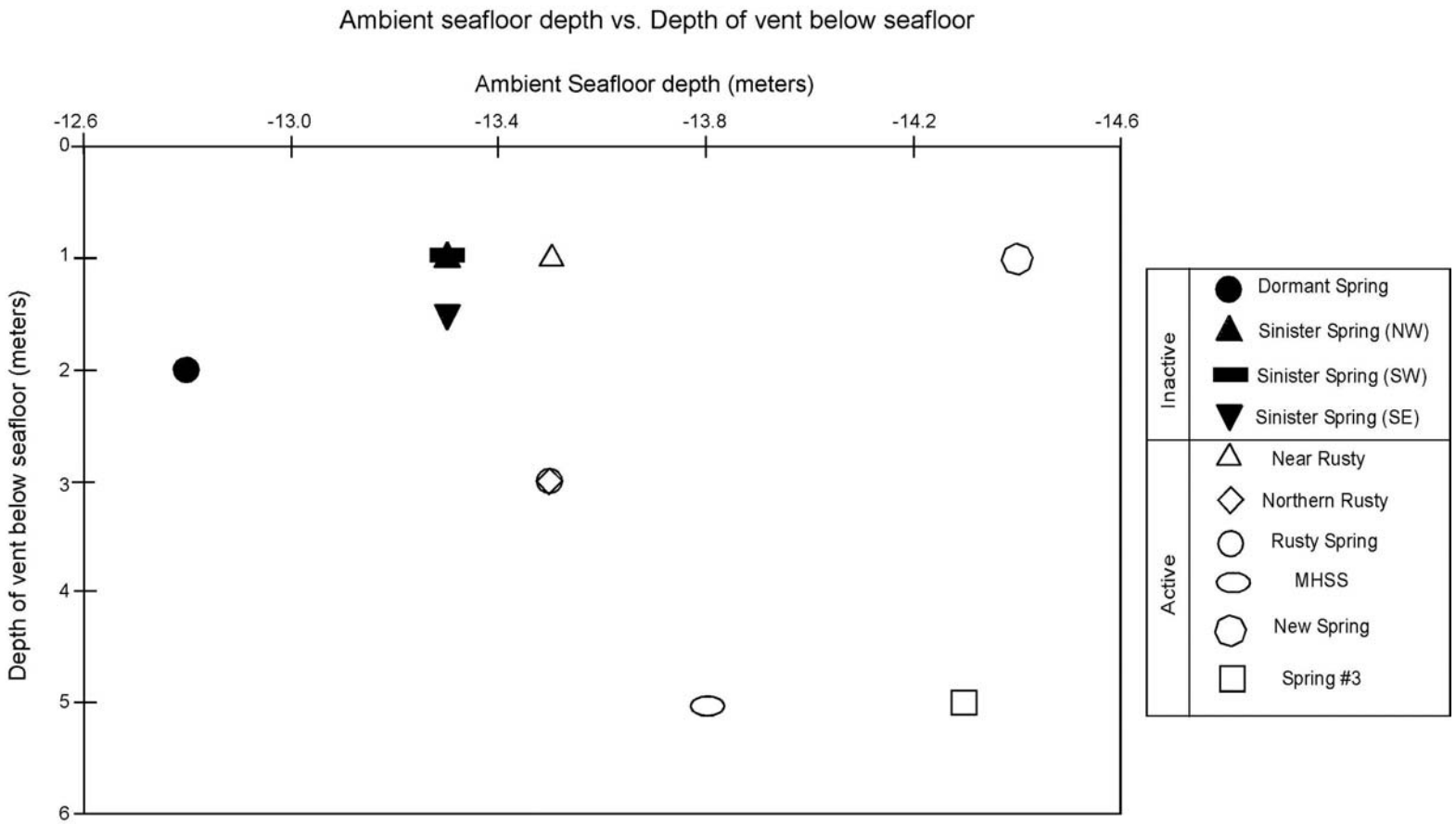

Figure 40. Depth of vent below seafloor vs. Ambient seafloor depth. The filled polygons represents vents that are 'extinct' or 'inactive'. Open polygons represents vents that are 'active'.

Ambient seafloor depths around vents are compared to maximum depths of below sea level in Figure 41. As expected, Figures 40 and 41 show similar patterns. As mentioned above, filled polygons represents springs that are inactive and open polygons are springs that are active. Dormant Spring, (inactive) Sinister Spring (inactive) and Near Rusty (active) have the shallowest maximum depths, 14.5, 14.6, 14.9 meters. These figures and tables show that active springs have the deepest maximum depths and are located at the deepest ambient seafloor depths compared to the two inactive vents.

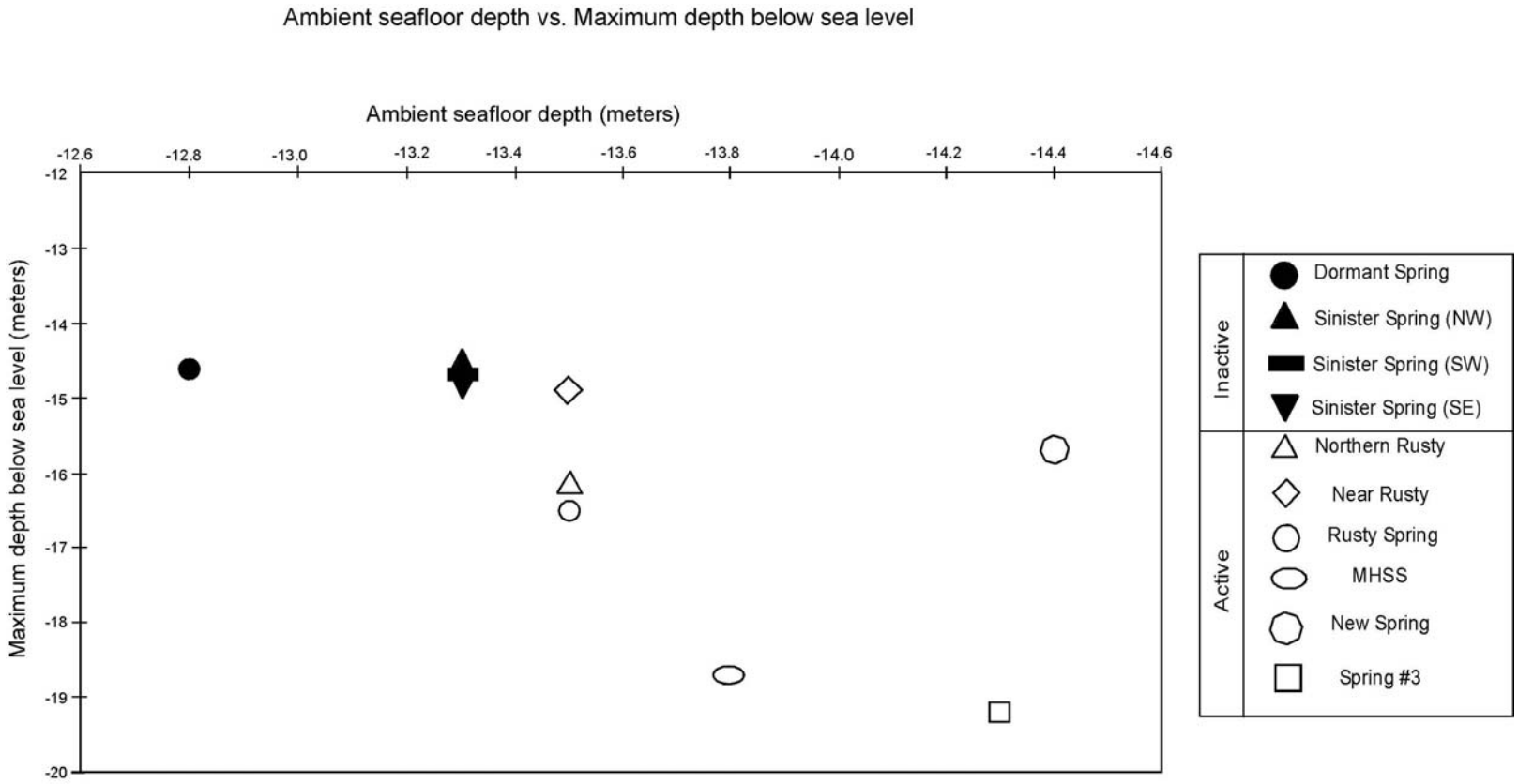

Figure 41. Ambient seafloor depth around vents vs Maximum depth below sea level. Filled polygons represents vents that are 'extinct' or 'inactive'. Open polygons represents vents that are 'active'.

Chapter 5

DISCUSSION

This chapter discusses results related to the research questions stated in Chapter One:

1. Do the spatial patterns of active and extinct vents line up with known vents on land as stated by Kohout (1977) and Breland (1980)?
2. If not, do seafloor structural trend in the MHSS study area correlate with vent distributions?
3. Does vent geomorphology vary from vent to vent?
4. Is there a correlation between the published geochemistry of the vent sites and vent geomorphology?

Spatial patterns of submarine springs and land springs

This study corroborates that there is a rough north-south correlation with vents on land compared to active and inactive (extinct) vents on the seafloor as shown in Figures 1, 2, 8, and 9. The submarine springs in the MHSS study area are situated along an axis of the Florida Platform near the west coast (Kohout 1965, 1967, and Schijf and Byrne, 2007) (Figures 1 and 9). However, in this study Figures 8 and 9 show the occurrence of land springs and submarine springs are predominantly located northwest of the red line (within the limits of observations of the Everglades and offshore). A probable

explanation of these occurrences may be due to the thickness of the upper confining units of the Floridan aquifer system (Figure 2). Most of the land and submarine springs are located in areas where the aquifer system is unconfined (upper confined unit is absent or thin) or thinly confined (upper confining unit is generally less than 100 feet thick, breached or both). However, where the Floridan aquifer system is confined (upper confining unit is generally greater than 100 feet thick and unbreached-separated by thick red line) several warm saline submarine springs (MHSS study area) occur off the west coast of Florida. Due to this confined area, lands springs may not occur. However, the dissolution of the limestone on the seafloor of the west Florida Platform provides a more probable outlet for seawater to escape. Thus, in view of the occurrence of the submarine springs found off the southwest coast of Florida, more geothermal vents may be discovered offshore.

In a study conducted by Schijf and Byrne (2007), several geochemical analyses were performed on four springs in the MHSS study area (MHSS, Spring #3, New Spring and Rusty Springs), Warm Mineral Spring (WMS) and Crescent Beach Submarine Spring (CBS). CBS is a warm water spring located off the northeastern coast of Florida in the Atlantic Ocean. When plotting the Na versus Mg as an indicator of dolomitization between CBS, groundwater, WMS, and the four submarine springs, they found that WMS and CBS seems to be a mixture of groundwater and spring effluent, thus confirming connection of WMS with the submarine springs system (Table 11 and Figure 42).

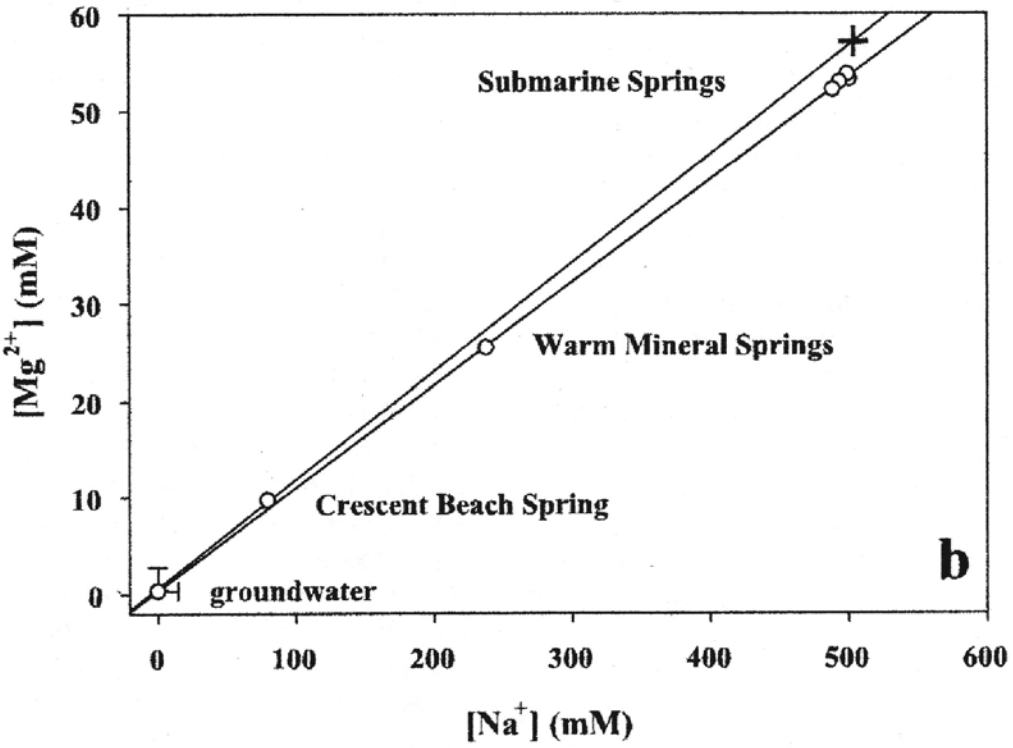

Figure 42. Mixing lines defined by Mg concentrations of fresh groundwater from the Floridan Aquifer System and of all spring effluents analyzed in this work (Table 11). The crosses represent ambient seawater. Points labeled "groundwater" are the median of 18 samples from Central Florida, analyzed by Back and Hanshaw (1970) and converted to millimolar units. The small error bars on these points indicate the upper bound of each concentration range. Solid lines are linear regressions. Figure from Schijf and Byrne (2007).

Table 11. Spring Effluent Compositions[a]. Table from Schijf and Byrne, 2007.

Location	$[Na^+]$	$[K^+]$	$[Mg^{2+}]$	$[Ca^{2+}]$	$[Cl^-]$	$[SO_4^{2-}]$	$[Sr^{2+}]$	$[Ba^{2+}]$
Seawater[b]	480	10.4	54.0	10.5	559	28.9	91[c]	30–72[d]
Rusty Springs	499 ± 10	10.8 ± 0.2	53.7 ± 1.0	14.1 ± 0.2	565 ± 13	29.6 ± 0.7	127 ± 2	164 ± 5
Spring 3	494 ± 4	10.6 ± 0.1	52.9 ± 0.6	14.0 ± 0.1	554 ± 4	29.3 ± 0.2	131 ± 0.3	200 ± 3
New Spring	489 ± 6	10.5 ± 0.2	52.1 ± 0.8	13.7 ± 0.1	557 ± 0.1	29.1 ± 0.04	134 ± 0.5	209 ± 1
MHSS	501 ± 9	10.8 ± 0.2	53.2 ± 0.9	14.5 ± 0.3	563 ± 11	29.6 ± 0.6	149 ± 3	244 ± 6
WMS	238 ± 4	4.8 ± 0.1	25.5 ± 0.4	12.7 ± 0.1	273 ± 2	18.0 ± 0.2	357 ± 3	320 ± 4
Published[e]	240	4.7	23.8	12.3	282	17.7	410	-
CBS[f]	79.6 (±0.6)	1.48 (±0.02)	9.78 (±0.09)	6.97 (±0.09)	92.4 (±0.3)	7.94 (±0.04)	97.7 ± 0.8	259 ± 2
Published[g]	87.00	1.07	8.72	6.49	96.75	7.77	90	300.7
Published[h]	88.74	1.64	10.37	7.39	102.39	8.50	100	-

[a]Standard seawater (S = 35.00) is shown for comparison. All concentrations in mM, except Sr (μM) and Ba (nM). Major ion concentrations determined by ion chromatography. Sr and Ba concentrations determined by ICP-MS. Values for each spring are the average of all samples collected during the period 1997–2003 (±1 standard deviation). Errors in parentheses are based on regression statistics; see text. Springs are arranged in order of increasing latitude (south to north; Figure 2).

[b]All concentrations, except $[Ba^{2+}]$, correspond to salinity 35.00; major ions after *Millero* [1996].

[c]After *Byrne* [2002].

[d]Range of surface water concentrations across the shelf break off the South Carolina coast [*Moore and Shaw*, 1998].

[e]*Scott et al.* [2004, Table 162].

[f]Sample kindly provided by P. W. Swarzenski, USGS, St. Petersburg, Florida.

[g]*Swarzenski et al.* [2001].

[h]*Toth* [1999, Table 3].

Seafloor structural trends

Vent distribution in the MHSS study area appears to correlate with the structural trend of the seafloor. According to Figures 14, 15, and 16 the vents, both active and inactive, appear to occur in areas of low relief, fine sediments, and/or a mixture of both fine sediments and coarse shells. However, rough areas, typically limestone outcroppings trending NE-SW may have venting without the characteristic circular depression seen in the sedimented areas. Fine and mixed sediments (sands) are distributed between the outcroppings and are evident where vents occur (Figure 39).

There appears to be a NE-SW structural trend of the overall sediment distribution along the seafloor (Figures 14 and 15). As one moves from the open ocean (west) of the MHSS study area towards the land (east), the seafloor becomes progressively shallower, with NE-SW bands of exposed limestone, and sediment bedforms (shown in orange). Evidence of this trend is shown by the orientation of the seafloor surrounding the vents. All of the vents, both active and inactive, have longer northern and eastern extents (Figures 20 and 21). The morphology of the seafloor in the study area may be dominated by low energy storm (wave) dominated or tide dominated processes (Brooks et al., 2003).

Variations in vent morphology

Geomorphology varies from vent to vent. Vent activity also seems to affect the geomorphology. Table 8 summarizes the activity and shape of each vent's W-E depression. Most of the active springs: MHSS, Spring #3, and New Spring, (with the exception of the vents within Rusty Springs depression) exhibit steeper walls than the inactive springs, Dormant Spring and Sinister Spring. It is important to note that the angle

of repose (the angle measured from horizontal at which grains start to roll is affected by size, mass, angularity and dampness of particles), is a lesser factor for infilling of depressions after vent activity ceases. According to Miller and Byrne (1966), variations of the angle of repose ranged from nearly 90^{o} to less than 20^{o}, depending on the following: grain sphericity, grain angularity, grain size , and grain sorting. Due to the variability of such factors, determining the angle of repose of marine sediments is a difficult problem. However, it is understood that particles that rest in deep pockets (i.e., marine sediments located in the deepest part of the vent depression) are harder to move than particles in shallow pockets (i.e., marine sediments more located near top of the depression), (Schmeeckle and Nelson, 2003). However, if one considers that any circular depression will slowly start to trap sediments that are redistributed during tidal flow, one would expect inactive vents to slowly fill up and become less steep and less deep. This expectation is supported by the results of the geomorphologic analyses of slope and relative depth in this study.

MHSS, has a high backscatter return and is located in an area mostly composed of gravel and coarse shells. The overall outline of the depression is irregular. However the depth of the conical "V"-shaped orifice is almost symmetrical with the western, eastern, northern, and southern slopes of 10^{o} (Figures 14 and 22). There appears to be some scouring towards the north of the depression (Figure 22 shown in light green).

Spring #3 and New Spring are both located in areas of low backscatter where the seafloor is mostly composed of sands and fine sediments. The ambient seafloor surrounding Spring #3 and New Spring is also similar at ~14 meters. The overall outline of the depression of these springs is circular, with a conical "V"-shaped depression and

sloped sides of ~10^{o}. MHSS, although situated in a different geomorpholoical setting than Spring #3 and New Spring, has the same “V”-shaped orifice and closely similar shape characteristics. It can be inferred that this difference may be due to a moderate flux of effluent flowing from MHSS.

Rusty and Near Rusty are located in an area of both low and high backscatter. The overall depression is situated in a very dynamic setting. The outline of the depression surrounding all the vents of Rusty Springs (Northern Rusty, Rusty Spring and Near Rusty) is irregular and appears to have a north by northeast orientation (Figures 24, 25 and 27). West of the depression there appears to be a limestone outcrop, to the north the bottom type appears to be mostly consisting of sands and fine grained sediments, and south of the depression the seafloor also appears to be mixed, probably rocks, gravel, and coarse shells (Figure 39). Such a variable seafloor setting can be a reason for the less steep slopes of both springs. Although the western, eastern, northern, and southern slopes of Northern Rusty and Rusty are very similar, the shape of the W-E depression of each spring differs (Table 8). The western and eastern slope of Northern Rusty is 3^{o}. The northern slope is 2^{o} and the southern slope is 6^{o}. Rusty’s western slope is 4^{o} and its eastern slope is 3^{o}, while its northern and southern slopes are the same as Rusty. Rusty exhibits a “V”-shape, while Northern Rusty has more of a “U”-shape. This difference may be related to a variation in effluent flux, and a possible long-term average flow of seawater in a more northerly direction. Strong flux would keep the depression steep and clear of sediments and suspend them into the water column where they would drift.The Near Rusty vent, although active, appears to have similar slopes and shapes to those of

the inactive vents. The western and northern slopes range from ~<1^{o} to 1^{o}, and its eastern and southern slopes are both 3^{o}.

The inactive or extinct vents, Sinister Spring and Dormant Spring, exhibit less steep slopes and "U"-shaped depressions (Table 8). The western slope of Dormant Spring is 2^{o}, its eastern slope is 1^{o} and its northern and southern slopes are both 1^{o}. The overall depression of Sinister Spring has three distinct orifices (northwest, southwest and southeast), and can be termed as an inactive "seepage field". The northwest depression of Sinister Spring has a western and eastern slope of 2^{o}. The northern and southern slopes are 2^{o}. The southwest depression of Sinister Spring has a western slope of 2^{o} and an eastern slope of 3^{o}. The northern slope is 1^{o} and the southern slope of the depression is 3^{o}. The western slope of Sinister Spring's southeast depression is 2^{o}, while its eastern slope is 5^{o}. The northern slope is 3^{o} and the southern slope is 5^{o}. The immediate depression of the seepage field is nearly circular, ~14 meters below ambient seafloor depth (Figures 29, 30, and 31). The orifice of Dormant Spring is shown with low backscatter suggesting fine sediments. The profile of Dormant Spring shows more of a "stair-step" shape from its deepest point to the ambient depth of the seafloor on the northern and southern edges (Figure 32). The suspected fine sediments located near the orifice of the vent may be attributed to the inactivity of the spring and subsequent infilling of the depression (Figure 14).

As described at the end of Chapter 4, the deepest vent depth and steepest slope are apparently related to active vent flux. However, the reason for an absence of active venting at shallow ambient seafloor depths is not clear.

Geochemistry and vent geomorphology

In a study by Schijf and Byrne (2007), spring effluent ratios of alkaline earth element to Na concentrations, where Na represents salinity, was normalized to corresponding seawater ratios (Table 11). To emphasize the small deviations in composition, Schijf and Byrne (2007) divided each ion/ion ratio in the spring effluents by the corresponding value in seawater. Note: all ratios are in mol/mol, except for Sr/Na (10^{-3} mol/mol) and Ba/Na (10^{-6} mol/mol). In order to remove all analytical bias three measured ambient seawater samples were averaged (Schijf and Byrne, 2007). The results are shown in Figure 43, with values smaller or larger than 1 indicates a depletion or enrichment of the numerator ion (dashed line) with respect to seawater. Figure 44 displays the elemental ratios of Ba/Na of Rusty Springs (B & C), MHSS (A), Spring #3 (E) and New Spring (F). The elemental ratio of Ba/Na of Rusty Springs (also named Rusty and Near Rusty) is 0.33 ±0.01. The Ba/Na ratio of: Spring 3 is 0.406 ±0.008, New Spring is 0.429±0.008, and MHSS is 0.488±0.009. In Figure 45, the elemental ratios of Sr/Na (refer to Table 11) for the submarine springs noted above is arranged in order of increasing latitude (Schijf and Bryne, 2007). The Sr/Na concentration of: Rusty Springs is 0.255±0.004, Spring 3 is 0.266±0.003, New Spring is 0.274±0.005, and MHSS is 0.298±0.003. The elemental ratio of Ca/Na in ambient seawater for: Rusty Springs is 0.0282±0.0003, Spring 3 is 0.0283±0.0002, New Spring is 0.0280±0.0002, and MHSS is 0.0289±0.0003 (Figure 46). The elemental ratios for Mg/Na are also shown in Figure 47. The concentration of: Rusty Springs is 0.1076±0.0005, Spring 3 is 0.1072±0.0005, New Spring is 0.1067±0.0003, and MHSS is 0.1063±0.0004. Schijf and Byrne (2007) noted the apparent depletion of Mg/Na in spring effluent as one moves north towards MHSS.

Rusty Springs is slightly more enriched than the remaining three active springs. The enrichment of Rusty Springs effluent may be directly influenced by its geomorphological setting (Figures 14 and 39).

There were no additional observations or spatial correlations discovered beyond those of Schijf and Byrne (2007) after the geochemical data were plotted directly on the high-resolution multibeam bathymetry data.

Table 12. Elemental Ratios in Ambient Seawater, Submarine Springs, WMS, and CBS[a]. Table from Schijf and Byrne, 2007

Location	K/Na	Mg/Na	Ca/Na	SO_4/Cl	Sr/Na	Ba/Na
Seawater[b]	0.0218	0.1126	0.0219	0.0517	0.190	-
1997[c]	0.0215 ± 0.0001	0.1128 ± 0.0001	0.0220 ± 0.0001	0.0519 ± 0.0001	0.175 ± 0.002	0.119 ± 0.005
1999[d,e]	0.0219 (±0.0002)	0.114 (±0.001)	0.0222 (±0.0003)	0.0517 (±0.0003)	0.178 (±0.002)	0.089 (±0.002)
2000[f]	0.0218 (±0.0002)	0.1134 (±0.0008)	0.0219 (±0.0002)	0.0519 (±0.0004)	0.173 (±0.002)	0.106 (±0.005)
Rusty Springs	0.0216 ± 0.0003	0.1076 ± 0.0005	0.0282 ± 0.0003	0.0524 ± 0.0004	0.255 ± 0.004	0.33 ± 0.01
Spring 3	0.0214 ± 0.0001	0.1072 ± 0.0005	0.0283 ± 0.0002	0.0529 ± 0.0003	0.266 ± 0.003	0.406 ± 0.008
New Spring	0.0215 ± 0.0002	0.1067 ± 0.0003	0.0280 ± 0.0002	0.0523 ± 0.0001	0.274 ± 0.005	0.429 ± 0.008
MHSS	0.0215 ± 0.0002	0.1063 ± 0.0004	0.0289 ± 0.0003	0.0526 ± 0.0003	0.298 ± 0.003	0.488 ± 0.009
MHSS[g]	0.0217	0.107	0.0299	0.0525	-	-
WMS	0.0202 ± 0.0001	0.1071 ± 0.0000_4	0.0535 ± 0.0003	0.066 ± 0.001	1.503 ± 0.008	1.345 ± 0.004
CBS[c]	0.0186 (±0.0003)	0.123 (±0.001)	0.088 (±0.001)	0.0860 (±0.0005)	1.23 (±0.01)	3.26 (±0.03)

[a]Values for each spring are the average of all samples collected during the period 1997–2003 (±1 standard deviation). Errors in parentheses were estimated from errors in the corresponding concentrations; see text. All ratios in mol/mol, except Sr/Na (10^{-3} mol/mol) and Ba/Na (10^{-6} mol/mol). Springs are arranged in order of increasing latitude (south to north; Figure 2).

[b]After *Millero* [1996] and *Byrne* [2002] (see Table 3).

[c]Collected in the vicinity of MHSS (depth ~7 m).

[d]Collected in the vicinity of CBS (surface).

[e]Sample kindly provided by P. W. Swarzenski, USGS, St. Petersburg, Florida.

[f]Collected in the vicinity of Rusty Springs (depth ~7 m).

[g]*Breland* [1980].

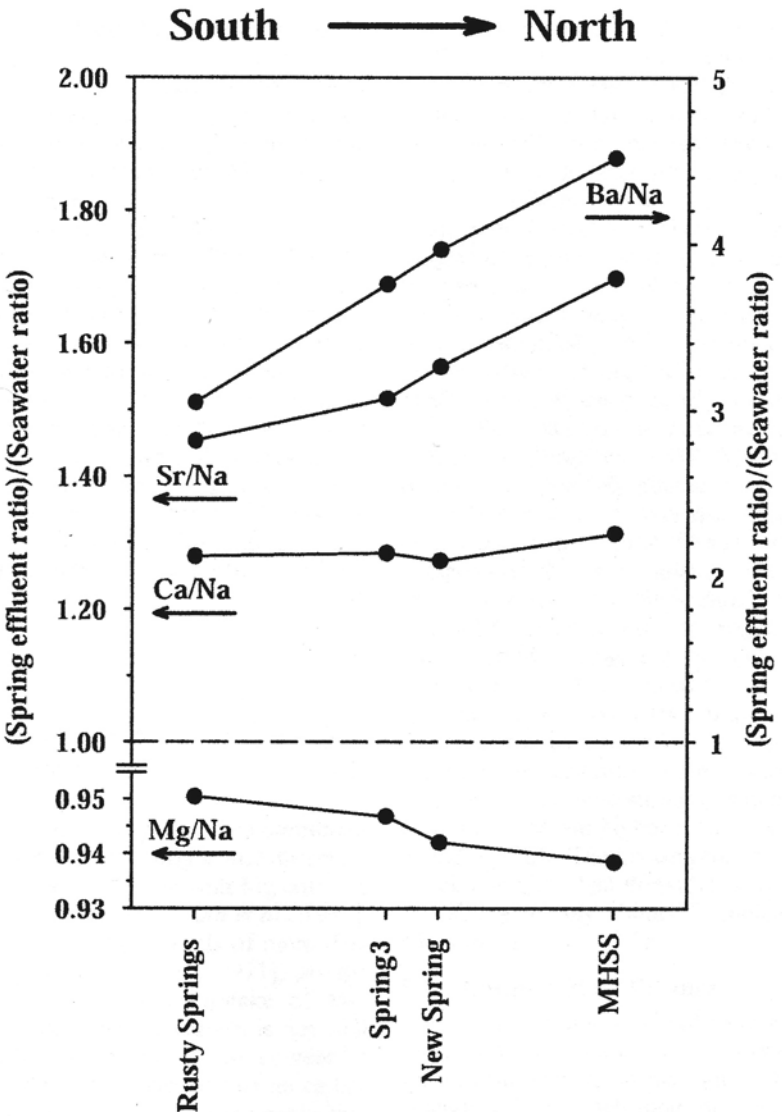

Figure 43. Spring effluent ratios of alkaline earth element to Na concentrations, where Na represents salinity, normalized to corresponding seawater ratios. Values below (above) the dashed line signify depletion (enrichment) with respect to ambient seawater. The small arrow underneath each label indicates whether the ratio should be read on the left or the right ordinate. Note the different scales. Figure from Schijf and Byrne (2007).

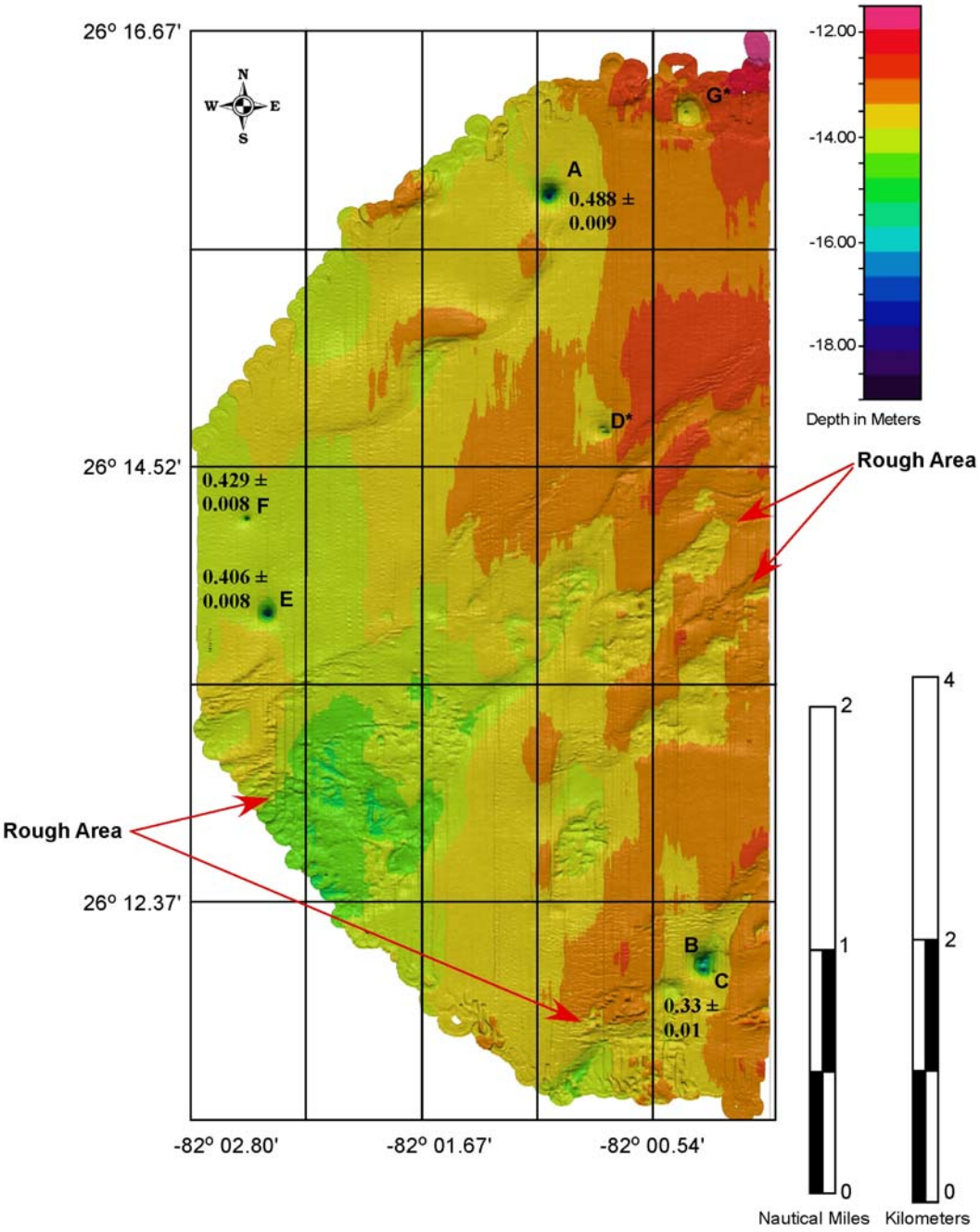

Figure 44. 2001 Mudhole Submarine Spring (MHSS) study area. Ba/Na concentrations of the active springs of MHSS (A), Spring #3 (E), New Spring (F), Northern Rusty and Rusty (B), and Near Rusty (C) (referred to as Rusty Springs in Schijf and Byrne, 2007). Refer to Table 11. Mean depth, interpolated 3D shaded relief image. The image is shown with aggressive surface editing, although some "striping" still occurs due to tide and sound velocity uncertainties. Black letters (A-G) denotes the location of the springs, refer to Table 6.

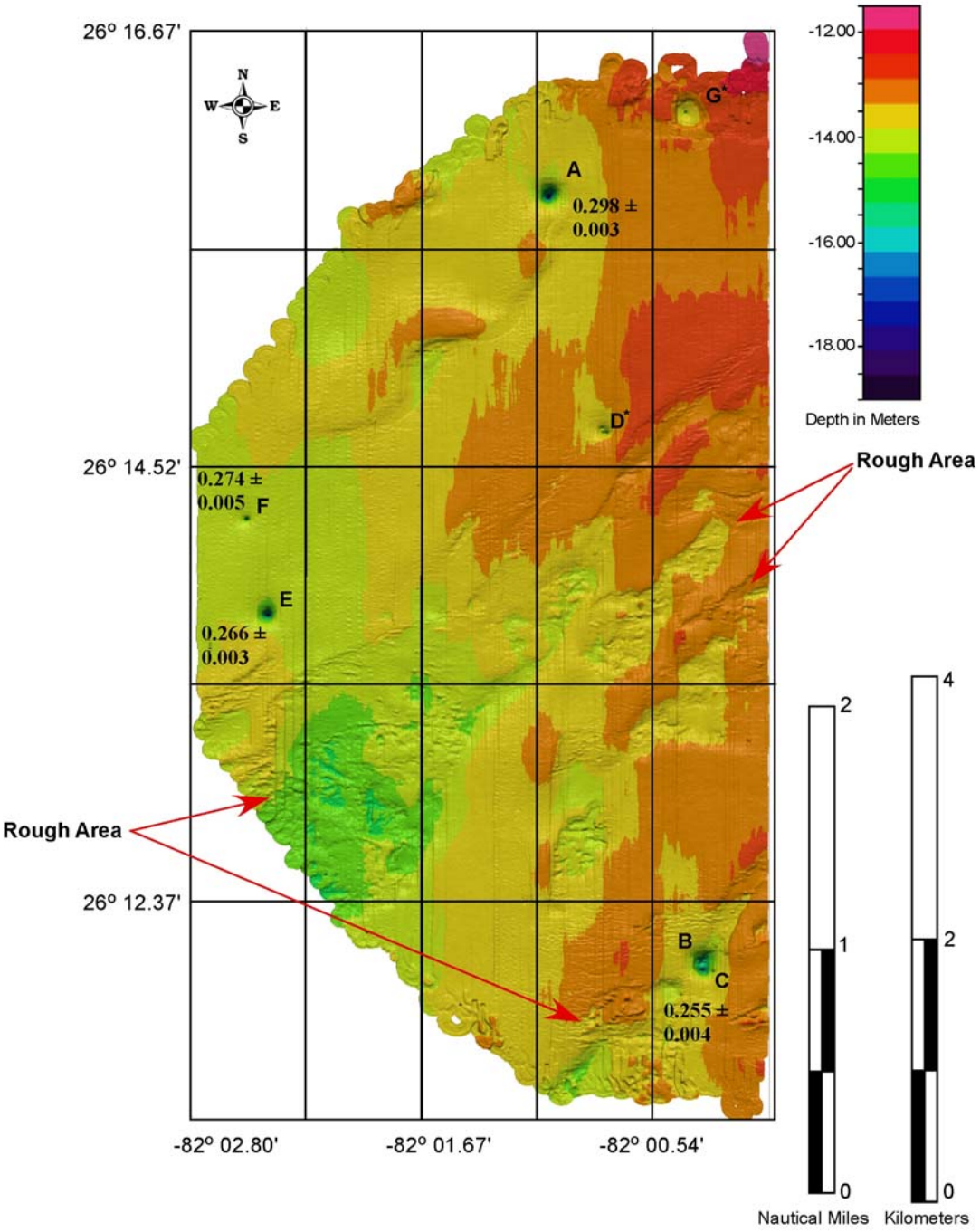

Figure 45. 2001 Mudhole Submarine Spring (MHSS) study area. Sr/Na concentrations of the active springs of MHSS (A), Spring #3 (E), New Spring (F), Northern Rusty and Rusty (B), and Near Rusty (C) (referred to as Rusty Springs in Schijf and Byrne, 2007). Refer to Table 11. Mean depth, interpolated 3D shaded relief image. The image is shown with aggressive surface editing, although some "striping" still occurs due to tide and sound velocity uncertainties. Black letters (A-G) denotes the location of the springs, refer to Table 6.

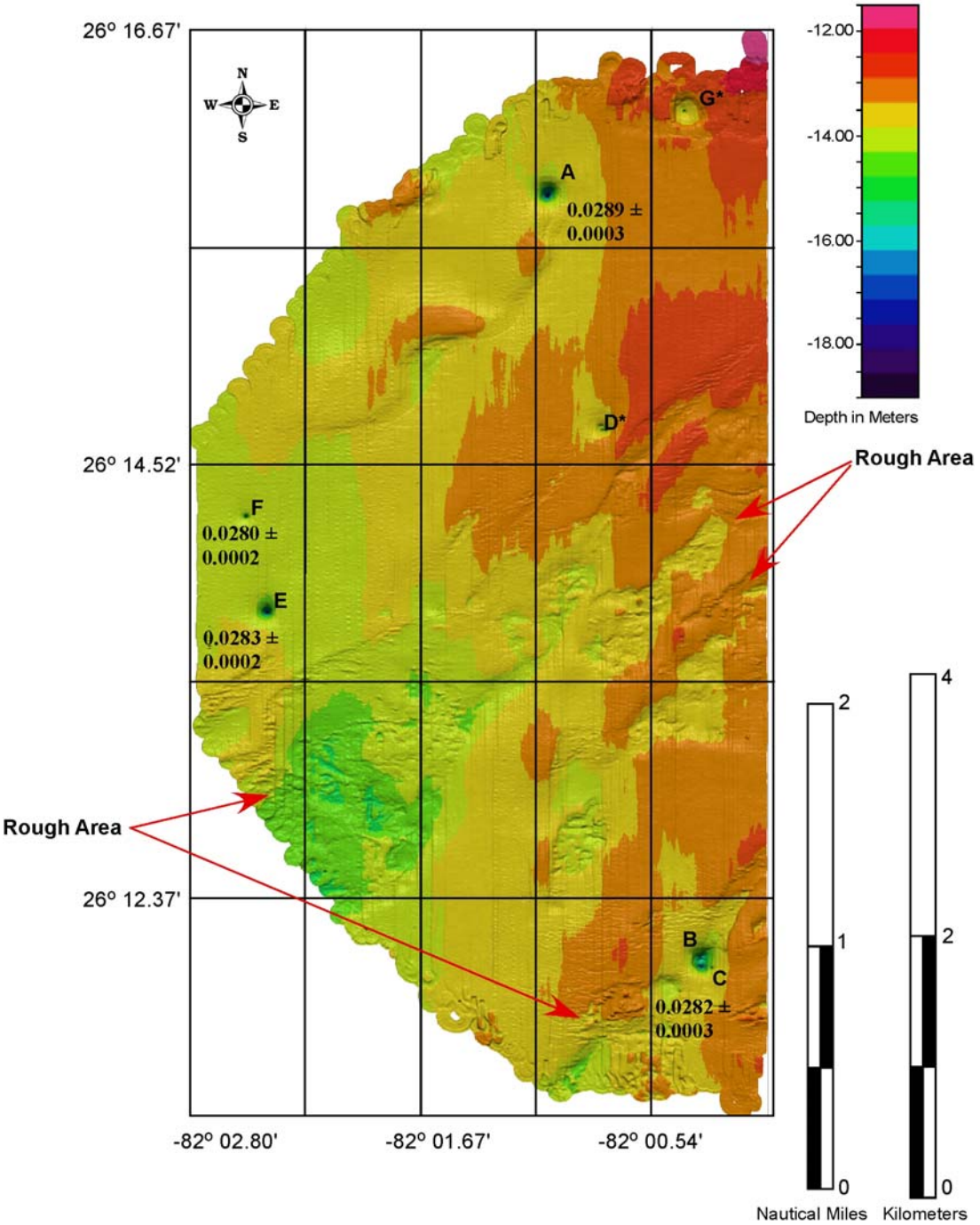

Figure 46. 2001 Mudhole Submarine Spring (MHSS) study area. Ca/Na concentrations of the active springs of MHSS (A), Spring #3 (E), New Spring (F), Northern Rusty and Rusty (B), and Near Rusty (C) (referred to as Rusty Springs in Schijf and Byrne, 2007). Refer to Table 11. Mean depth, interpolated 3D shaded relief image. The image is shown with aggressive surface editing, although some "striping" still occurs due to tide and sound velocity uncertainties. Black letters (A-G) denotes the location of the springs, refer to Table 6.

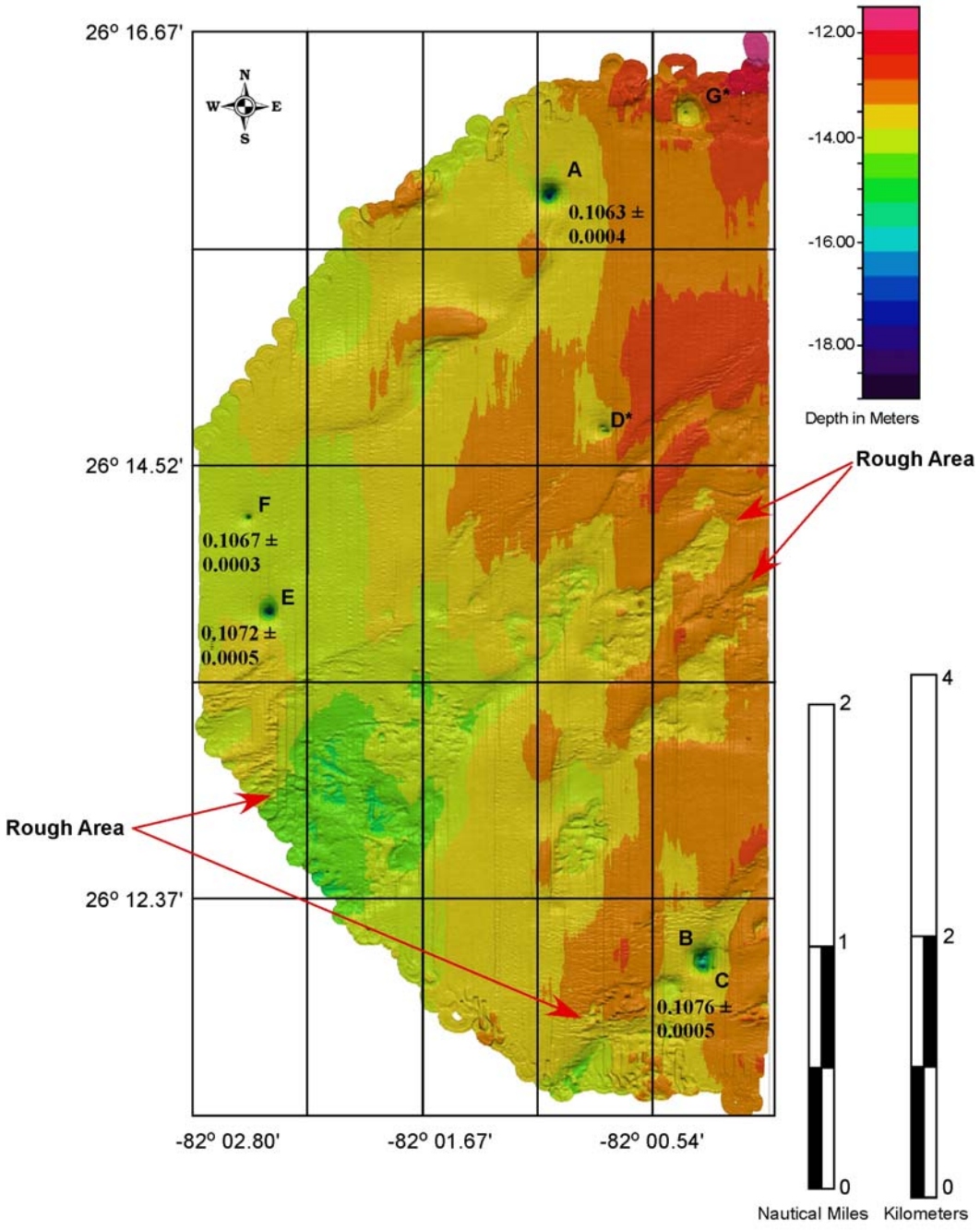

Figure 47. 2001 Mudhole Submarine Spring (MHSS) study area. Mg/Na concentrations of the active springs of MHSS (A), Spring #3 (E), New Spring (F), Northern Rusty and Rusty (B), and Near Rusty (C) (referred to as Rusty Springs in Schijf and Byrne, 2007). Refer to Table 11. Mean depth, interpolated 3D shaded relief image. The image is shown with aggressive surface editing, although some "striping" still occurs due to tide and sound velocity uncertainties. Black letters (A-G) denotes the location of the springs, refer to Table 6.

Chapter 6

CONCLUSION

The vent distribution in the MHSS study area correlates with NE-SW structural pattern of the seafloor, which is delineated by the overall pattern of sediment and limestone hardbottom. Inactive vents appear to correlate with the shallowest ambient seafloor depth, shallowest vent depression depth, and less steep vent slopes. The geomorphology of each vent varies throughout the study area.

The inactive springs, Dormant Spring (~14.5 m) and Sinister Springs (average depth of entire seepage field ~14.7 m) have a lower maximum depth than the active springs and are located in shallower ambient seafloor depths. Most of the active vents had slopes between 6^{o} or greater, with the exception of the vents within the Rusty Springs depression whose slopes ranged from $\sim<1^{o}$ to 6^{o}; whereas the inactive vents had slopes of $\sim5^{o}$ or less. Most of the active springs show evidence of steeper walls or greater slopes than the inactive springs. In the absence of strong vent flux, subsequent infilling of these depressions may be the cause of the less steep profiles, and lesser relief (between vent depth and ambient seafloor). Most of the active springs also have a “V”-shaped conical depression, with the exception of Northern Rusty and Near Rusty. The inactive vents have shallower slope profile and more of a “U”-shaped west-east depression.

The geology, based on backscatter data and very limited samples and SCUBA observations, is likely to vary from vent to vent. MHSS is located in an area probably composed of limestone gravels and coarse shells. Northern Rusty, Rusty, and Near Rusty Spring are most likely in a similar area, but appear to have fine sediments towards the southeastern edge of the depression. The geology of Sinister Spring is probably limestone, with some coarse shells, rocks and gravel. Spring #3 and New Spring are located in an area that may be interpreted as fine sediments and in a nearly flat area. Dormant Spring is in areas that probably consists of sands and fine sediments, some sand and/or shell debris.

High-resolution multibeam bathymetry and backscatter data are useful in determining overall seafloor depths and detailed morphology. Geomorphological analysis provides a potential means of assessing probable vent flow. Future work for this study area could include: (a) repeated multibeam bathymetry mapping to monitor potential changes in the geomorphology of the vents and ambient seafloor; (b) extended multibeam mapping toward the southwest in order to search for additional submarine springs; and (c) systematic bottom sampling using backscatter data as a guide to better define the seafloor geology.

References

Back, W. and B.B. Hanshaw, 1970. Comparison of chemical hydrogeology of carbonate peninsulas of Florida and Yucatan. Journal of Hydrology. 10: p. 330-368.

Berman, G.A., 2002. Geophysics and hydrodynamics of Egmont channel: An anomalous inlet at the mouth of Tampa Bay, Florida, Master's Thesis, USF, St. Petersburg, 95pp.

Berman, G., D.F. Naar, A.C. Hine, G. Brooks, S.F. Tebbens, B.T. Donahue, and R. Wilson, 2005. Geologic structure and hydrodynamics of Egmont Channel: An anomalous inlet at the mouth of Tampa Bay, Florida. Journal of Coastal Research. 21 (2): p. 331-357.

Blondel, P. and B. J. Murton, 1997. Handbook of Seafloor Sonar Imagery. New York: John Wiley & Sons, 303 pp.

Breland, A.J., 1980. Chemical and physical characteristics of a saline, geothermal spring off Florida's southwest coast, Master's Thesis, University of South Florida, 105 pp.

Brooks, G.R., L.J. Doyle, R.A. Davis, N.T. DeWitt, and B.C. Suthard, 2003. Patterns and controls of surface sediment distribution: West-central Florida inner shelf. Marine Geology. 200: p. 307-324.

Brooks, H.K., 1961. The submarine spring off Crescent Beach, Florida. Quarterly Journal of Florida Academy of Sciences. 24 (2): p. 122-134.

Byrne, R. and D. F. Naar, 2002. Coordinated investigation of the geochemistry and bathymetry defining the impact of nearshore geothermal vent input on the south-central west Florida shelf. Cruise Report. FIO/USF.

Davis, K.S., N.C. Slowey, I.H. Stender, H. Fiedler, W. R. Bryant, and G. Fechner, 1996. Acoustic backscatter and sediment texture properties of inner shelf sands, northeastern Gulf of Mexico. Geo-Marine Letters. 16 (3): p. 273-278.

Donoghue, J.F., R.J. Anuskiewicz, J.S. Dunbar, P.R. Gerrell, and M. Faught, 1995. Evidence of early humans on the northeastern Gulf of Mexico continental shelf: Ray Hole Spring. The 1st SEPM Congress on Sedimentary Geology. p. 48.

Doyle, L.J. and T.H. Sparks, 1980. Sediments of Mississippi, Alabama, and Florida (MAFLA) continental shelf. J. Sediment. Petrol. 50: p. 905-916.

Fanning, K., R. Byrne, J. Breland III, and P. Betzer, 1981. Geothermal springs of West Florida shelf: Evidence for dolomitization and radionuclide enrichment. Earth and Planetary Science Letters. 52: p. 345-354.

Finkl, C.W., L. Benedet, and J.L. Andrews, 2005. Submarine geomorphology of the continental shelf off southeast Florida based on interpretation of airborne laser bathymetry. Journal of Coastal Research. 21 (6): p. 1178-1190.

Ford, D. and P. Williams, 1989. Karst geomorphology and hydrology. London: Unwin Hyman Ltd., 601 pp.

Gould, H.R., and R.H. Stewart, 1955. Continental terrace sediments in the northeast Gulf of Mexico. In: Finding ancient shorelines. Soc. Econ. Paleontologists Mineralogists, Special Publication, 3.

Hanshaw, B.B., W. Back, and R.G. Deike, 1971. A geochemical hypothesis for dolomitization by groundwater. Economic Geology. 66: p. 710-724.

Henry, H.R., and F.A. Kohout, 1972. Circulation patterns of saline groundwater affected by geothermal heating—as related to waste disposal. Underground waste Management and Environmental Implications, p. 202-221.

Hine, A.C., and D.F. Belknap, 1986. Recent geological history and modern sedimentary Processes of the Pasco, Hernando, and Citrus county coastline: West-central Florida. Florida Sea Grant College Publication no. 9, 160 pp.

Hugget, Richard J., 2003. Fundamentals of geomorphology. New York: Routledge, 386 pp.

Hunn, J.D., and R.N. Cherry, 1969. Remote sensing of offshore springs and spring discharge along the gulf of central Florida. Earth Resources Aircraft Program. 3: p. 39-1-39-7.

Huvenne, V.A.I., Ph. Blondel, and J.P. Henriet, 2002. Textural analyses of sidescan sonar imagery from two mound provinces in the Porcupine Seabight. Marine Geology. 189: p. 323-341.

Kohout, F. A., 1965. A hypothesis concerning the cyclic flow of salt water related to geothermal heating in Floridan Aquifer. Transactions of the New York Academy of Sciences, Series 2. 28 (2): p. 249-271.

Kohout, F.A., 1966. Submarine springs: a neglected phenomenon of coastal hydrology.

Central Treaty Organization's Symposium on Hydrology & Water Resources Devel. Feb. 5-13. p. 391-413.

Kohout, F.A., 1967. Ground water flow and the geothermal regime of the Floridan Plateau. Trans. Gulf Coast Ass. of Geological Societies. 17: p. 339-354.

Kohout, F.A., M.C. Kolpinski, and A.L. Higer, 1973. Sensing of hydrothermal springs: Floridan Plateau and Jamaica, West Indes. International Symposium on Ground Water, p. 571-578.

Kohout, F.A., H. Henry and J. Banks, 1977. Hydrogeology related to geochemical conditions of the Florida Plateau. In: D. Smith and G. Griffen (eds). The geothermal nature of the Floridan Plateau. Florida Dept. of Nat. Resources Special Publication. 21: p. 1-41.

Lane, E., 1986. Karst in Florida. Florida Geological Survey Special Report, no.29,100 pp.

McIntyre, M.L., 2003. Testing a model for deriving bathymetry from airborne hyperspectral data by comparisons with multibeam data, Master's Thesis, USF, St. Petersburg, 79 pp.

McIntyre, M., D.F. Naar, K.L. Carder, B.T. Donahue, and D.J. Mallison, 2006. Coastal Bathymetry from hyperspectral remote sensing data: Comparisons with high Resolution multibeam bathymetry. Marine Geophysical Researches. 27, 2: p.126-136.

Miller, L. R. and R.J. Byrne, 1966. The angle of repose for a single grain on a fixed rough bed. Sedimentology. 6 (4): p.303-314.

Naar, D. F., and R. Byrne, 2001. Coordinated investigation of geochemistry and bathymetry defining impact of nearshore geothermal vent input on the south-central west Florida shelf. Cruise report- Leg I & II. FIO/USF.

Naar, D., R. Byrne, B. Donahue, D. Williams, and J. Schijf, 2000. High-resolution multibeam bathymetry surveys of the Mudhole submarine springs area near Fort Myers, Florida. Proceedings of the American Academy of Underwater Sciences, Diving for Science, Twentieth Annual Scientific Diving Symposium, October, p. 60.

Parrott, R., J.H. Clarke, G. Fader, J. Shaw, and E. Kamerrer, 1999. Integration of multibeam bathymetry and sidescan sonar data for geological surveys. OCEANS '99 MTS/IEEE. Riding the Crest into the 21st Century. 3: p.1129-1133.

Randazzo, A.F., and D.S. Jones, 1997. The Geology of Florida. Tampa: University Press of Florida, 327 pp.

Rosenau, J.C., G.L. Faulkner, C.W. Henry, and R.W. Hull, 1977. Springs of Florida. Florida Department of Natural Resources, Bureau of Geology Special Bulletin, Florida Geological Survey, http://www.flmnh.ufl.edu/springs_of_florida/ Geological Bulletin No. 31(revised). 469 pp.

Schijf, J. and Robert H. Byrne, 2007. Progressive dolomitization of Florida limestone recorded by alkaline earth element concentrations in saline, geothermal, submarine springs. Journal of Geophysical Research.112: p.1-17.

Schmeeckle, W. M., and J.M. Nelson, 2003. Direct numerical simulation of bedload Transport using a local, dynamic boundary condition. Sedimentology. 50: p. 279-301.

Soulsby, Richard, 1997. Dynmaics of marine sands: a manual for practical applications. Telford: London, 245pp.

Spechler, R.M. and D.M. Schiffer, 1995. *Springs of Florida*. U.S. Geological Survey Fact Sheet FS-151-95, 2 pp.

Stringfield, V.T., 1936. Artesian water in the Florida peninsula: U.S. Geological Survey Water-Supply Paper 773-C, p.1115-195.

Stringfield, V.T., Warren, M.A., and Cooper, H.H., 1941. Artesian water in the coastal area of Georgia and northeastern Florida. Economic Geology, 36 (7): p.698-711.

Stringfield, V.T. and H.E. LeGrand, 1969. Hydrology of carbonate rock terrains- A review with special reference to the United States. Journal of Hydrology. 8: p. 349-417.

Tihansky, A.B., and L.A. Knochemus, 2001. Karst features and hydrogeology in West-central Florida-A field perspective. In: Eve L. Kuniansky (Ed.). U.S. Geological Survey Karst Interest Group Proceedings, Water-Resources Investigations Report 01-4011, p. 198-211.

Wilcove, Raymond, 1975. The great Red Snapper Sink. National Oceanic and Atmospheric Administration press release reprint April 1975, 5 (2): 2 pp.

Wong, Wing and M. Gourley, 2003. Sound velocity corrections for Simrad EM Data. Caris. Fredericton, Canada: 1-15 pp.

Wolfson, M. L., 2005. Multibeam observations of mine scour and burial near Clearwater Florida, including a test of the VIMS 2D burial model. Masters' Thesis, 256 pp.

Wolfson, M.L., D.F. Naar, P.A. Howd, S.D. Locker, B.T. Donahue, C.T. Friedrichs, A.C. Trembanis, M.D. Richardson, and T.F. Wever, 2007. Comparing predicted mine scour and burial to multibeam observations offshore of Clearwater, Florida. In: Wilkens R.H and M.D. Richardson (Editors) Mine Burial Processes. *IEEE Journal of Oceanic Engineering*.

Zaleski, L., and R. Flood, 2001. Changes in bottom morphology of Long Island Sound near Mount Misery Shoal as observed through repeated multibeam surveys. http://pbisotopes.ess.sunysb.edu/lig/Conferences/abstarcts01/zaleski/zaleski-abst.htm